POLITECNICO DI TORINO

Faculty of Engineering

Department of Mechanical and Aerospace Engineering

Master's Degree in Aerospace Engineering

Master's Degree Thesis:

Advanced Numerical Models for Electromechanical Actuators

Supervisors

Prof. Matteo D.L. Dalla Vedova

Eng. Gaetano Quattrocchi

Prof. Paolo Maggiore

Candidate

Rosario Aresco

A.Y. 2022/2023

1 Abstract

Electromechanical actuators are increasingly being used in aerospace, mainly due to the new design concept, the more electric aircraft (MEA), such as the Boeing 787, which uses electric power to directly operate some actuators, such as the brake system, to feed the hydraulic system, or to power systems that manage the onboard environment, making the aircraft bleed-less. In the most recent airbus aircrafts are used electric actuators for secondary systems, but for primary systems are used hybrid actuators, such as the Electro Hydrostatic Actuators (EHA), which use both electric power and local hydraulic power. Actuators are safety critical components, especially when used for systems of primary importance, and for this reason it is necessary to identify all possible faults associated with it and, if possible, assess the degraded state of the actuator to maintain a high level of safety. Nowadays, electric actuators are used for secondary systems because the failure risks and accumulated reliability experience are absent. The predictive maintenance is the ability to know the remaining useful life of a generic system, based on prognostic methods, in order to plan maintenance before a critical failure. With data-driven prognostic methods there is a need for a high amount of data from sensors to evaluate the performance of the system. These data are collected and run through machine learning algorithms in hopes of detecting correlations and using these to make prognoses of future failures. The purpose of this work is to implement a thermal model within an existing model of Electromechanical Actuator (EMA), provided by Prof. M.D.L. Dalla Vedova and the Eng. G. Quattrocchi, in order to evaluate the thermal effects due to the energy dissipation inside the stator conductors, and the consequent heat flows on the other components of the electric motor, as the resistance of the windings is a function of their temperature. The EMA model provided is based on Permanent Magnet Synchronous Motor (PMSM), which is an AC synchronous motor whose field excitation is provided by permanent magnets, such as the Brushless DC electric motor, and that has a sinusoidal back EMF waveform. Several variables related to the failure modes of servomechanism are implemented within the model, the partial shortage of each phase, a variable that evaluates the static eccentricity, and a variable that evaluates the phase of this imbalance. Once created the thermal model, and compared the system response with the previous model provided, the following step is related to the simulations performed taking into account different operating conditions, varying parameters such as the partial shortage of each phase, so as to sample as much data as possible and use prognostic methods, in order to evaluate the Remaining Useful Life (RUL) of the actuator

Contents

2 Introduction

The purpose of this thesis is to implement a possible thermal model of the electric motor PMSM, in order to evaluate the effects of the temperature change, and the relative thermal exchanges between the various components of the motor, on the operation of the Electromechanical Actuator (EMA) under certain operating conditions.

The following paragraphs focus mainly on explaining the Control system, starting from the actuator types, explaining their functionality, to evaluate their use within the aircraft. After explaining the operational use of the actuators, the paper focuses on the operation of Brushless electric motors, as contained in the actuator model under consideration.

The development of actuator models is due to the relatively premature electric actuator technology, which requires an optimal knowledge of actuator behaviour to assess safety aspects. The main purpose is to incorporate fault tolerance and redundancy tools into the design of the actuator, with health monitoring through the incorporation of sensors inside the actuator, in order to consider predictive maintenance, also associated with Artificial Neural Network models.

The thermal model implemented on the system is based on an existing EMA model, developed using MATLAB Simulink software. Specifically, chapter 5 explains in detail all the blocks contained in this model, which emulate the actuator's real behaviour. A model-based approach in the engineering field is favoured in the development of a system as it allows to easily modify some parameters of the model, decreasing costs and increasing productivity with shorter development timelines.

The EMA model provided is based on an existing test bench used to assess the model's behaviour in relation to the real case, by performing tests, necessary for the validation of this.

With the implementation of a thermal model in Simscape, although not numerically accurate, it is possible to evaluate the macroscopic effects of temperature on the system, creating a modularity that allows, through the use of different blocks, to easily evaluate different setups.

After having implemented the thermal model within the EMA model, it is useful to evaluate the difference between the old and the new model, in order to evaluate its correct functioning, as well as evaluate the effects of temperature on the system. Specifically, in chapter 6, the fault modes introduced in the model under examination are explained. One of the test simulations also implements one of these, the short circuit fault, in order to verify its effect on the system response.

3 Aircraft Overview

3.1 Actuation system

The actuation system is a fundamental element of the aircraft which has been updated over time through the introduction of new technologies.

The main purpose of the actuators on aircrafts is the actuation of control surfaces, by transferring the pilot's command, for example via the yoke, to the elements that control the aircrafts themselves.

There are different types of actuators, such as:

1. Hydraulic actuator
2. Electro-Hydraulic
3. Electro-Hydrostatic actuator (EHA)
4. Hybrid configuration (EBHA)
5. Electro-Mechanical actuator (EMA)

The least used configuration in aerospace is the EMA model, due to lack of knowledge of failure modes, one of the most important things for safety reasons.

Every configuration has in common the purpose of tracking the commanded position of the actuator itself, and therefore the inclination of the surface.

Every type of actuator previously introduced will be explained in the following paragraphs.

3.1.1 Hydraulic actuator

This type of actuator was the most used in the past as it did not include any electric drive because the pilot's command is directly transferred to the servomechanism and then the surface, via hydraulic power.

In this case the input signal is given directly from the pilot to a series of levers, connected to the servo valve contained in the servo mechanism, which moves a spool in a typical configuration.

This spool with its motion open ducts and supplies pressurized hydraulic fluid to one of the actuator chambers, which control the actuator jack movement.

In this case the feedback loop is closed by the jack's movement because this is directly connected to the input command linkage. When the jack moves, the instant centre of rotation changes and the spool of the servo valve return to the neutral position whenever the error between the input command and the real position is null.

This type of actuator has been mostly used in the past, as it makes direct use of the pilot's command through mechanical linkages, in order to enhance it and make the piloting of the aircraft easier, without limiting the accuracy and the reliability.
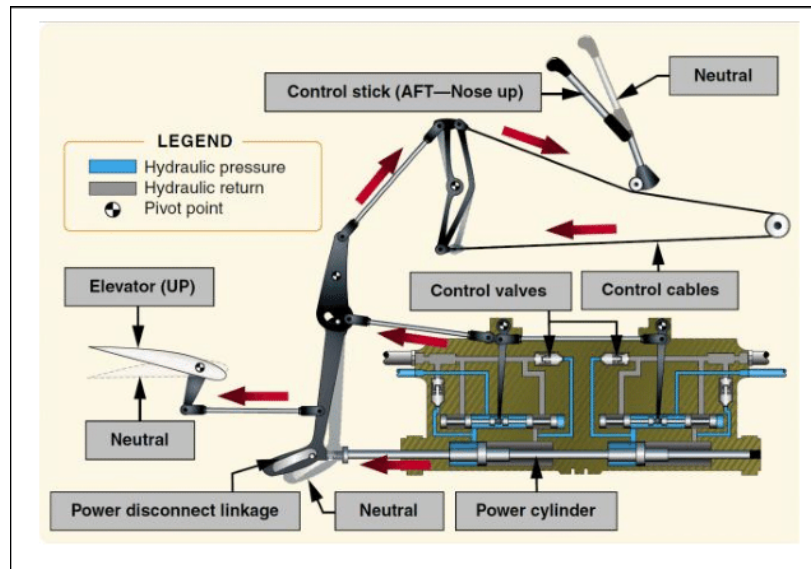

FIGURE 3-1 CONVENTIONAL AIRCRAFT FLIGHT CONTROL SYSTEM

3.1.2 Electro-Hydraulic actuator

The evolution of the hydraulic actuator is related to the use of the electrical system to control the movement of the servomechanism.

In this case the main power for the jack's movement it always comes from the pressurized hydraulic fluid from the hydraulic circuit, but the servo valve spool is moved by an electrical signal.

There are different types of Electro-Hydraulic actuator, such as Jet pipe solution or Direct Drive Valve actuator, but the most adopted solution is related to the use of a two-stages flapper nozzle servo valve.

This type of valve uses an electric torque motor that directly moves a flapper, i.e., the first stage of the valve, which obstructs the flow of hydraulic fluid from the nozzle, in order to create a pressure difference between right and left side of the main spool, i.e., the second stage of servo valve.

As seen in the previous case, the spool's movement open and closed ducts between pressurized flow and the actuator chambers.
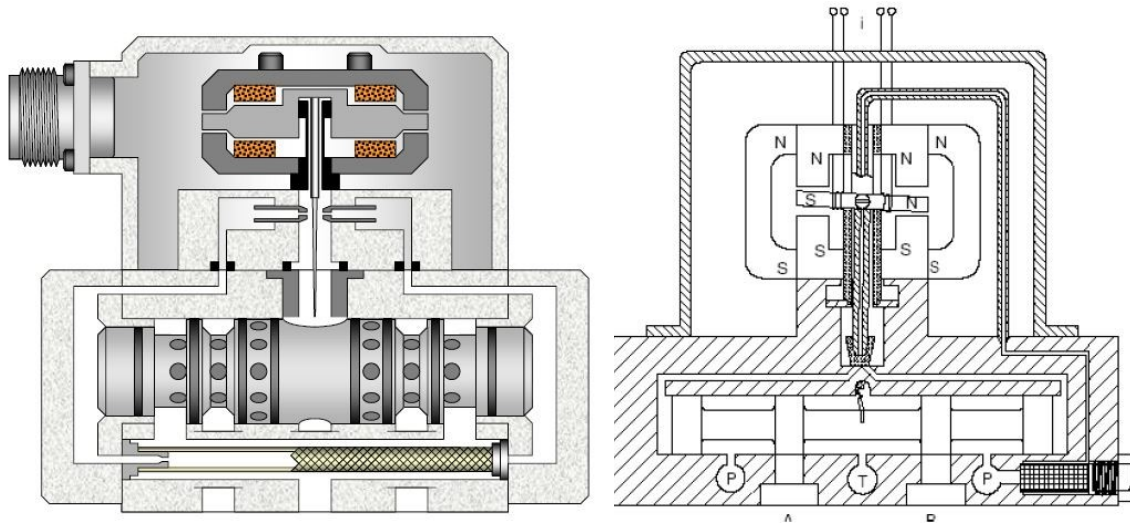
FIGURE 3-2 FLAPEER NOZZLE VALVE (LEFT) VS JET PIPE VALVE

In this case the feedback loop is closed by a particular element contained in the servo valve, the feedback spring, connected directly to the flapper, which takes care of bringing back the flapper in the neutral position, depending on the position of the spool, and therefore on the error between the input command and the actual position of the servo mechanism.

As already mentioned, there are other typed of electro-hydraulic actuators. An evolution of the flapper nozzle model is the Jet pipe hydraulic valve. In this case the electric torque motor does not moves a flapper but the position of a Jet pipe towards two holes, directly connected to the right and left chambers of the spool.

The movement of the Jet pipe makes it pass more pressurized hydraulic flow to a chamber of the spool than the other, and the kinetic component of the flow causes a pressure difference between right and left part of the spool. In this case the feedback loop is closed with a spring connected to the spool.

The latest configuration introduced is the Direct Drive valve. In this case a solenoid moves directly the spool making the position control more accurate.

This configuration is used in modern application thanks to the new technologies introduced in the electrical field, making the system more reliable. A two-stage valve, like the conventional ones previously seen, implies a narrow operating bandwidth of about 50 Hz. For this reason, for applications that require a high operating frequency, it is possible to solve the problem using single-stage valves, and one of these is DDV valve.
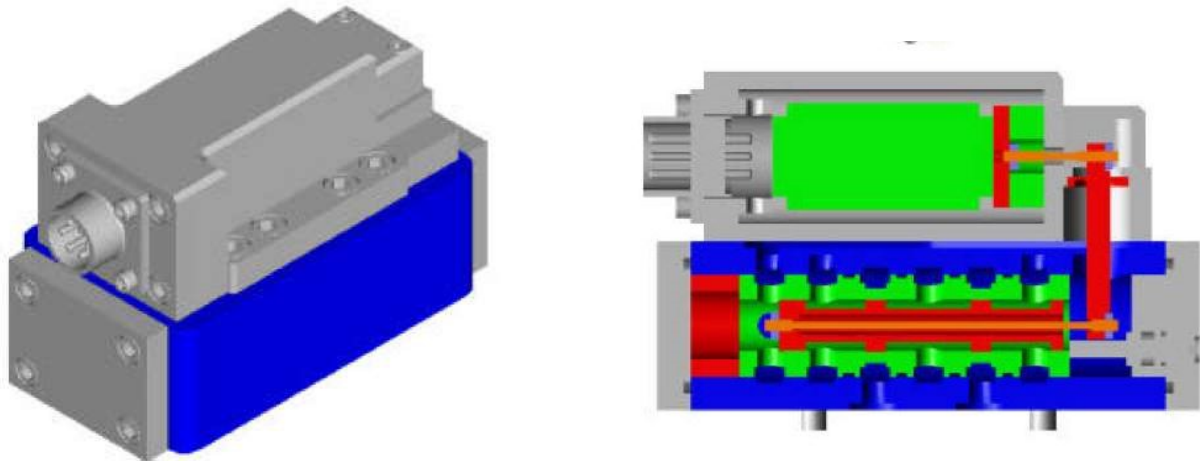
FIGURE 3-3 DDV VALVE

3.1.3 Electro-Hydrostatic actuator (EHA)

In the last few years, the More Electric concept became predominant in aircraft development and his subsystems. In particular, the increased use of electrical power for actuators has brought specific benefits in terms of overall weight and control of motion of the servo mechanism.

FIGURE 3-4 EHA ARCHITECTURE

The centralized hydraulic system of the aircraft is replaced by a local pump, in the actuator drive area. In this case the overall system is composed by the hydraulic jack, the same of the previous configurations, a hydraulic pump, usually an axial piston pump, driven by an electric motor that in aerospace refers to a BLDC, the Brushless DC electric motor.

FIGURE 3-5 FCC ARCHITECTURE
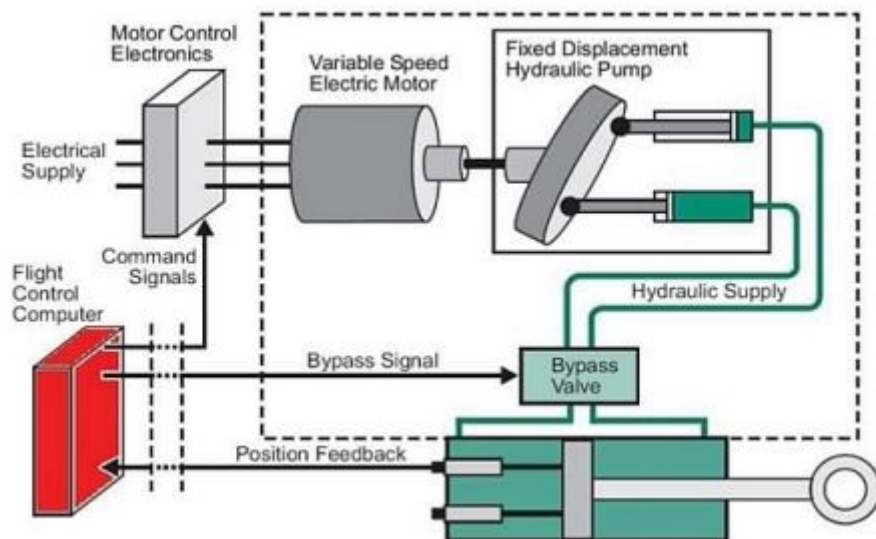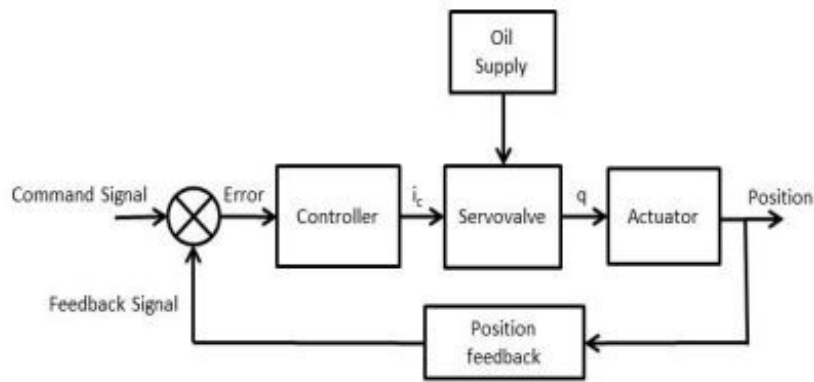
The feedback loop for the error estimation is closed by a position sensor, usually an LVDT, which detects a mechanical linear movement as displacements and converts it to electrical signals.

The pilot's input signal and the sensor feedback are managed by the FCS, that through the error manages the input to be given to the actuator.

The main advantage of this configuration is the absence of hydraulic lines along the aircraft, replaced by light electrical wires, and the greater accuracy in surface position due to lower hydraulic losses.

The first civil aircraft to use this type of actuator was the Airbus A380, and later the Airbus A350, while in military aircraft they are used by the new generation fighters, the Lockheed Martin F22 and F35 Lightning II.

ù

3.1.4 Hybrid configuration (EBHA)

This typology of actuator is very similar of the previous one, but in this case the primary source of power comes from the centralized hydraulic system. The local pump is only used in emergency cases when there are problems on the primary power source. In this case the actuator shuts down the connection with the centralized hydraulic system and engage the local pomp, driven by an electric motor, the BLDC.
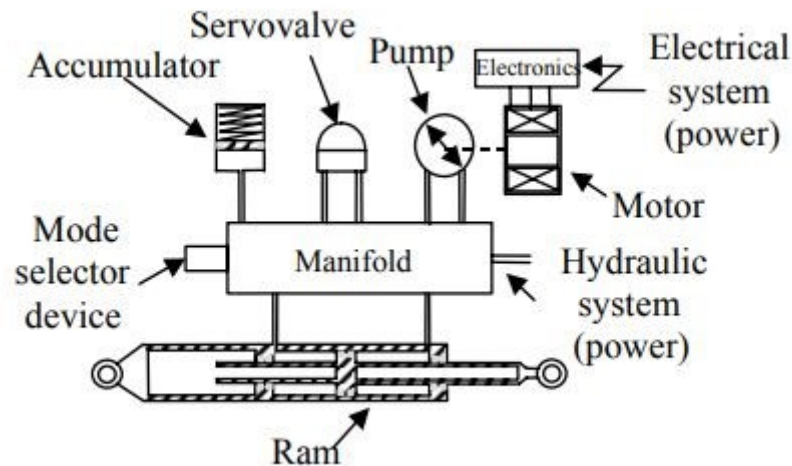
FIGURE 3-6 EBHA ARCHITECTURE

This type of actuators is used for those control surfaces where the centralized hydraulic system has its benefits, but in emergency cases there is a backup system which keep operative the actuator.

3.1.5 Electromechanical actuator (EMA)

The previously introduced actuators refers to a more electric design concept but in both cases the main power source derives from the hydraulic power system, with a local hydraulic pump for the EHA, and the centralized hydraulic system with a local electric backup for the EBHA.

The next step for a real More electric concept actuator is the elimination of the hydraulic power source, using only the electrical power. This type of actuator is di Electromechanical actuator (EMA).

The system is composed by an electric motor, such as BLDC in aerospace applications, connected to a rotatory to linear motion converter, i.e., ball screw, jackscrew, or a roller screw. As seen for previous actuators, there is a feedback loop to estimate the error between the input command and the real jack position, consist in a sensor that is usually an RVDT, which measure a rotational displacement.

The main advantages of this type actuators are the overall lower weight, for the actuator itself and the absence of hydraulic lines, and ease of maintenance compared to hydraulic actuators.

They are rarely used in aerospace because this is a recent technology, and their fault modes need to be studied to be used on primary flight control. For this reason, there aren't sufficient resource to understand their reliability level, preferring the most used EHA actuators.

Currently the only applications of this type of actuators are restricted only to the UAV, which do not have a hydraulic system due to costs and application, and for secondary control surfaces or for backup power source.
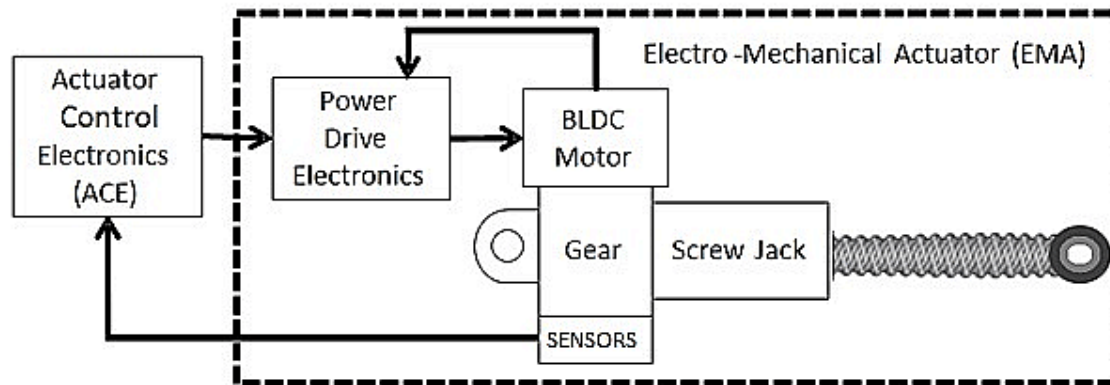

FIGURE 3-7 EMA ARCHITECTURE

A typical EMA setup includes the following items:

- **ACE (Actuator Control Electronics):** this is an electronic control unit which implements a control logic of the actuator. In this system the input command, from FBW system, is compared with the sensor signals, calculating the error signal
- **PDE (Power Drive Electronics):** this is a static power converter which transform the DC into a three-phase alternating current for the BLDC phases, based on error signal from the ACE module.
- **BLDC (Brushless DC motor):** this is the source of mechanical power.
- **Reduction Gear:** this component modulates the RPM of the electric motor.
- **Rotational to linear converter:** Convert the rotational motion of the electrical motor in a translational motion. Usually this is a ball screw, a jack screw or a roller screw.
- **RVDT (Rotary Variable Differential Transducer):** this is the angular position sensor, used for the feedback loop. In some cases, this is coupled with a LVDT, located in the jack, for redundancies.

This type of actuator includes a gearbox because the BLDC generates a low torque at very high RPMs while the payload, such as a control surface, requires a low angular speed, in the order of tens of degrees for second.

An important parameter for this actuator type is the Transmission ratio, that is the ratio between the electric motor angular velocity and the gear box output angular velocity. This ratio is also related to the torques because these angular velocities are a function of motor torque, the output torque, and the transmission efficiency.

$$\tau = \frac{\dot{\theta}_m}{\dot{\theta}_u} = \frac{1}{\eta}\frac{T_u}{T_m}$$

In aerospace the required angular velocity is of the order of $50 - 60\,^{\circ}/_{s}$ for the primary surfaces, and it is of order of $5 - 10\,^{\circ}/_{s}$ for the secondary surfaces.

The application of this type of actuators is limited due to major safety issues because, unlike the hydraulic actuators, fault modes have not yet been thoroughly studied. In addition, one of disadvantages of using an electric motor for a direct transmission of input command is the difficult to keep a fixed position when the input command is null.

FIGURE 3-8 BALL SCREW [LEFT] VS ROLLER SCREW [RIGHT] CONVERTERS

For this reason, there may be oscillations in the surfaces control following an incorrect design, due to the torque values function of the error between the input command and the real position of the surface.

Another problem is related to the continuous operative of the same stator phases, as explained in the previous example, that could lead to malfunctions and overheating.

The problems introduced so far relate to a reversible transmission. these could be solved by the introduction of components that make the transmission irreversible, maintaining the desired position when they are not powered.

3.2 Application of Actuators

3.2.1 More electric aircrafts

The main application of these actuators in aerospace concerns the control surfaces actuation. At the beginning the main power source for the movement of these surfaces was the human strength, thanks to steel cables through the entire aircraft.

Through the years, ever larger planes needed a greater force to control their trim and for this reason it was necessary to implement innovative solutions, based on hydraulic system and a new type of actuator, the hydraulic one.
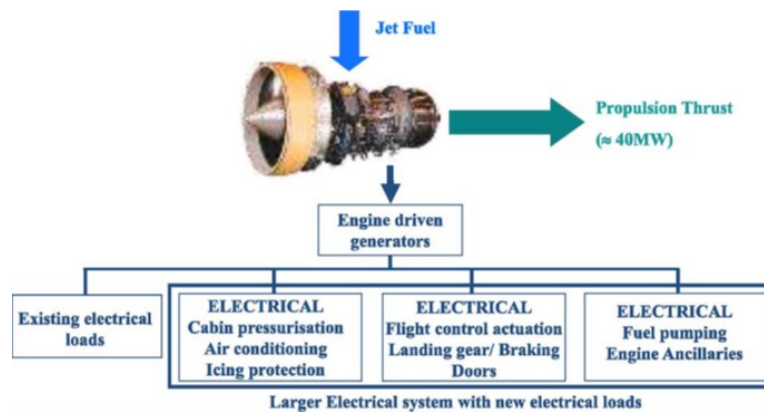

FIGURE 3-9 B787 POWER DISTRIBUTION

The More Electric concept for aircraft design is leading to an increasing use of electric power on the aircraft, such as the motion of control surfaces.

The recent civil aircrafts, such as the Airbus A350 or the Boeing 787 implements innovative solutions for the electric power system and subsystems.
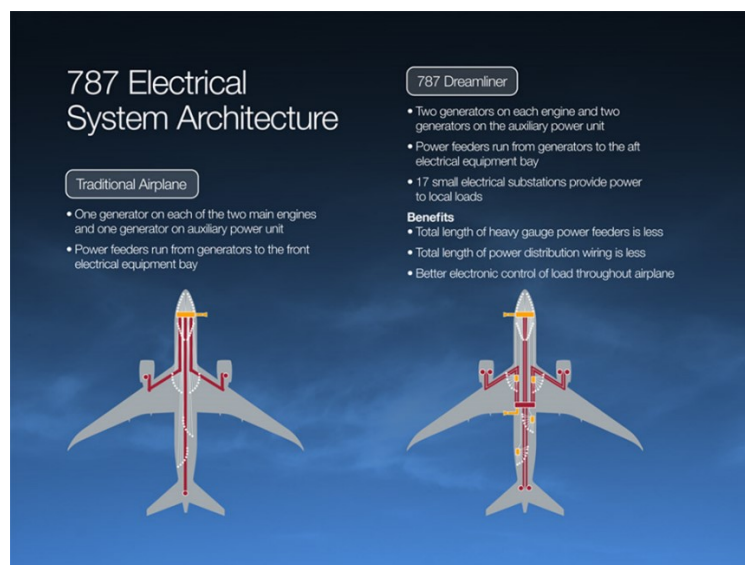

FIGURE 3-10 B787 ELECTRICAL SYSTEM ARCHITECTURE

In particular, Boeing has revolutionized this system by eliminating the air bleed system and converting all the subsystems that used the compressed air to an electric functioning, such as the propulsion system start up, but in this case the main power used to control the surfaces motion always comes from the centralized hydraulic system, powered by electric pumps.

The Airbus concept for the A350 design involves the implementation of More electric actuators, such as EHA and EBHA, to reduce the use of the centralized hydraulic systems preferring local pumps or local back-up systems in order to reduce the overall

weight of this system, implementing only two hydraulic lines compared to the three of the Boeing 787.

3.3 Motion control

The main purpose of the actuators is the motion of control surfaces in order to control the attitude and the trajectory of the airplane. Aircraft flight control systems consist of primary and secondary systems. The ailerons, elevator (or stabilator), and rudder constitute the primary control system and are required to control an aircraft safely during flight. Wing flaps, leading edge devices, spoilers, and trim systems constitute the secondary control system and improve the performance characteristics of the airplane or relieve the pilot of excessive control forces.

3.3.1 Primary flight controls

The motion of these surfaces creates a local modification of aerodynamic forces and depending on their position along the aircraft create pitch, roll and yaw moments (M_{XB}, M_{YB}, M_{ZB} in body axis).

Movement of any of the three primary flight control surfaces (ailerons, elevator or stabilator, or rudder), changes the airflow and pressure distribution over and around the airfoil. These changes affect the lift and drag produced by the airfoil/ control surface combination and allow a pilot to control the aircraft about its three axes of rotation.
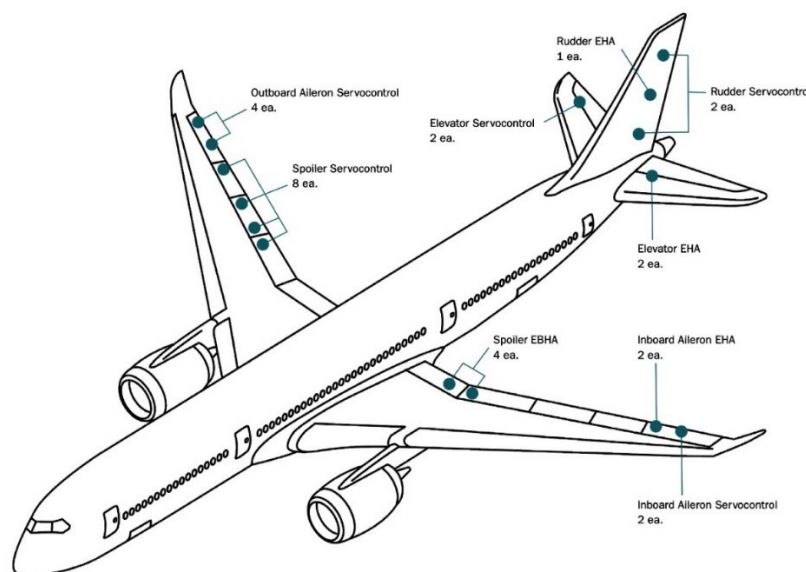

FIGURE 3-11 AIRBUS A350 PRIMARY SURFACES CONTROL

The purpose of these design limits is to prevent the pilot from inadvertently overcontrolling and overstressing the aircraft during normal manoeuvres. A properly designed aircraft is stable and easily controlled during normal manoeuvring. Control surface inputs cause movement about the three axes of rotation. The types of stability an aircraft exhibits also relate to the three axes of rotation.

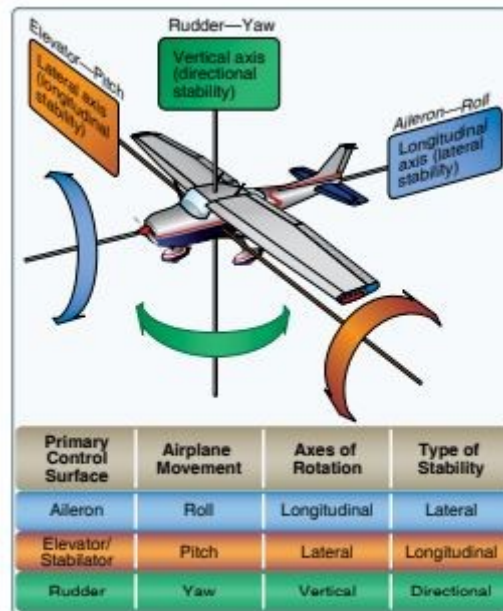| Primary Control Surface	Airplane Movement	Axes of Rotation	Type of Stability
Aileron	Roll	Longitudinal	Lateral
Elevator/ Stabilator	Pitch	Lateral	Longitudinal
Rudder	Yaw	Vertical	Directional

FIGURE 3-12 CONSEQUENCES OF MOVEMENT OF PRIMARY SURFACES

In a conventional architecture, such as the Boeing 737, there is a yoke connected directly to the hydraulic system of the aircraft, then with direct control of the main moving surfaces. In case of failure of the hydraulic systems of the aircraft a manual reversion is available, for roll and pitch control, associated with components such as the balance tab, present in elevators and ailerons, which help the pilot in the control of the aircraft in the absence of servomechanisms.

As already explained above, in modern aircrafts there is no need of pilot power because control system uses the hydraulic or electrical power system for the surface control. The input command from the cockpit's stick or pedals is transmitted to the FCS (Flight Control System) through the FBW (Fly by Wire) or FBL (Fly by Light) systems.

The signal is processed by the on board computer in order to analyses the input command and output the appropriate signal, based on flight data (such as speed, acceleration, altitude, attitude and other parameters) to prevent exceedance of the normal flight envelope. In emergency cases there are backup systems, such as batteries or the Ram Air Turbine (RAT) which allow the normal operation of the on-board computers, in order to control the aircraft main surfaces.
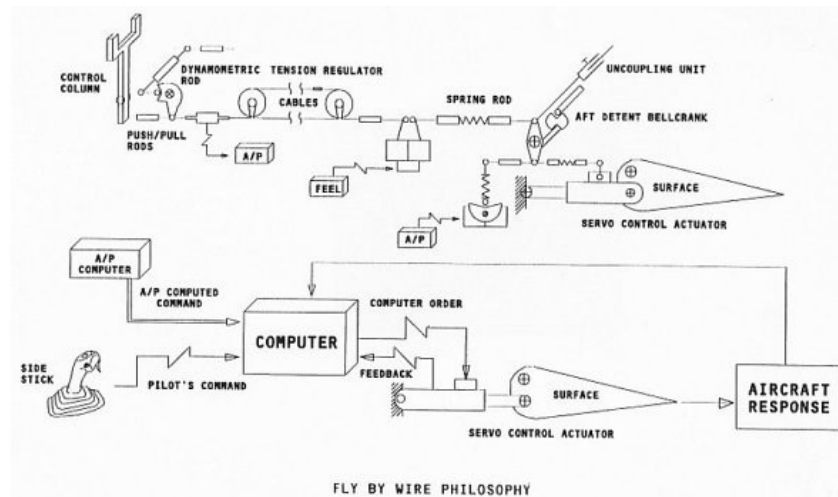
FIGURE 3-13 CONVENTIONAL VS FBW ARCHITECTURE

The FBW system in civil aircrafts was introduced by Airbus on the A320 family and the main advantages are weight reduction, easier maintenance, flight envelope protection, augmented stability, reduction of fatigue stresses on structures due to the input command processing by the FCS.
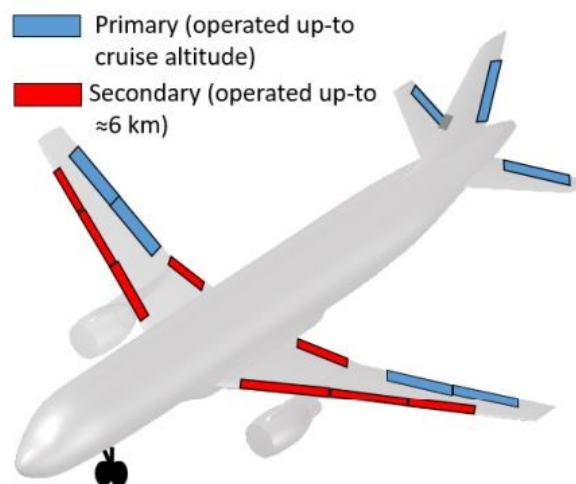

FIGURE 3-14 MAIN FLIGHT CONTROL SURFACES IN A TYPICAL MID-SIZED AIRCRAFT

In the next lines will be explained the functions of the primary flight control surfaces in a conventional configuration:

- **Ailerons**: Ailerons control roll about the longitudinal axis. The ailerons are attached to the outboard trailing edge of each wing and move in the opposite direction from each other. Moving the control wheel, or control stick, to the right causes the right aileron to deflect upward and the left aileron to deflect

downward. The movement of the surface increase or decrease the lift in one of the two wings for control the aircraft roll moment.

- **Elevators**: The elevator controls pitch about the lateral axis. The up-elevator position decreases the camber of the elevator and creates a downward aerodynamic force, which is greater than the normal tail-down force that exists in straight-and level flight. The overall effect causes the tail of the aircraft to move down and the nose to pitch up.

- **Rudder**: The rudder controls movement of the aircraft about its vertical axis. This motion is called yaw. When the rudder is deflected into the airflow, a horizontal force is exerted in the opposite direction. Rudder effectiveness increases with speed; therefore, large deflections at low speeds and small deflections at high speeds may be required to provide the desired reaction.

There are also different configurations from the conventional one:

- **V-Tail**: The V-tail design utilizes two slanted tail surfaces to perform the same functions as the surfaces of a conventional elevator and rudder configuration. The fixed surfaces act as both horizontal and vertical stabilizers. The movable surfaces, which are usually called ruddervators, are connected through a special linkage that allows the control wheel to move both surfaces simultaneously. The V-tail design is more susceptible to Dutch roll tendencies than a conventional tail, and total reduction in drag is minimal.

- **Canard**: The canard design utilizes the concept of two lifting surfaces. The canard functions as a horizontal stabilizer located in front of the main wings. The canard creates lift and holds the nose up. A benefit obtainable from a control-canard is the correction of pitch-up during a wingtip stall. This solution is mainly used for military aircraft, which require high control.

- **Elevons**: The elevons implements both the characteristics of elevators and ailerons. When these surfaces are moved simultaneously in the same direction they control the pitch moment, otherwise if operated in different directions they control the roll moment.

- **Flaperons**: This type of control surface combine aspects of both flaps and ailerons. The flaperon system implements a mixer to combine the two pilot inputs. With no ailerons input command, the surface is positioned like adjacent flaps, but these can move if a roll moment is required. This helps to reduce stall speed and improves low speed handling characteristics.

- **Tailerons**: These are aircraft control surfaces combining the effects of ailerons and elevators and they are located on the rear of the aircraft and operated like elevons.

3.3.2 Secondary flight controls

Secondary flight control systems may consist of wing flaps, leading edge devices, spoilers, and trim systems. The main purpose of these surfaces is to improve the performance of the aircraft in certain phases of flight, such as landing or take-off because the speeds are lower than cruising phase and consequently the lift generated is less.

In the next lines will be explained the functions of the secondary flight control surfaces in a conventional configuration:
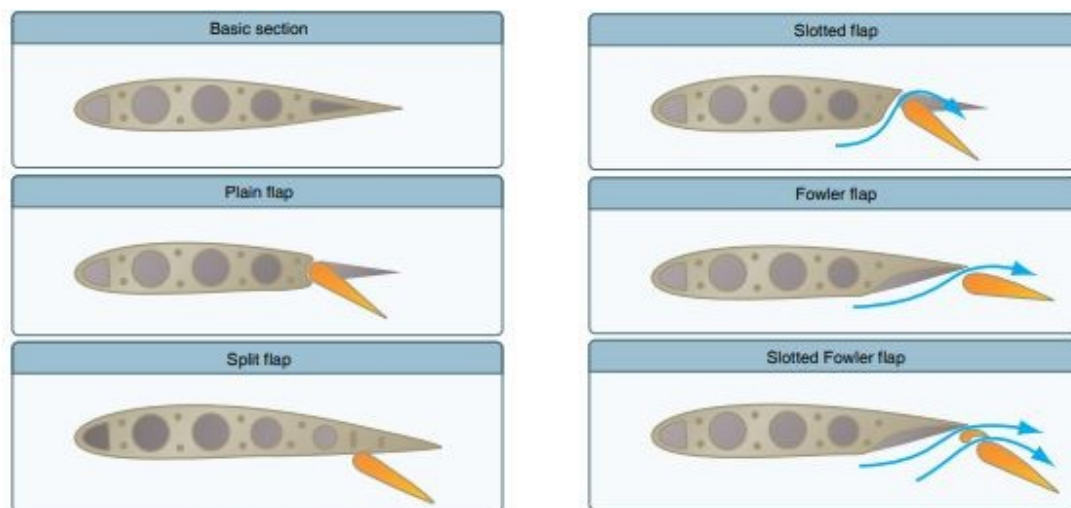

FIGURE 3-15 FLAPS TYPICAL CONFIGURATIONS

- **Flaps**: Flaps are the high-lift devices used on aircraft. These surfaces increase both lift and induced drag for any given angle of attack. Flaps allow a compromise between high cruising speed and low landing speed because they may be extended when needed and retracted into the wing's structure when not needed. There are four common types of flaps: plain, split, slotted, and Fowler flaps.

- **Slats**: Along with the flaps, the slats are high lift devices located on the leading edge of the wings. Their purpose is to increase lift during low-speed operations such as take-off, initial climb, approach, and landing. They accomplish this by increasing both the surface area and the camber of the wing by deploying outwards and drooping downwards from the leading edge.
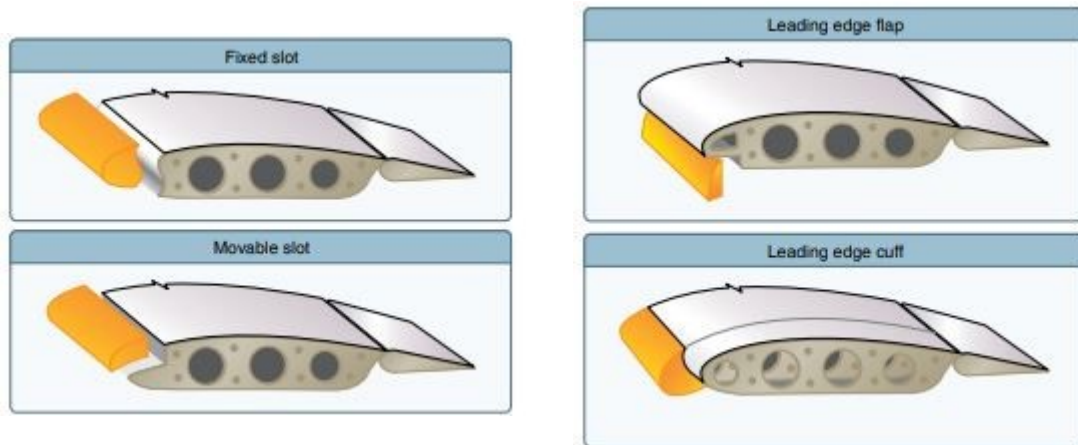
FIGURE 3-16 SLATS TYPICAL CONFIGURATIONS

- **Spoilers:** Spoilers can be used to slow an aircraft, or to make an aircraft descend, if they are deployed on both wings. Spoilers can also be used to generate a rolling motion for an aircraft, when operated in one of the two wings because they increase the Drag, and decrease the Lift.

FIGURE 3-17 SPOILERS DEPLOYMENT

4 Electric drives

Electric drives are the future for the actuation system, but their application is limited due to fault aspects. As previously introduced, there are hybrid actuators that make use of both electric power and hydraulic power, introduced on the Airbus A380, such as EHA and EBHA actuators.
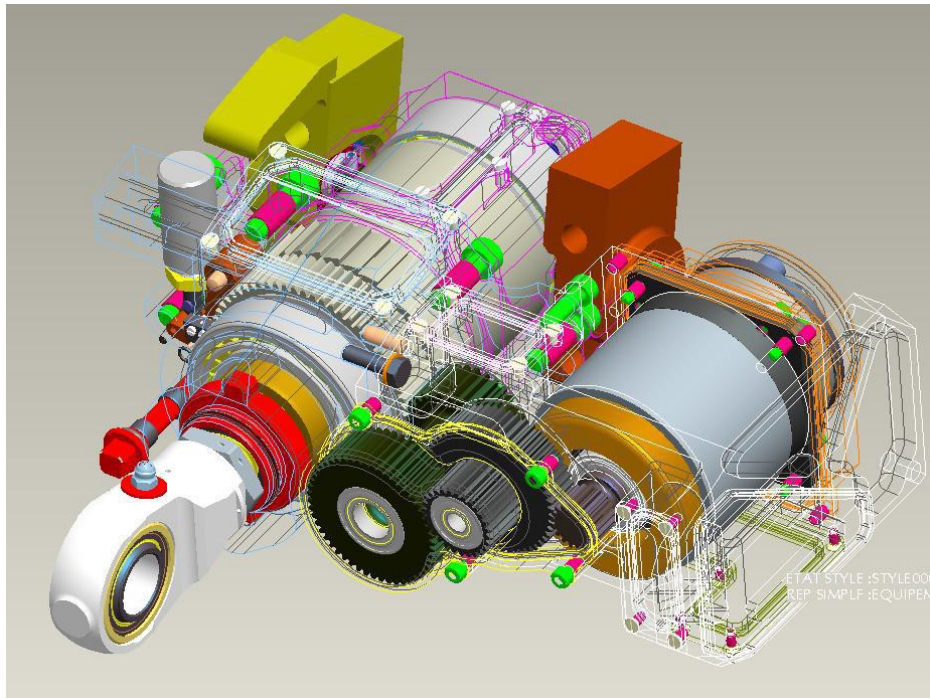

FIGURE 4-1 ELECTRIC DRIVE

Generally, an electric drive is composed by the following elements:

- Electric motor
- Static power converter
- Controller
- Mechanical transmissions
- Actuated element (Load)

The main advantage of the electric powered actuators is the lower weight and the lower costs than the hydraulic powered one because electricity can be transported by light wires, preferring a More Electric design concept.
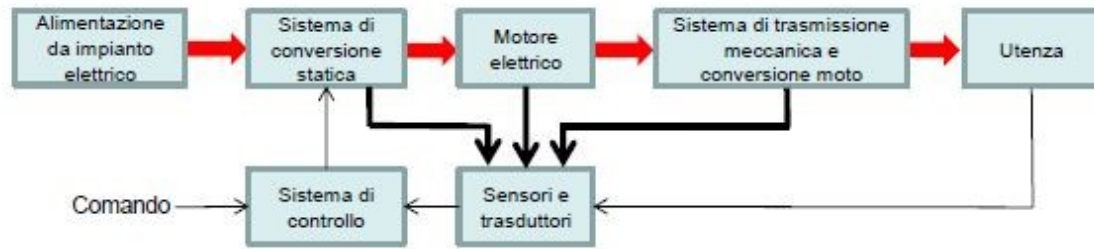
FIGURE 4-2 ELECTRIC DRIVE ARCHITECTURE

The scheme in Fig 4-2 describes an electric drive with three main lines, the high-level power system, from which comes the power for the actuation, the low-level power system, concerning the sensor and transducer system and the signal line for the commutation control. The main purpose of the control system is to modulate the voltages and frequencies inputs to the electric motor.

4.1 Operation of an electric motor

A classic DC electric motor consists in an external fixed part, the stator, and an internal rotating part, the rotor.
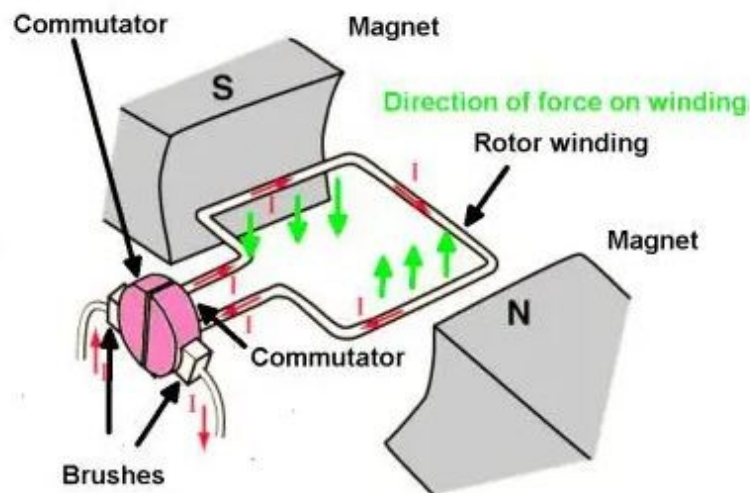

FIGURE 4-3 DC MOTOR OPERATION

The operating principle of this electric motor type is based on Lorentz force, because when electric current passes through a coil in a magnetic field, the magnetic force produces a torque which turns the rotor winding. For high torques it is preferred to have higher magnetic fields or high currents in the coil compared to the increase in the length of the conductor.

The main disadvantage of this solution is the commutator, which it is used to reverse the current direction at each half turn. In aerospace it is not permitted because this commutator composed by sliding contact could lead to safety issues, related to the consumption of these, that creates reliability problems, and any sparks.
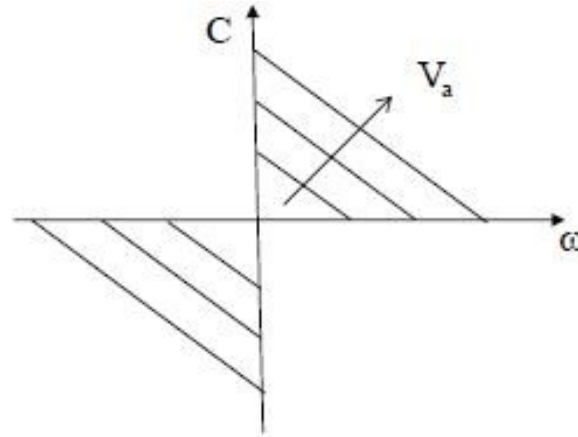

FIGURE 4-4 TYPICAL TORQUE-ANGULAR VELOCITY CURVES AS A FUNCTION OF VOLTAGE

Analysing the torque as a function of angular velocity, due to the Back-electromotive force, linked to the angular velocity, there is a linearity because a coil that rotates within a magnetic field generates a voltage that opposes the passage of current.
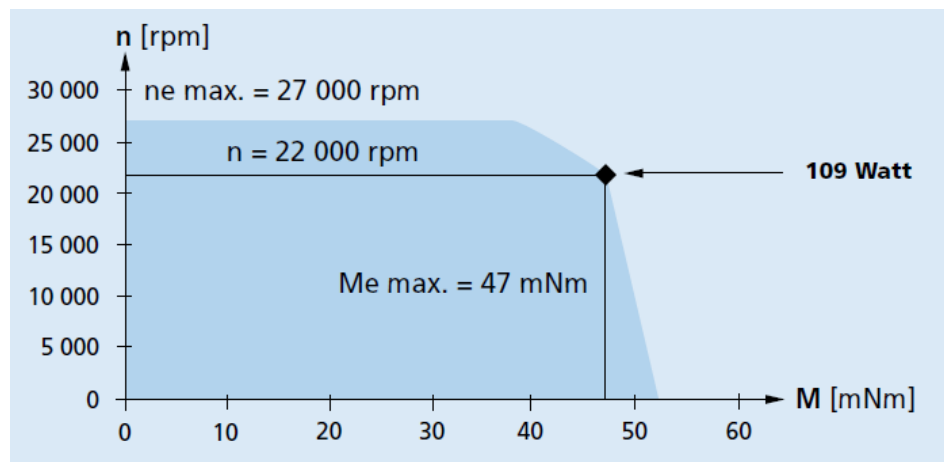

FIGURE 4-5 REAL TORQUE-ANGULAR VELOCITY CURVE

In the real case there are torque and angular speed limitations because at low angular speeds there is a lower limitation of current in the coils, due to lower BEMF levels, that could lead to electric motor damages, and at high angular speed there are mechanical limitation, due to bearings and sliding contacts. Another limitation concerns the maximum power delivered by the electric motor, as a function of the torque and the angular speed.

4.2 BLDC electric motor

The Brushless DC motor is the best solution for aerospace application because it solves the DC conventional electric motor issues due to brushed commutator. There are also called Permanent magnet synchronous motor because the magnetic field and the angular velocity have the same frequency.
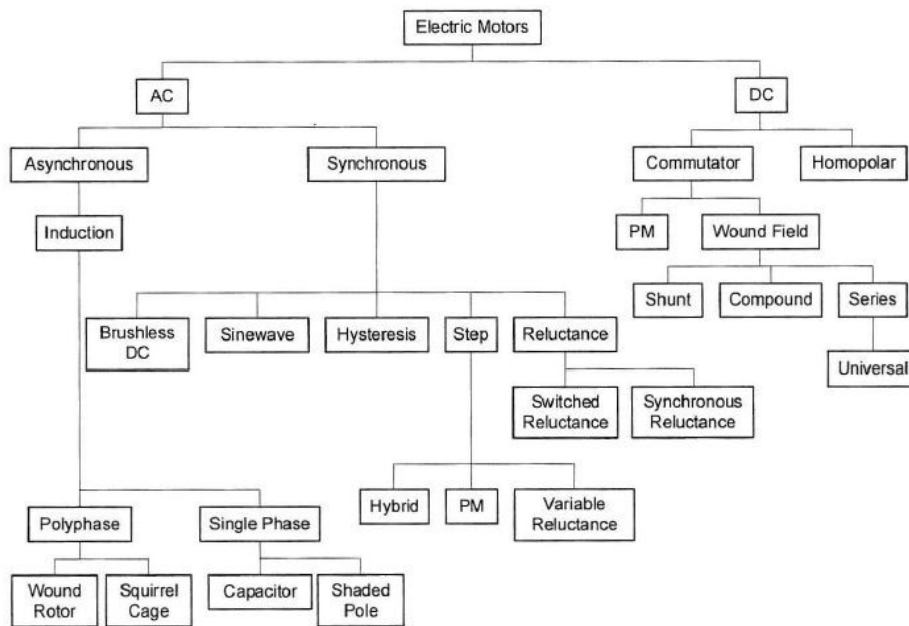

FIGURE 4-6 ELECTRIC MOTORS FAMILY

The main advantages of this type of electric motor are the high overall efficiency (no voltage drop across brushes), a long operating life, because there are no easily worn components such as brushes, a noiseless operation, reducing the electromagnetic interferences, and higher speed ranges. These are preferred for aerospace applications also because the ratio between the delivered torque and the size of the motor is higher than another one.
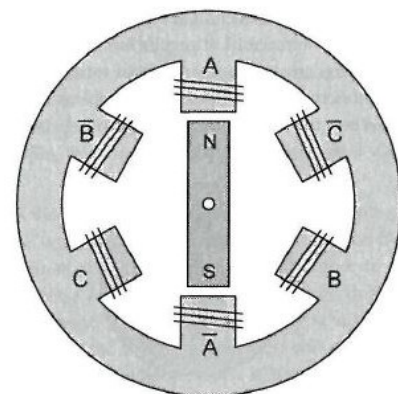

FIGURE 4-7 PERMANENT MAGNET ELECTRIC MOTOR

In this case the permanent magnet is attracted by the opposite electromagnet pole which create the formally called alignment torque. The generic case involves the use of several stator slots for many reasons, to turn continuously the rotor and to avoid torque fluctuations due to the distance between coils. These are also called phase windings.

The previously introduced conventional DC motor uses mechanical commutator for the current commutation in the rotor coils. The BLDC electric motor has a permanent magnet as a rotor and stator slot, in addiction of current carrying coils used as electromagnets, which are electronically commutated with a solid-state controller that switches the power supply of the stator windings.

The electronic speed control (ESC) must know the rotor angular position to switch motor phases, and then adjust the motor speed. There two different system architecture, sensored or sensorless motor.
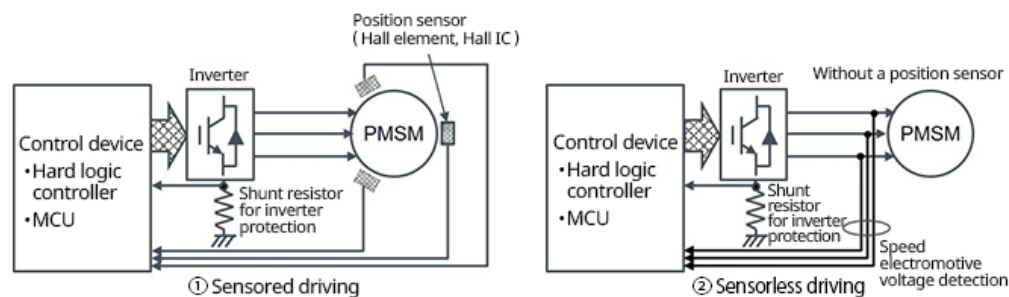
FIGURE 4-8 BASIC CONFIGURATION OF MOTOR DRIVING SYSTEM

In the first case the electric motor is equipped with sensors that in the most common case are Hall effect sensors. r the rotor magnetic poles pass near the Hall sensors, they give a high or low signal, indicating the N or S pole is passing near the sensors. Based on the combination of these three Hall sensor signals, the exact sequence of commutation can be determined. With these the electric motor can accelerate right from zero RPM, in order to produce more torque at low speeds than the other solution. Sensored motors also are able to allow safe operation of the motor by monitoring its condition.
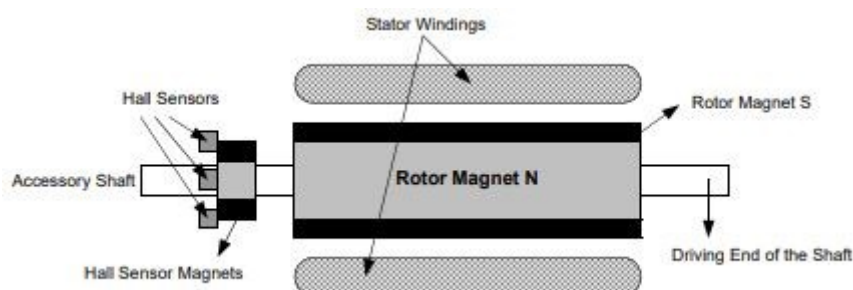
FIGURE 4-9 HALL SENSORS ARCHITECTURE

This solution is the most used in the aerospace due to the greater precision of control, although the reliability is less because the sensors can fail.

The sensorless motor high speed performance is much higher than low speeds because ESC can determine rotor position from the Back-EFM, as the rotor is in motion.

The main advantages of this electric motor type are the lower weight than the sensored one, it is less complicated, and it increase his reliability.

A further classification of BLDC electric motors involves the shape of BEMF, trapezoidal or sinusoidal. These two categories are created through the type of magnets and windings of the electric motor.
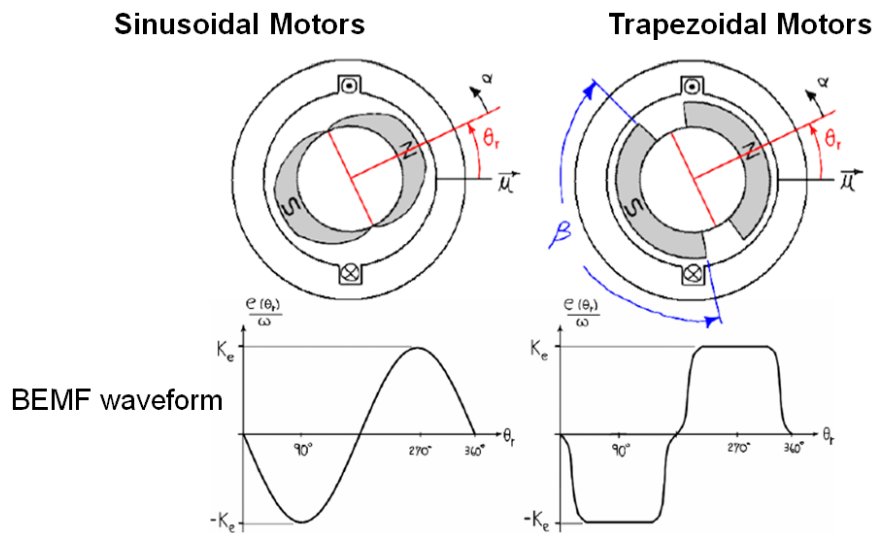

FIGURE 4-10 SINUSOIDAL VS TRAPEZOIDAL MOTOR ARCHITECTURE

As their names indicates the trapezoidal motor gives a BEMF with trapezoidal shape, and the same for sinusoidal motors.

In addition to the back EMF, the phase current also has trapezoidal and sinusoidal variations in the respective types of motor. This makes the torque output by a sinusoidal motor smoother than that of a trapezoidal motor, with lower noise and vibrations, in addition to less switching complexity, but the trapezoidal motor has higher power density and torque peak. However, this comes with an extra cost, as the sinusoidal motors take extra winding interconnections because of their distribution on the stator periphery, thereby increasing the copper intake by the stator windings.

4.2.1 Stator Architecture

The stator of the BLDC motor consists of laminated steel elements used to mitigate the effects of eddy currents. In this block are then obtained the slots for the phase windings, which generate the rotating magnetic field.

Eddy currents are induced currents caused by the change in the magnetic field, and it is an effect that can be had in BLDC because the rotor consist in a permanent magnet. From faraday's induction law the rate of change of the magnetic flux generates an electromotive force, in this case in the stator, which induces a flow of electric current. These currents generate resistive losses that transform the energy into heat by Joule effect, which reduces efficiency of stator iron core.

In electric motor these eddy currents generate a magnetic field that is opposed to the magnetic field generated by the phase windings. This effect is minimized by selecting a different type of material for the stator, which have low electrical conductivity, or by using a series of sheets of steel, insulated each other. This splits the core in many individual magnetic circuits and restricts the flow of the eddy currents through it.
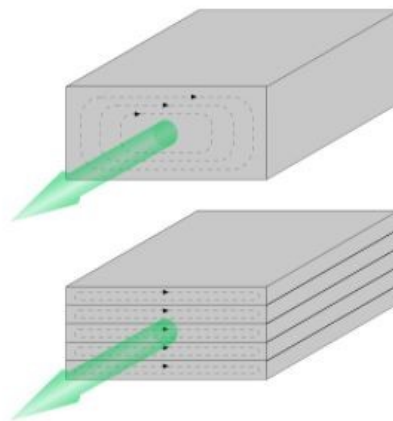
FIGURE 4-11 CORE LAMINATION

In the most common cases the BLDC have three stator windings connected each other with a star architecture. In this case these coils generate the magnetic field only when there are powered, which will attract or repel the permanent magnet. In this case the phase voltage is equal to $\frac{1}{\sqrt{3}}$ of line voltage (Fig 4-12).
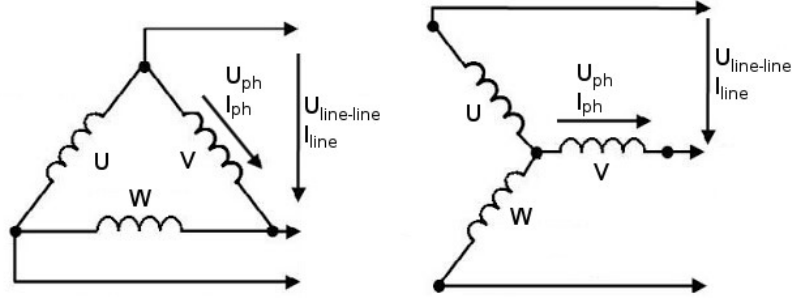
FIGURE 4-12 WINDINGS DELTA CONNECTION [LEFT] VS STAR CONNECTION [RIGHT]

A second configuration involves the use of delta architecture of the phases and in this case the phase voltage is equal to the line voltage. This implies higher currents in the windings and higher torque than the same motor with a star architecture. The main disadvantage of this architecture is the commutation sequence, which is different than the previous configuration, in addition to the fact that the phases are always fed.

There are different solutions for winding layouts, the nonoverlapping scheme, or the overlapped one, as seen in the figure below.
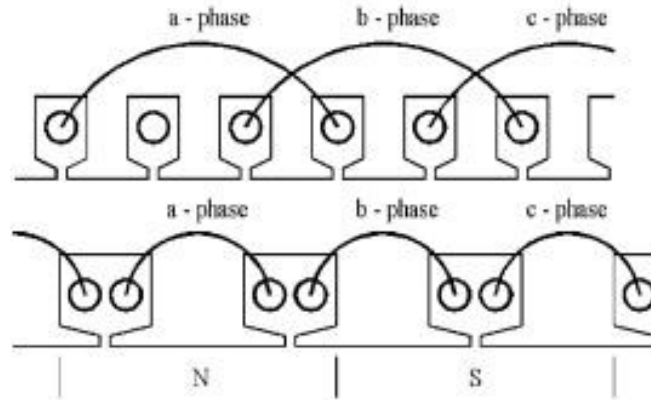
FIGURE 4-13 OVERLAPPING LAYOUT [TOP] VS NON-OVERLAPPING LAYOUT [BOTTOM]

In the first case the main advantage is the short length of the winding, resulting in lower copper losses than the overlapping scheme, but to make an optimal evaluation of the two schemes it is necessary to evaluate the relation between the delivered torque and copper losses.

$$\frac{T_{(no)}}{p_{Cu(no)}} \approx \frac{T}{p_{Cu}} \cdot \left(k_{w\,(no)}^{2} \frac{1 + \frac{2.5}{p} \frac{D}{L}}{1 + 1.2 \frac{\pi}{Q} \frac{D}{L}} \right)$$

Where $k^2_{w(no)}$ is the winding factor, related to coil layout and the number of poles per slot (ex. It is equal to one for one slot per pole per phase and no skewing), p is the number of poles, Q is the slots number and $\frac{D}{L}$ is the ratio between the inner stator diameter and his length.

2p	Q	k_p	k_d	k_w	L/D
2	3	0.866	1	0.866	2.50
4	3	0.866	1	0.866	1.25
	6	0.866	1	0.866	1.25
6	9	0.866	1	0.866	0.84
8	6	0.866	1	0.866	0.63
	9	0.985	0.96	0.945	2.32
	12	0.866	1	0.866	0.63
	15	0.743	0.96	0.711	0.007
10	9	0.985	0.96	0.945	1.85
	12	0.966	0.97	0.933	1.43
	15	0.866	1	0.866	0.50
	18	0.766	0.96	0.735	0.04

TABLE 1 WINDING FACTOR WITH POSSIBLE CONFIGURATIONS

Based on this relation, with a small number of poles the nonoverlapping configuration is better than the other if the stator length L is higher than the inner stator diameter. For a high number of poles this configuration is convenient if the stator length is smaller than the inner stator diameter.

4.2.2 Rotor Architecture

The rotor of BLDC electric motor is made of permanent magnet (PM), and it can typically be composed of ferrite or different materials, such as rare earth.

The choice of magnet composition is linked to several parameters, such as the magnetic coercivity, the Curie temperature and the saturation remanence. The first parameter is the material's resistance to demagnetization, the second is the temperature value for which the material lose his permanent magnetic properties, the third parameter is the maximum value of magnetization remaining after a large magnetic field is applied, related to the hysteresis loop.

Ferrite magnet is composed by iron oxide and metallic elements, but unlike other ferromagnetic materials these are not electrically conductive, thus mitigating the effects of eddy currents. These magnets are relatively expensive, but they have the disadvantage of low flux density, and this implies increased geometries and therefore also greater weight than other types.

Aluminium Nickel Cobalt (AlNiCo5) offer the lowest intrinsic coercivity levels and these are an optimal solution for higher temperatures, but the saturation remanence is lower than other materials and this leads to bigger size of the rotor.

Neodymium magnet is an optimal solution for aerospace application in BLDC electric motors because they have a high level of saturation remanence in order to produce higher levels of magnetic even with small geometrical dimension. this kind of magnets are however very expensive due to the material of which they are composed (Rare earth element). The main disadvantage of this magnets is the operative temperature, because at higher values of T they become unstable.

Samarium cobalt magnets are the post option for BLDC electrical motors because they have the highest remanence and energy product levels, and they are stable at higher temperature than Neodymium, and for this they are used in small and powerful electric motors. In this case the main disadvantage is the higher cost due to the extremely rare element of which they are composed.

Property	Reference values of properties	Weak	←	→	Loud
Magnetism	Remaining/Maximum energy produced	Ferrite	Alnico	Samarium-cobalt	Neodymium
Repeated adsorption	Holding power	Alnico	Ferrite	Samarium-cobalt	Neodymium
Hardness	-	Samarium-cobalt	Ferrite	Neodymium	Alnico
Corrosion/rust resistance	-	Neodymium	Alnico	Samarium-cobalt	Ferrite
Thermal stability	Curie Temperature/Maximum Permissible Operating Temperature	Neodymium	Samarium-cobalt	Ferrite	Alnico

TABLE 2 PERMANENT MAGNET MATERIALS CHARACTERISTICS

Another aspect to consider in rotor design is the number of pole pairs. Increasing the number of pairs of poles decreases the distance between them and therefore this implies a greater torque. Increasing the number of pairs of poles decreases the distance between them and therefore this implies a greater torque. The choice of the number of poles is also linked to the angular speed of the motor as this implies a faster phase switching. The relationship between electrical angle and mechanical angle is related to the number of magnet poles on the rotor.

$$\theta_e = \frac{N_m}{2} \theta_m$$

Where θ_e is the electrical angle, θ_m is the mechanical angle and N_m is the number of poles. It is also possible to evaluate the frequency starting from the angular velocity and therefore that relative to the commuting.

$$f_e = \frac{N_m}{120} \cdot RPM$$

The electrical frequency f_e influences the design of the power electronics because if this parameter increases the switching speed of the phases must be higher. If the

electric motor is composed of 4 poles, or 2 pole pairs, there are four electrical cycles per mechanical revolution.

FIGURE 4-14 2 POLE PAIRS ROTOR [LEFT] VS 5 POLE PAIRS [RIGHT]

4.3 Theory of Operation

The BLDC electric motor operation is based on the generation of a rotating magnetic field by the switching of the different phases. The aim is to have the maximum repulsion between the magnetic vector of the permanent magnet and the induced magnetic vector generate from the stator windings.

As already introduced it is possible to implement sensors, such as those with Hall effect, to identify the exact angular position of the rotor and act optimally on the feeding of the windings. The phases are fed by a special electric converter, the inverter.
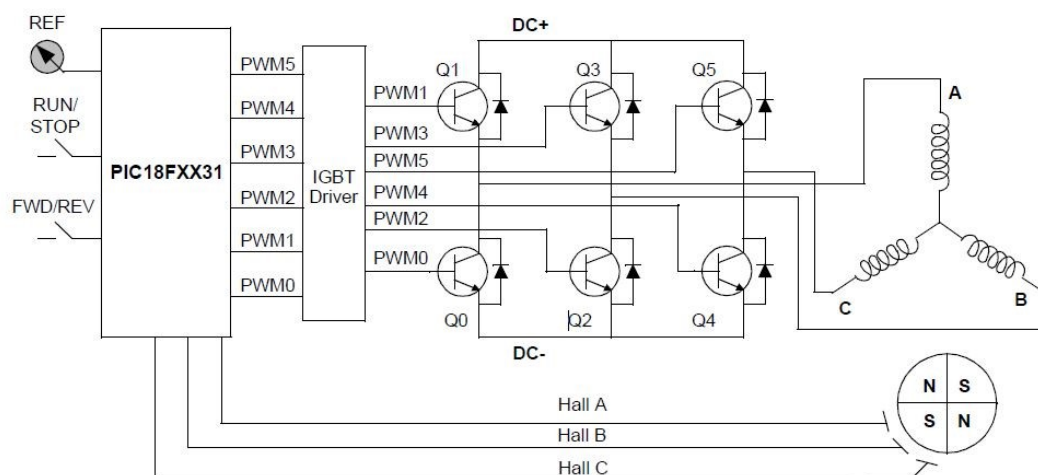
FIGURE 4-15 TYPICAL PERMANENT MAGNET MOTOR ARCHITECTURE

Inside this component are contained transistors, driven by a control module, and diodes used to protect these from any inductive effects of the electric motor.

The transistor is a semiconductor device used to amplify or switch electrical signals and power. This element is composed by a base, a collector, and an emitter. A small current at the base terminal can control a much larger current between the collector and the emitter terminals.

there are different types of transistors, and each has its own operating field but in aerospace Mosfets and Igbt are mainly used because they have a higher control frequency even if they withstand lower voltages and currents

As already introduced transistors are coupled to diodes due to the inductive currents that are generated when opening the circuit, which may damage the transistor itself, for temperature rise due to Joule effect, or create unwanted voltage arcs.
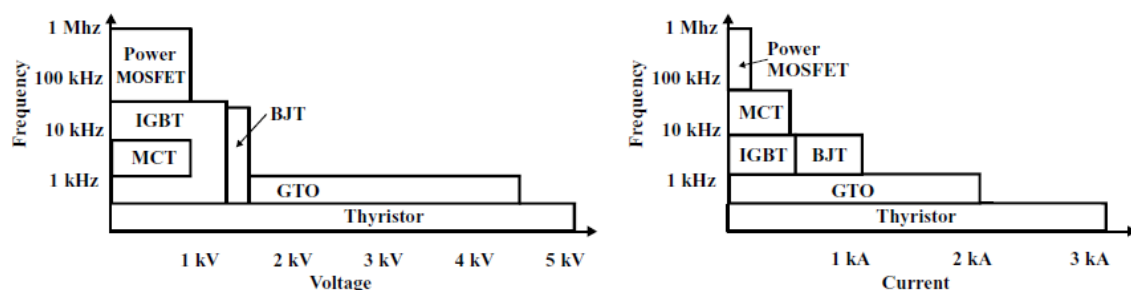

FIGURE 4-16 DIFFERENT TRANSISTORS CHARACTERISTICS

The control of the electric motor drive can be carried out exclusively by varying the motor supply voltage because the signal from the sensors is used for the optimal control of the electric motor, due to have a constant angle between the magnetic vectors. A first technique, analogue type, involves the use of variable resistances due to vary the voltage of the motor, but this implies a high dissipated power and therefore lower efficiency.
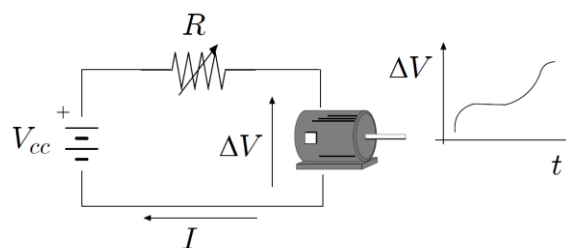

FIGURE 4-17 VARIABLE RESISTANCE MOTOR CONTROL

A more efficient way to regulate the voltage of the phases is to implement a Pulse Width Modulation logic, which is based on breaking the signal into pulses with its duty cycle. If the modulation frequency is high enough, the current is not affected by this impulsive trend also due to the inductive effects of the motor. the output of this modulation is an average power signal value compared to the duty cycle.
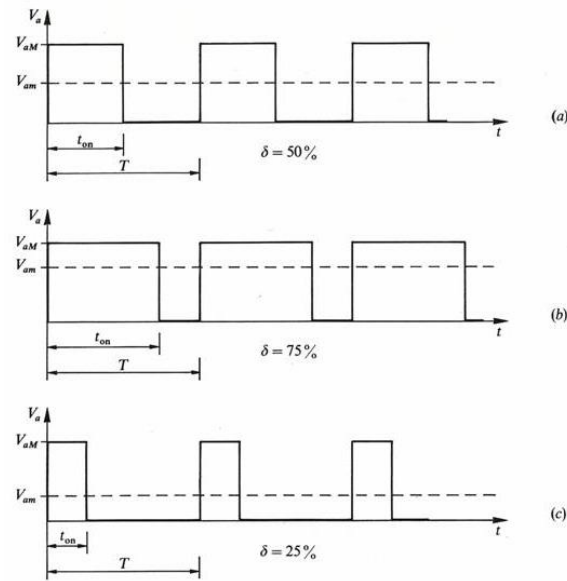
FIGURE 4-18 PWM LOGIC

The sinusoidal motor is based on this modulation logic and allows a very precise phase switching as all the windings are fed simultaneously in order to have a continuous rotation of the magnetic vector generated by the windings.
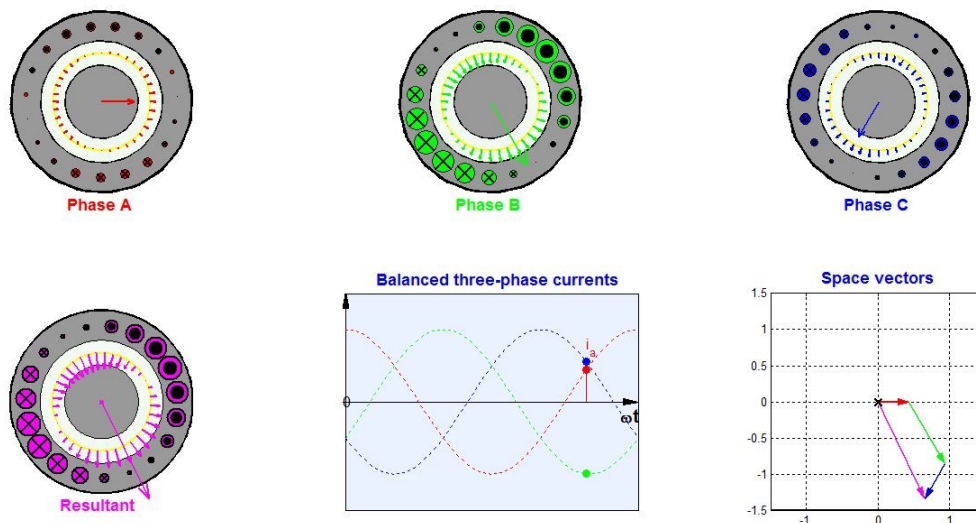
FIGURE 4-19 PM SINUSOIDAL MOTOR OPERATION

In three-phase trapezoidal motors the phases are fed in pairs for a certain mechanical angle, function of the electric motor configuration (poles-windings) and this makes the switching easier than the previous case.

For a three-phase, three slot motor and one pole pair there are 6 commutations in a single mechanical revolution of the rotor, one every 60 degrees.

Table 3 describes the commutation logic for a trapezoidal electric motor over one mechanical revolution of the rotor. The sensor included in the stator core, in this case Hall effect sensors, evaluate the rotor position following a High-Low logic depending on the rotor pole close to it, and then feeding the phases so that the magnetic vectors related to the rotor and stator are in quadrature.

Every 60 degrees, in this particular case, one of Hall sensors change the state due to the rotation of the permanent magnet and therefore the control system of the electric motor switches the phases in order to maintain an optimal condition. In this condition it takes six steps to complete an electrical cycle.

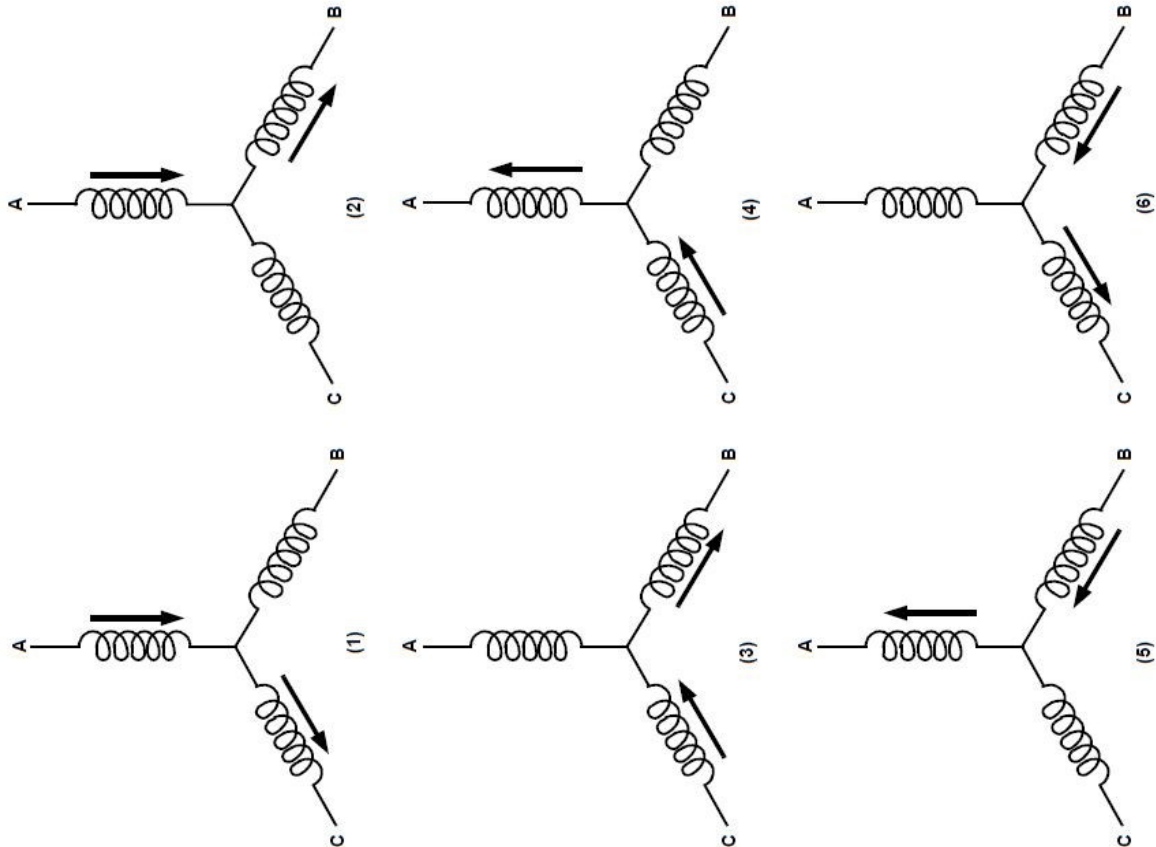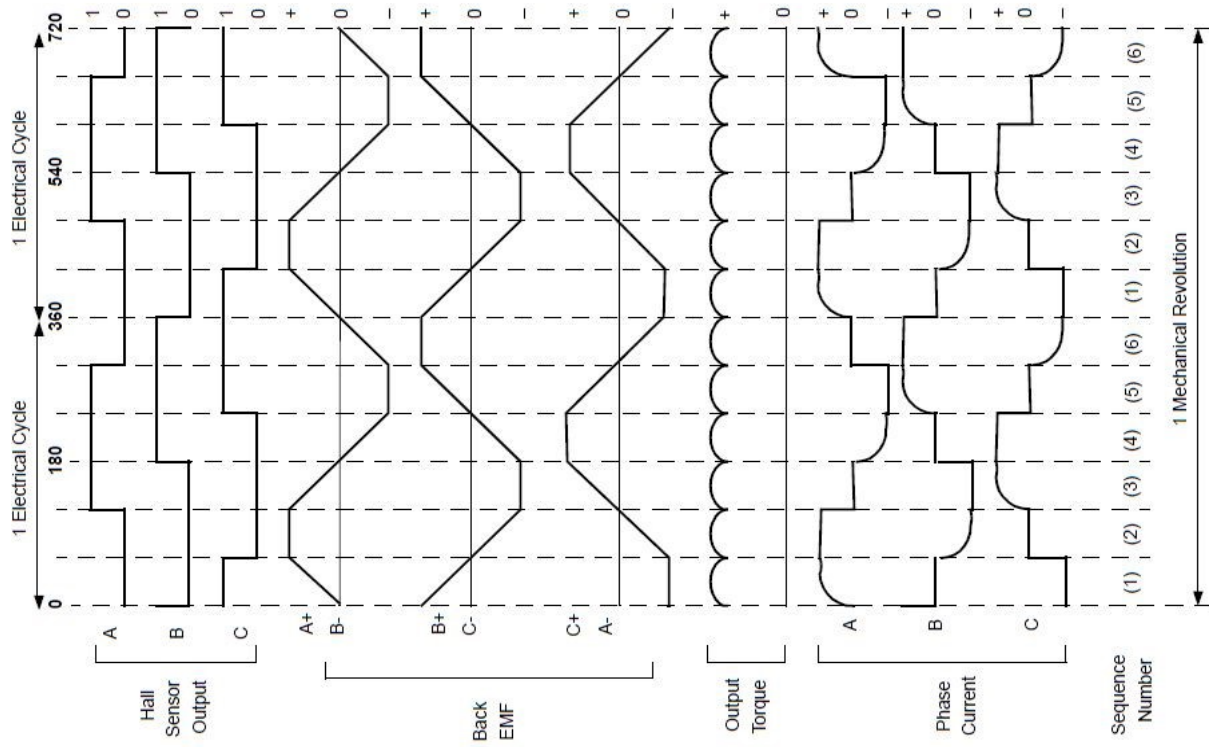| Sequence #	Hall Sensor Input			Active PWMs		Phase Current		
	A	B	C			A	B	C
1	0	0	1	PWM1(Q1)	PWM4(Q4)	DC+	Off	DC-
2	0	0	0	PWM1(Q1)	PWM2(Q2)	DC+	DC-	Off
3	1	0	0	PWM5(Q5)	PWM2(Q2)	Off	DC-	DC+
4	1	1	0	PWM5(Q5)	PWM0(Q0)	DC-	Off	DC+
5	1	1	1	PWM3(Q3)	PWM0(Q0)	DC-	DC+	Off
6	0	1	1	PWM3(Q3)	PWM4(Q4)	Off	DC+	DC-

TABLE 3 COMMUTATION LOGIC BLDC

FIGURE 4-20 TRAPEZOIDAL BLDC 6 STEP OPERATION

The main advantage of this solution, in which the phases are fed in pairs, is relative to the thermal aspect of the electric motor, because for every commutation one of the three phases is not fed, but at the same time the disadvantage is related to the lower torque generated by the motor itself.

Sensorless electric motors can be commutated by monitoring the Back-EMF signal without using any type of sensor. It is possible to evaluate a relationship between the BEMF and the change of hall sensor status. As shown in fig. 4-20, in an ideal case every time the sensor identifies a change in status, as a function of the rotation of the magnet, BEMF crosses from a positive to negative or from negative to positive value. In the real case there will be a delay due to the winding characteristics, but it should be compensated by the motor controller.

As previously introduced, sensorless motors do not work well at low speeds due to the proportionality between angular velocity and BEMF, making it difficult to detect the zero-crossing. the solution adopted in most cases involves the start of the electric motor with an open-loop architecture. When a suitable speed is reached, the loop is closed and the BEMF values are then considered for phases commuting.
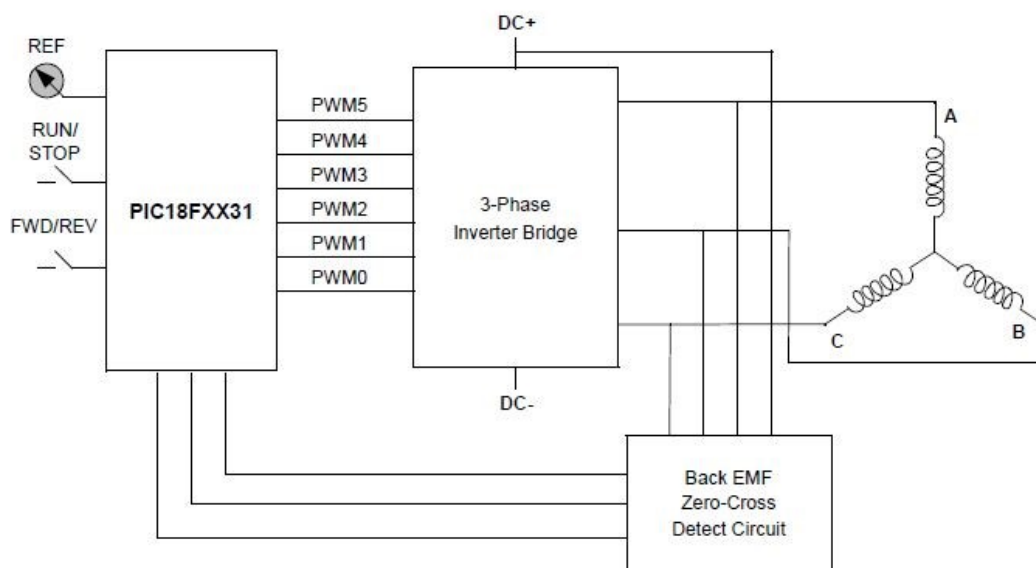
FIGURE 4-21 SENSORLESS BLDC ARCHITECTURE

4.4 Torque and efficiency

Torque in an electric motor is generated by the interaction between the magnetic fields generated by the permanent magnet and the electromagnet composed of the phase windings. In general, it is possible to evaluate the moment of dipole generated by the single phase, when fed, approximating it as a solenoid composed of N coils, powered by a current I and a cross-section of area A.

$$\bar{m} = NiA \, \bar{n}$$

Evaluated the dipole moment generated by the solenoid it is possible to calculate the mechanical moment, and therefore the torque, due to the interaction with the magnetic field generated by the permanent magnet, as a cross product between the magnetic dipole vector and magnetic field.

$$\bar{M} = \bar{m} \times \bar{B}$$

By replacing the previous ratio of the magnetic dipole, it is possible to evaluate the parameters that affect the torque value generated by the electric motor, such as the cross section of the solenoid, the number of the coils of them, the Magnetic field generated by the permanent magnet or the current value flowing in the windings.

The torque reaches his maximum value when these two vectors are perpendicular, when the angle between them is 90 degrees. In trapezoidal electric motors phase switching does not vary for a certain mechanical angle value of the rotor, and this explains the possible torque fluctuations as the angle between these two vectors varies, as seen in fig. 4-20.

It is possible to vary the torque values generated by the electric motor acting on two aspects, some characteristics of the motor itself, as previously mentioned, or on the current amplitude, as the mechanical moment is directly proportional to this parameter, but its increase also implies greater power dissipated by the Joule effect in the windings.

the use of rare earth for the manufacture of permanent magnets improves the performance of electric motors, as at the same volume, these generate a greater magnetic field than ferrite magnets.

The torque generated by the electric motor can be expressed as a function of two parameters, the current I, which can vary, and a torque constant K_T, function of electric motor design.

$$T = K_T I$$

Another aspect to consider in the operation of electric motors is the electromotive force is generated by the relative rotation between stator and rotor. In addition to the induction of the windings, which is opposed to the change in current, the change in magnetic flux linked to the rotation of the rotor generates a Back Electromotive force that opposes the normal operation of the electric motor, in accordance with Faraday's law. Therefore, current and torque are progressively reduced as speed increases because:

$$V = RI - K_{BEMF}\omega$$

The constants K_{BEMF} and K_T have different names but have the same numeric value as the geometry to which the BEMF refers is the same that generates the torque, even if expressed in different units ($\frac{V}{RPM}$ and $\frac{Nm}{A}$).

$$K_{BEMF} = K_T$$
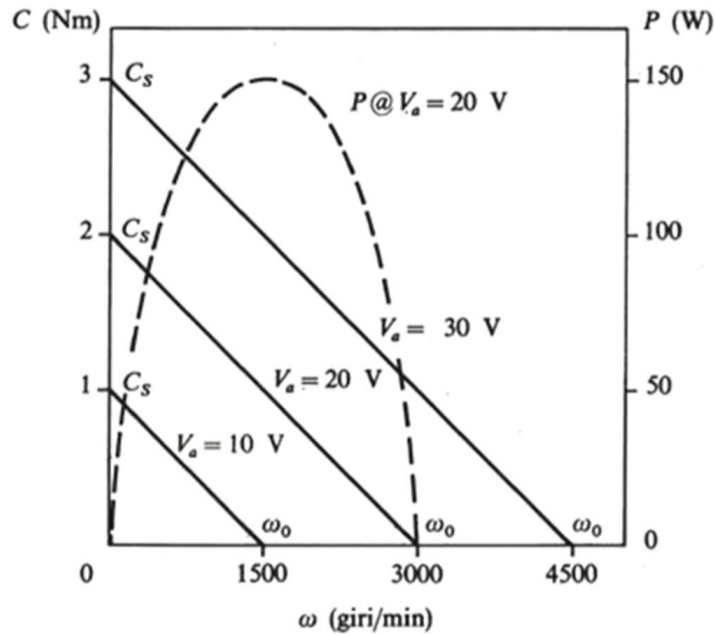
FIGURE 4-22 TYPICAL OUTPUT POWER CURVE

From the previous relationship it is possible to evaluate the power generated by the electric motor as a function of torque and angular speed, as shown in fig. 4-22

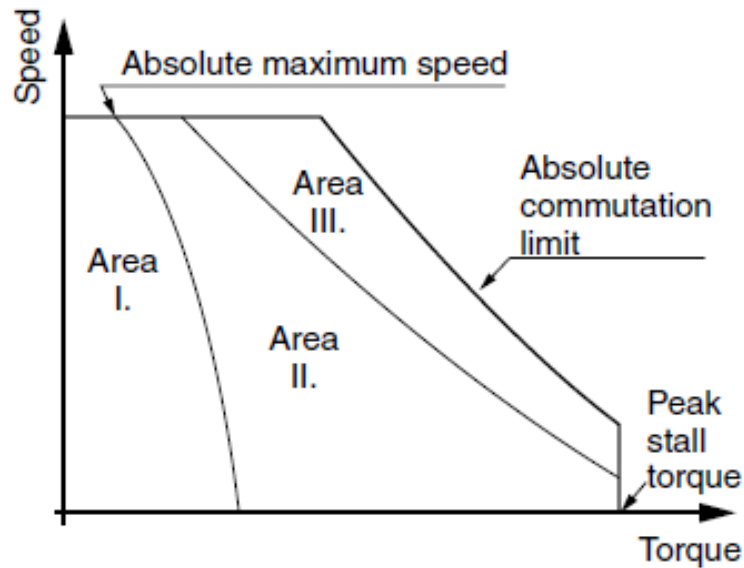$$P_{OUT} = T\omega = \frac{V K_T}{R}\omega - \frac{K_T^2}{R}\omega^2$$

FIGURE 4-23 REAL ELECTRIC MOTOR OPERATION CURVE

Figure 4-23 shows a real case of operation of the electric motor as there are limitations related to different aspects. Area I is the continuous operating area, area II is the intermittent operating area and area III can be used only for accelerating and decelerating. These areas are limited by absolute maximum speed, an absolute commutation limit and the peak stall torque. The speed and the torque (current) control loops must consider these limitations of the DC servo motor. The torque limitation is also linked to the resulting high current values in the windings, which could break the insulation layers, or high temperatures that could damage the electric motor.

4.5 PMSM Motor Control

4.5.1 Speed vs Torque control

In a speed controller, the parameter controlled by the system is the speed of the electric motor. By implementing in the system sensors that identify the speed of the motor shaft, it is possible to monitor and act directly on this parameter, used as a feedback loop.

To vary the speed of the shaft, the voltage of the stator phases is increased or decreased, and therefore indirectly the current flowing in them, which influences the torque generated by the motor.

As shown in previous paragraphs, a more efficient way to control the electric motor operation requires the implementation of Pulse width modulation (PWM) model, which applies high frequency pulse signal with a variable duty cycle.

To control the voltage of the phases, the duty cycle of the PWM is directly controlled, thus varying the average signal value.

A Speed control model can control the motor speed in either directions, clockwise and anti-clockwise, by applying a positive or negative voltages, as a function of the error between this parameter and the required speed value.
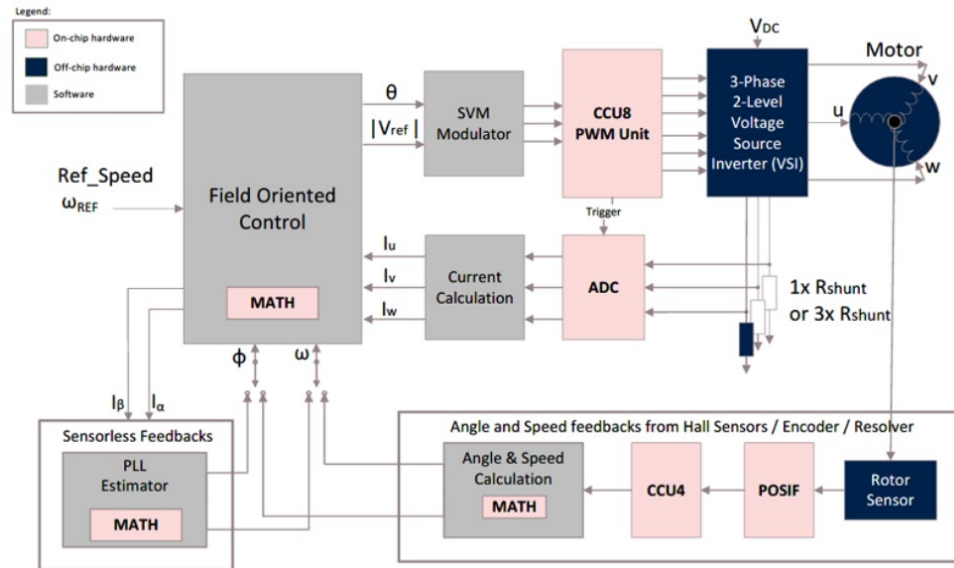
Some applications do not require speed control, in order to follow a desired speed, but torque control, implementing a system architecture that gives a constant torque value as output, even if the system is subject to external loads.

The torque generated by the electric motor depends on the distribution of magnetic flux between windings and permanent magnet, but a detailed study would require the implementation of very complex finite element models (FEM). A simplification is to consider the torque proportional to the current flowing in the windings, function of the torque constant k_T.

Evaluating the current, function of the supply voltage of the windings, the total torque value generated by the electric motor is obtained as a function of the contributions of the three phases, and then subsequently compared with the required torque value.

$$T_M = \sqrt{2} \left(\sum k_{T,i-th\ phase} I_i \right)$$

For both cases, the calculated error is given as input to a controller, PID in the most common case, which aims to modify the duty cycle within the PWM controller, changing the average voltage to which the windings are subject, and therefore the current flowing through them.

4.5.2 Protection control system

There are operating conditions of the electric motor that lead to irreversible failures, for this reason it is necessary to implement a motor protection algorithm, which overrides the normal control of the electric motor, in order to preserve it. In the following points are explained some methods of motor protection that can be implemented in the model of the electric motor:

- **Peak Current Limit**: This is the maximum current allowed in transition condition, such as starting the motor from a zero-speed condition. The control system limits the output of the PWM if this threshold is exceeded.

- **Maximum working current**: Unlike the previous point, which refers to transition conditions, this parameter refers to the maximum current value allowed in the normal condition of use.

Implementing protection systems for the two previous cases is a function of the operating conditions, as in the transition phase the motor speed is low, and consequently also the BEMF, which quickly increases the current flowing in the windings, causing overheating, due to Joule effect, the damaging of conductor insulation or the permanent magnet demagnetization if his temperature rises over the Curie Temperature. In the normal operating conditions of the motor, it is necessary to limit the current because also in this case it is necessary to limit possible effects due to the Temperature, or possible fault due to electric circuits damages.

- **Undervoltage Protection**: Undervoltage occurs when the average supply voltage drops below a certain value, typically 90% of the normal condition, for long periods. This implies that the motor must absorb extra current to meet the power requirements, resulting in heating of the windings. This phenomenon is to be considered especially in electric motors powered by accumulators, as they are more subject to voltage drops due to failures of their internal components. This protection system consists in the implementation of a relay that blocks the operation of the motor in case a certain voltage error threshold is exceeded.

- **Resolver fault protection**: It is necessary to implement fault detection systems that identify faults in the resolver, necessary component to assess the position and speed of the shaft of the electric motor. An unidentified failure could lead to incorrect operation of the actuator, and in the worst case even its failure. The detection system involves the implementation of procedures that reveal the presence of a fault and the subsequent reconfiguration of the system in order to maintain the operation of the entire system.

5 Electromechanical actuator model (EMA)

To examine the performance of a system in a given command imposed, it is common practice to make use of different types of models to simplify the problem.

There are two types of models, the physical model, the realization of a model, possibly in scale, to study the response to an imposed input command, or mathematical models, a set of equations that describe the behaviour of the system itself, which depend on its physical characteristics.

The mathematical model is generally divided into subsystems and components as it is easier to model and especially test the individual blocks, subsequently joined to form the complete system. One aspect to consider is the complexity of the system to be modelled. Complex models may contain parameters that are difficult to evaluate, such as modelling friction between contact surfaces, but simple models may not reflect the real behaviour of the system. The choice of a system abstraction level could be a source of error because improper use of the model beyond its field of validity could lead to incorrect evaluations.

The modelling of such a system is usually associated with an iterative process, so that this is evaluated and if necessary redesigned. The use of such models is useful in several respects, such as for economic reasons, as a mathematical modelling is based on software, when the system is still being developed, making the process efficient, or when prognostic methods are used to estimate the operating life of components following inner component failures.
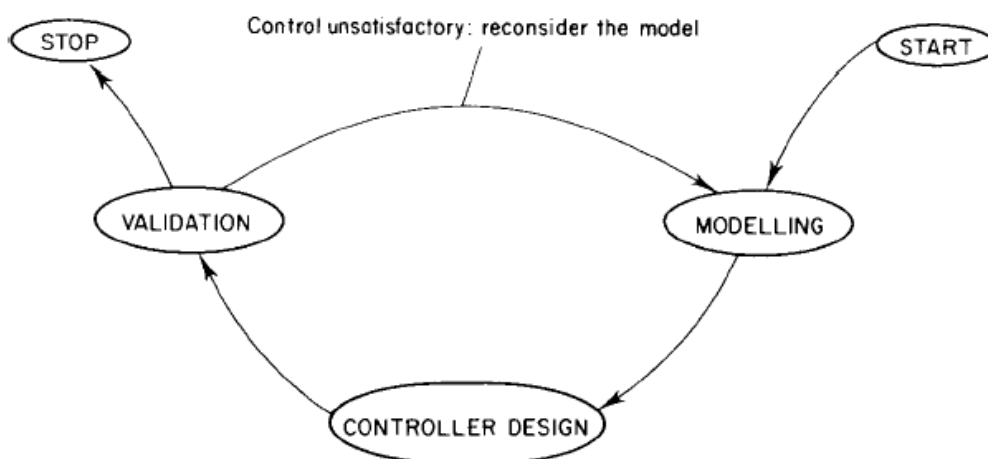
FIGURE 5-1 MATHEMATICAL MODELLING V-SCHEME

The Electromechanical Actuator was modelled following a block diagram, implementing all the component equations included within the actuator. The purpose of this model is to evaluate the behaviour of the system following a command imposed by the user, and then make assessments of the state of the actuator, implementing innovative prognostic methods.

The model is developed using Matlab® software in which inside are contained the toolboxes Simulink and Simscape, where Simulink is a graphical programming environment for modelling, simulating and analysis of dynamic systems, Simscape is a Physical modelling part in Simulink environment. The signal flow in Simulink is unidirectional and in Simscape the signal flow is bi-directional between blocks.

Simscape toolbox is used to evaluate the thermal characteristics of the BLDC electric motor, for the following considerations in prognostic field. In the following paragraphs all the blocks of the EMA model are explained.

5.1 EMA Simulink Model

5.1.1 Overview

The figure below (fig. 5-2) shows the overall schematic of the electromechanical servo motor model. The user sets the values related to the command (Com block) and any external loads (Load block), the response of the actuator is evaluated in the time domain, giving output several characteristic parameters, such as mechanical angle and mechanical angular speed of the electric motor, mechanical angle after the gear box and the equivalent current value from the electric motor, evaluated graphically with the scope block.
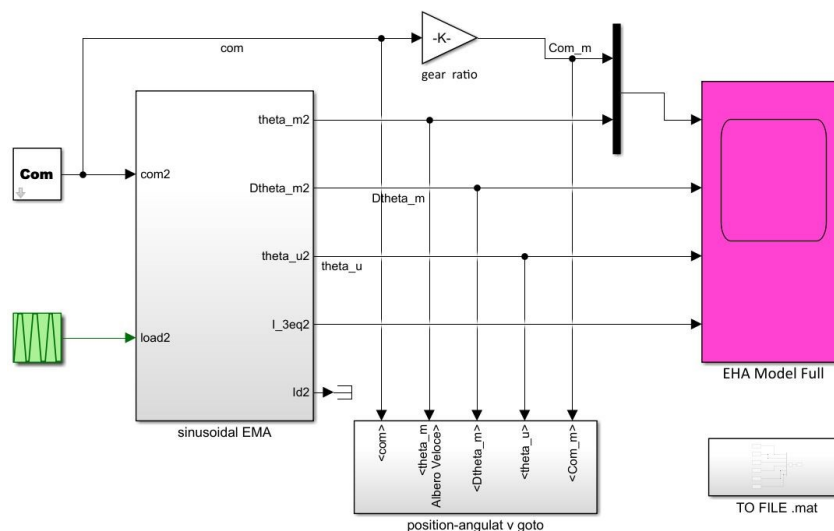
FIGURE 5-2 GENERAL MODEL OVERVIEW

5.1.2 Command block

Within the command block, different types of input signal to the actuator model are included, depending on the type of analysis required by the user. The signal to be selected refers to a given angle value required by the electric motor, and then output to the entire actuator.

Each type of command must be properly set by changing certain characteristic parameters, in addition it is possible to select even more than a single command directly from the custom user interface (Mask).
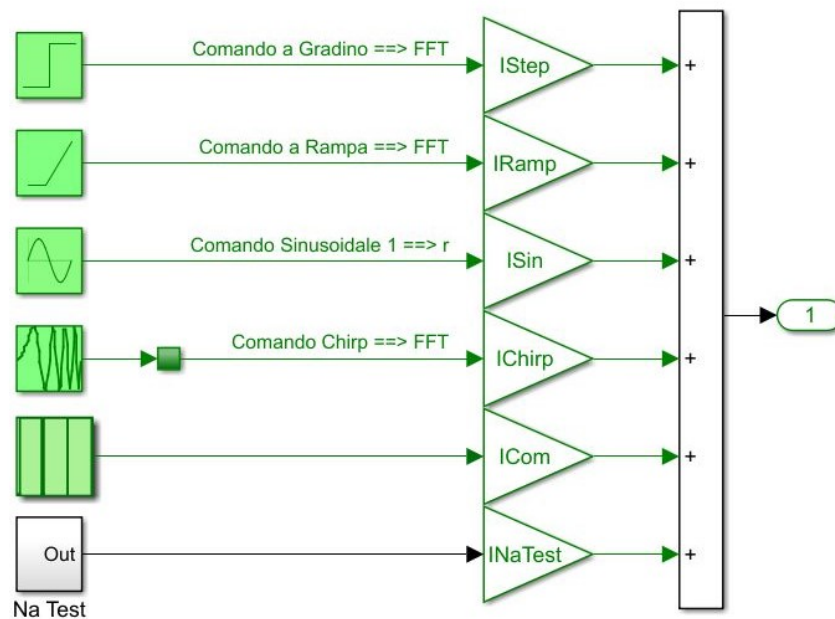

FIGURE 5-3 COMMAND BLOCK

5.1.3 Sinusoidal EMA block

As shown in Fig 5-4, the sinusoidal EMA block includes all the main elements of the actuator model under consideration. This system includes all the part related to the electrical, electronic, mechanical, and thermal subsystems. Go-to blocks are needed to save simulation data, used for later evaluation.

Unlike the figure shown, there is a real connection between the inverter block and the thermal PMSM block, carried out through go-to blocks from the Pulse Width Modulator (PWM) towards the tri-phase H bridge that feeds the phases of the electric motor.

In the following paragraphs will be deepened the subsystem blocks contained in this Thermal SSC model.
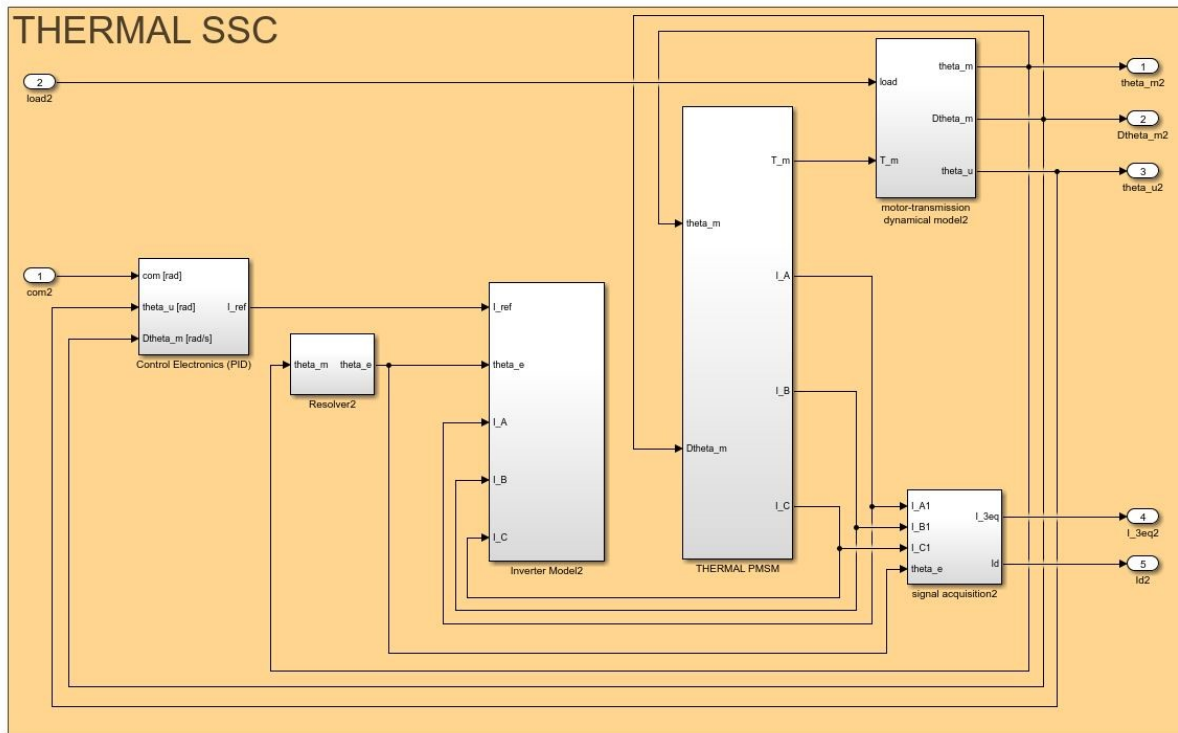
FIGURE 5-4 SINUSOIDAL EMA BLOCK

5.1.4 Control electronics (PID) block

The first subsystem introduced is the Control electronics (PID) block, in which input data are given on the command, the instantaneous position of the user and its angular velocity in order to evaluate the reference current.
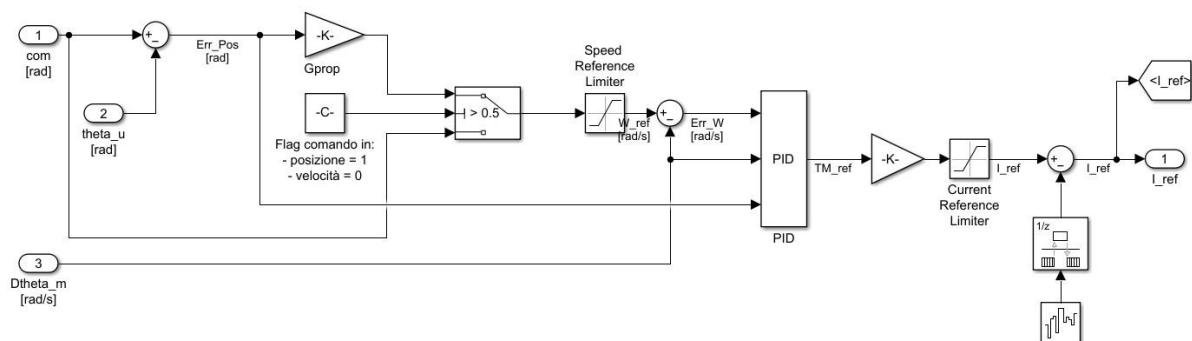
FIGURE 5-5 CONTROL ELECTRONICS (PID) BLOCK

Its purpose is to evaluate the error between controlled position and real position, to evaluate the reference speed by introducing a gain of the controller, and then calculate the speed error subsequently given in input to the real PID controller.

This controller applies a correction based on a combination of three terms, the Proportional gain, which determines the ratio of output response to the speed error

signal, the Integrative term, which sums the error values over time in order to drive steady-state error to zero, and a Derivative term, which his response is proportional to the rate of change of controller input error. The Derivative response is highly sensitive to noise in the process variable signal and if it is noisy the derivative term can make the control system unstable.
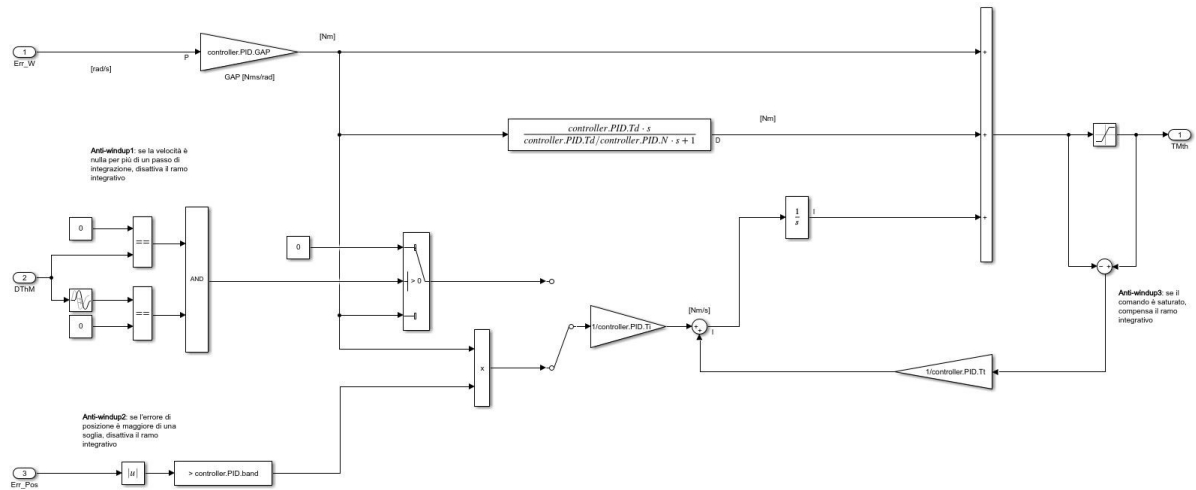
FIGURE 5-6 PID BLOCK

In the figure 5-6 is shown the block of the PID controller, with the three main components. In addition to the three branches (PID), within it are contained terms called anti-windup. The presence of elements such as saturators, also a function of the physical characteristics of the component, implies possible problems during controller operation as the Integral term accumulates a significant error even if the output command remains constant due to saturation itself. To obviate this, terms have been introduced that limit the integrative action only in the case of specific operating conditions (Ex. If the speed error exceeds a certain threshold). When the desired torque is known, the current value is calculated by multiplying this value by the torque constant of the electric motor under consideration.

Some electrical noise is added in order to include small, realistic disturbance to the main signal (block on the right side of Fig 5-5).

5.1.5 Resolver block

To evaluate the current of the three phases, starting from the reference value, it is necessary to calculate the value of the electrical angle, as seen above. To do this a block called resolver is modelled, in which inside is introduced the relationship that binds the value of the angles as a function of the number of poles of the Permanent Magnet inside the rotor.

$$\theta_e = 2\pi(\frac{p\theta_m}{2\pi} - floor\left(\frac{p\theta_m}{2\pi}\right))$$

This relationship is necessary to correlate the angle value of the magnetic vector generated by the phases, depending on the position of the rotor and the number of the poles of this.
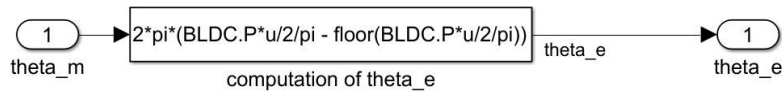

FIGURE 5-7 RESOLVER BLOCK

5.1.6 Inverter block

Inside the Inverter block are contained the necessary components to optimally supply the windings of the electric motor, as shown in Fig. 5-8.
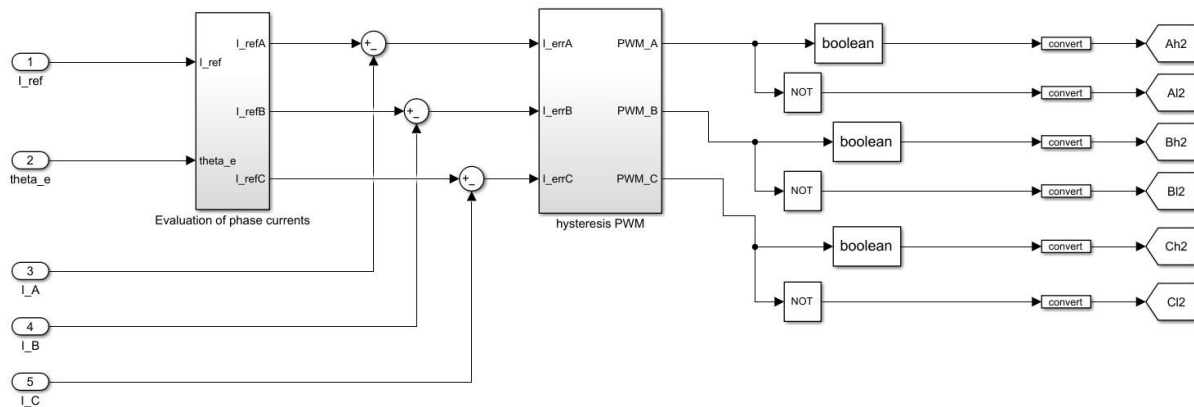

FIGURE 5-8 INVERTER BLOCK

Starting from the left, the first block is related to the evaluation of phase currents, starting from the reference value, output from the controller, and the electric angle value. Inside it there is the Direct-quadrature-zero transformation, which breaks down the currents into three terms, one for phase, according to a reference system attached to the rotor, necessary to have an optimal condition, that is a 90-degree shift between the two magnetic vectors, the rotor and that generated by the windings.
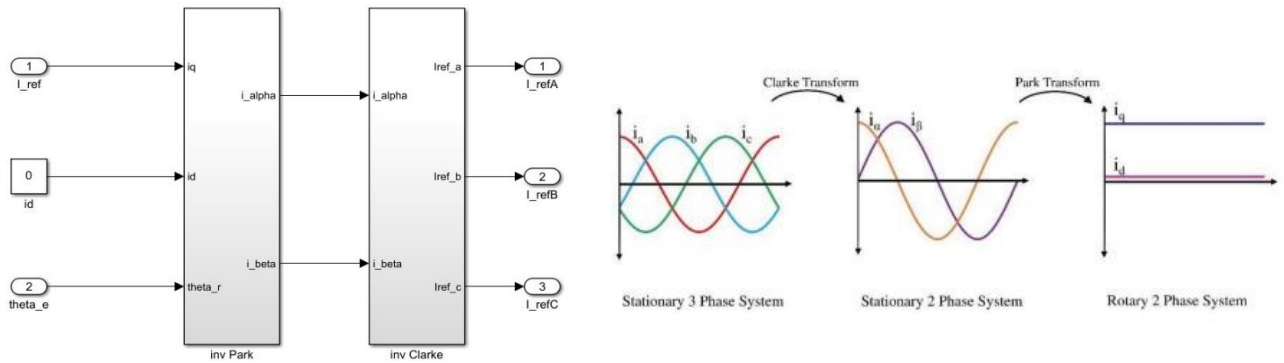
FIGURE 5-9 EVALUATION OF CURRENTS BLOCK

Then these three phase currents are conveyed into a block called Hysteresis PWM, which returns 1 if the input is greater than +hb, that is greater than half of the set dead-band, 0 if it is less than −hb and keeps the previous value until the signal gets inside the dead-band value. The dead-band determines the PWM carrier frequency. For the Theorem of Nyquist-Shannon, this frequency needs to be one order of magnitude bigger than the inverter switching frequency to avoid aliasing problems.
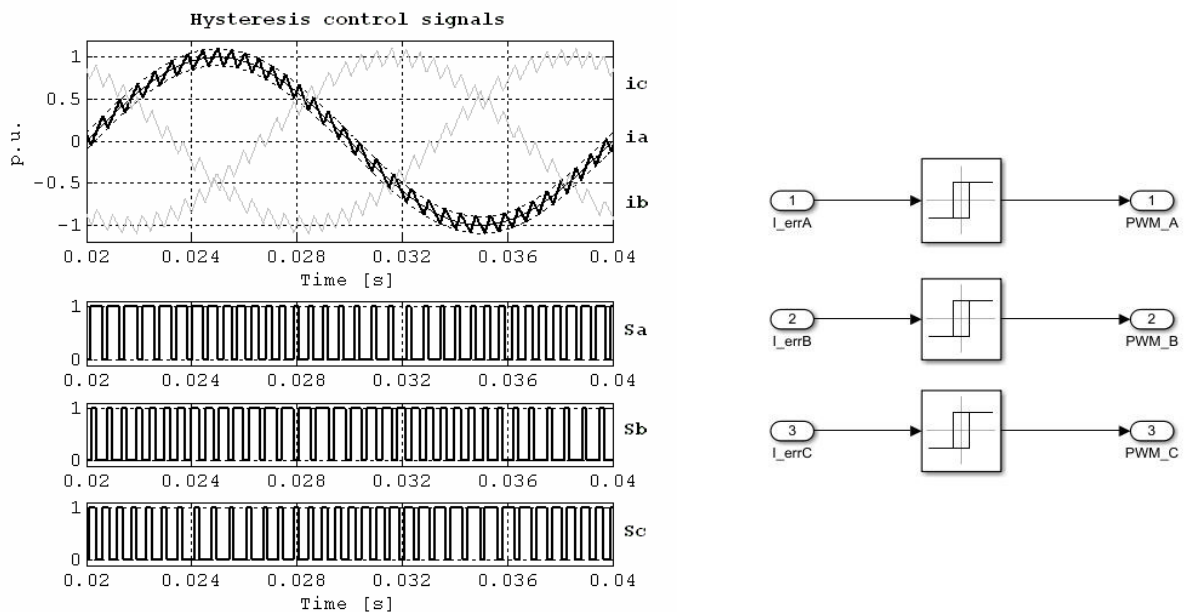
FIGURE 5-10 HYSTERESIS PWM BLOCK

After the Hysteresis PWM block, the signal is transferred to the Thermal PMSM block which inside is also contained the H-bridge that drives the windings, modelled through Simscape electrical elements.

5.1.7 Transmission dynamic model block

The Transmission Dynamic Model subsystem is used to estimate the angular positions of the user and the shaft of the electric motor and its angular velocity, starting from the torque value generated by the electric motor and the external load value.

Electric motor-transmission coupling is evaluated as a second-order system in which viscous effects, due to engine components and any brake system, inertial and non-linearity effects are included. Non-linear effects include the implementation of operating limits (end-stops), friction effects, described by the modern Borello model, an improvement of the simpler Coulomb model, or backlash effects. It can be defined as the maximum distance or angle through which any part of a mechanical system may be moved in one direction without applying appreciable force or motion.
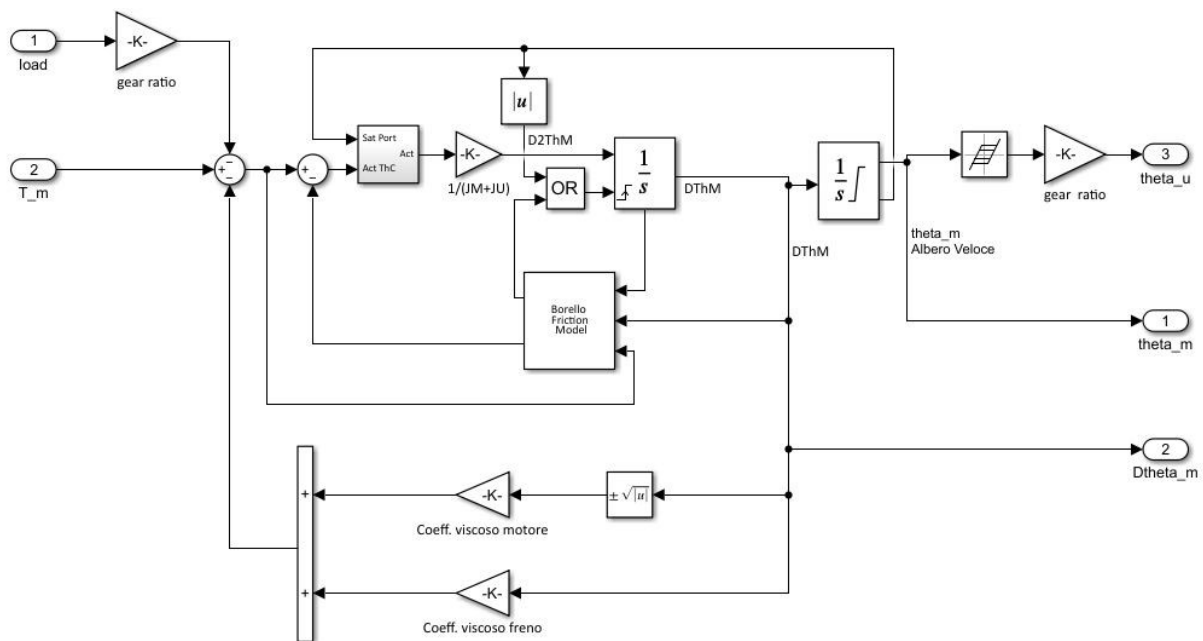
FIGURE 5-11 TRANSMISSION DYNAMIC MODEL BLOCK

5.1.8 Thermal PMSM

The last, but not the least subsystem of the complete model is the Thermal PMSM block, which includes all components evaluating the interaction between stator and rotor.

45

On the left side in Fig 5-12, the first block contained in this subsystem calculates the back-EMF coefficients, which in general can be introduced as:

$$K_{BEMF} = \frac{BEMF}{\omega_m}$$

The change in magnetic flux linked to the rotation of the rotor generates a BEMF that opposes the normal operation of the electric motor, in accordance with Faraday's law, but another aspect to consider is the effect of static eccentricity of the rotor, which leads to variations in these coefficients according to the relationship:

$$k_{BEMF,i} = k_{e,i}(\theta_m) \left\{ 1 + \zeta \cos\left[\theta_m + \frac{2(i-1)}{3}\pi\right] \right\}$$

Where $k_{e,i}$ is the sinusoidal normalized BEMF relative to the i-th phase, $\zeta = \frac{x_0}{y_0}$ is the ratio between the rotor axis from the centre and the nominal air gap, evaluated in the following paragraphs.

Once these coefficients are calculated, they are then multiplied by the angular velocity of the rotor to calculate the BEMF value to be given in input to the electrotechnical components (RL model). Calculated these coefficients are then multiplied by the angular velocity of the electric motor rotor to calculate the value of BEMF to be given in input to electrotechnical components (RL model).
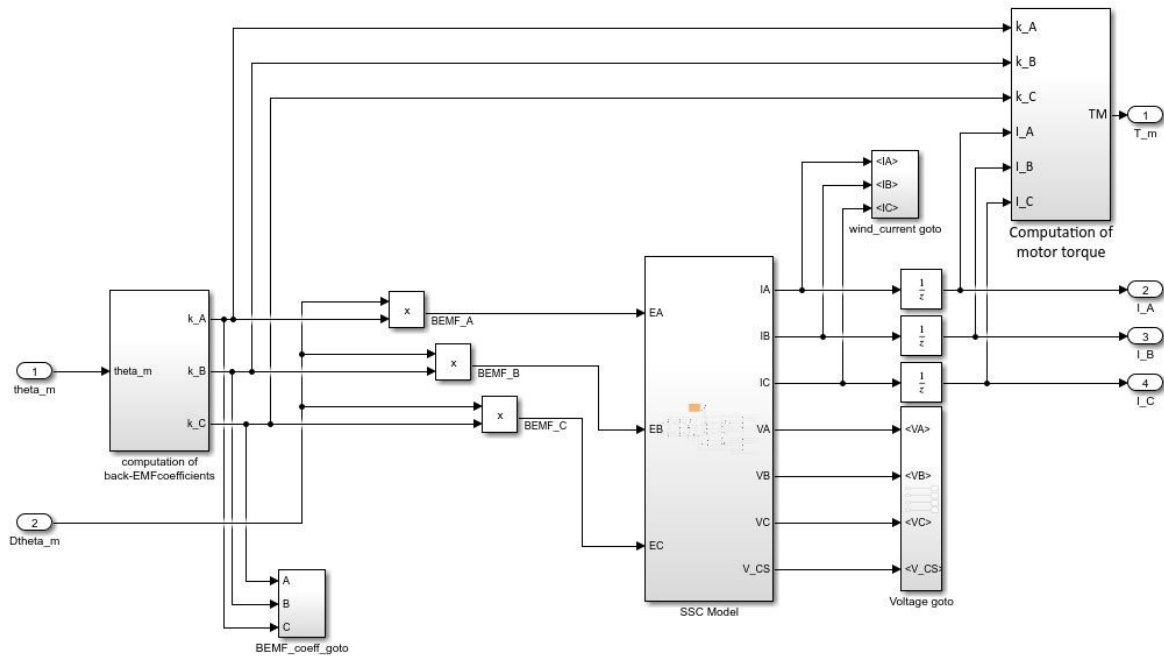
FIGURE 5-12 THERMAL PMSM BLOCK

In the right part of the Fig. 5-12 there is the block relative to the computation of motor torque delivered by the electric motor, obtained as the sum of the effects related to the

three phases, multiplying the BEMF constant by the current of the single winding, the whole multiplied by the root of two to consider the peak value, since the components that generate it refer to the RMS value.
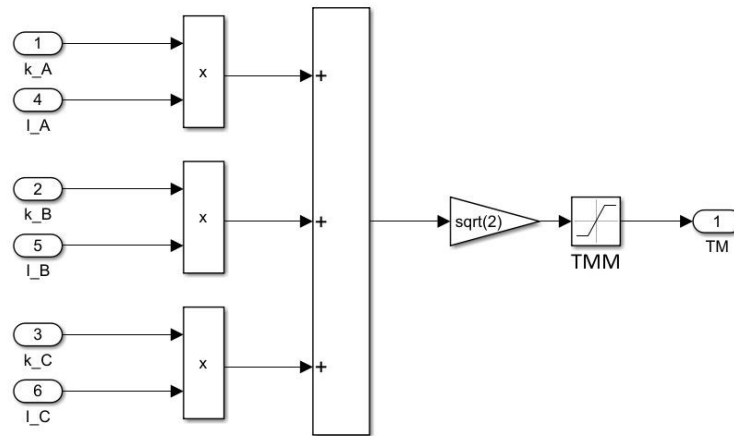

FIGURE 5-13 COMPUTATION OF MOTOR TORQUE BLOCK

Downstream of this computation is implemented a saturation block that considers the maximum torque value that the electric motor can deliver in its operation.

5.1.9 Solid state contactor model

In the last block contained in this subsystem are modelled all the coils contained in the rotor of the electric motor, the H bridge used to commutate each phase, and a thermal model of the complete electric motor, all modelled using Simscape.
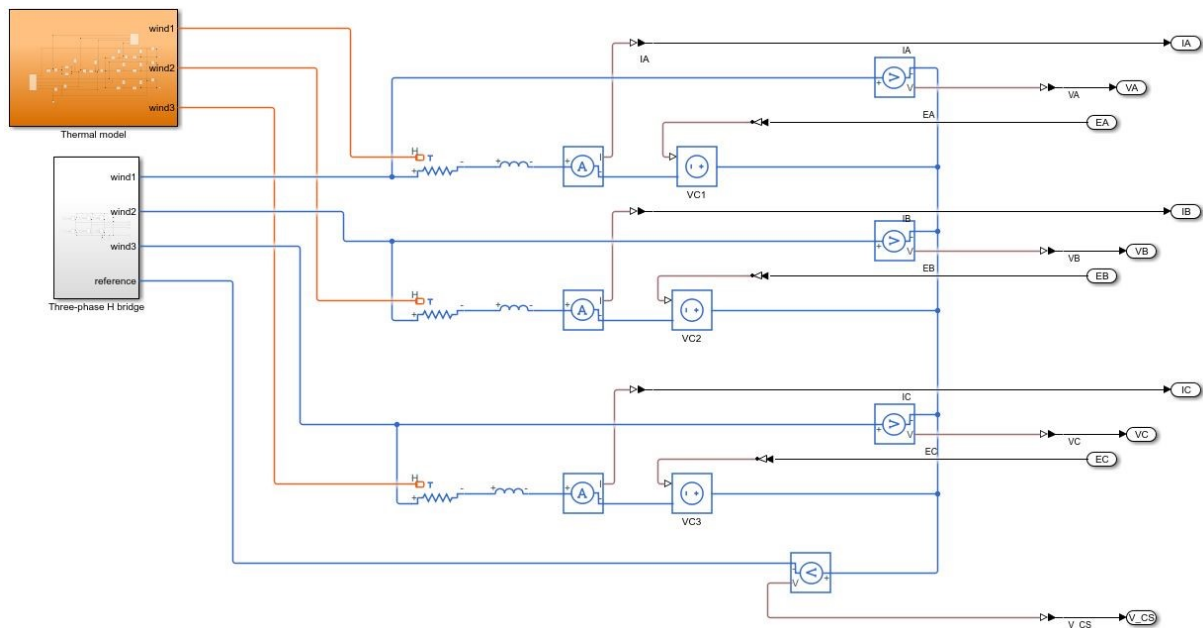
FIGURE 5-14 SSC BLOCK

The output from the inverter block is used to switch the phases, using an H bridge, an electronic circuit that switches the polarity of a voltage applied to the phases of the electric motor. As shown in Fig. 5-15, this circuit is modelled by using switches driven by the same inverter and powered by a constant voltage source. The operation of one of the two switches present in each phase determines the polarity of the winding itself.
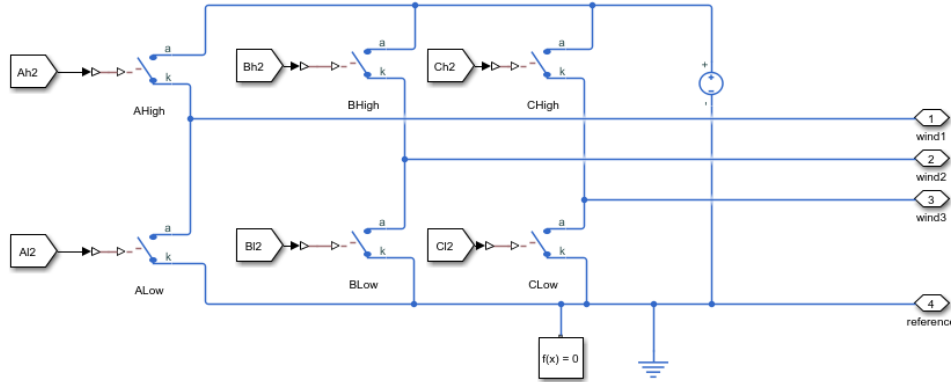
FIGURE 5-15 THREE-PHASE H-BRIDGE BLOCK

The output of this component is directly connected to the RL model which describes the electrical architecture of the motor itself. In this case there is a thermal resistance, an inductance, a phase voltage generator, used as a source for BEMF, and other components such as voltage and current sensors, which are used for other evaluations previously introduced, as shown in Fig. 5-14,

The thermal resistor block is used for two purposes, take into account the influence of temperature on the resistance of the windings, and take into account the dissipative effects by Joule effect of the conductors. When the temperature at the thermal port is T, the resistance is:

$$R = R_0(1 + \alpha(T - T_0))$$

Where R_0 is the nominal resistance at the reference temperature T_0 and α is the temperature coefficient. The following equation describes the thermal behaviour of the block:

$$Q = K_a t_c \frac{dT}{dt} - i^2 R$$

Where Q is the net heat flow into port H, K_a is the Dissipation factor, t_c is the Thermal time constant, $\frac{dT}{dt}$ is the rate of change of the temperature and it is the current through the resistor.

Starting from these components is then built a thermal model of the electric motor through an architecture with lumped parameters. The purpose of this model is to determine the temperature distribution inside the PMSM to evaluate the influence of temperature on the operation of the electric motor, because the phase resistance depends on the temperature of the conductor, and to evaluate the thermal stability of the motor itself.

The components used for modelling are:

- Thermal Mass block, which represents a thermal mass that reflects the ability of a material to store internal energy. The mass of the material and its specific heat characterize this property. This component is used for the phases winding, the stator core, and the case of the electric motor. The thermal mass is described by the equation:

$$Q = c\,m\,\frac{dT}{dt}$$

  Where Q is the heat flow, c is the specific heat of the material, m is the mass and T is the temperature.

- Conductive Heat Transfer block, which represents the heat transfer by conduction. For a flat surface, the Fourier law describes the transfer:

$$Q = k\,\frac{A}{D}(T_A - T_B)$$

  Where k is the thermal conductivity of the material, A is the Area normal to the heat flow direction, D is the distance between the layers and T are the temperatures between the sides of the layer.

- Convective Heat Transfer block, which represents heat transfer by convection between two bodies by means of fluid motion. The Newton law of cooling describes the transfer:

$$Q = k\,A(T_A - T_B)$$

  Where k is the convection heat transfer coefficient and A is the surface area. This component is used to evaluate the convective heat transfer between the motor case and the ambient.

- Radiative Heat Transfer block, which represents a heat transfer by radiation between two bodies. The transfer is governed by the Stefan-Boltzmann law:

$$Q = k\, A(T_A{}^4 - T_B{}^4)$$

Where k is the radiation coefficient and A is the emitting body surface area.

- Temperature Source block, which represents an ideal source of thermal energy that is powerful enough to maintain specified temperature at its outlet regardless of the heat flow consumed by the system. For this model the temperature value is set to 298.15 K, or 25˚C.

Other components are implemented in the model, used for later evaluations, such as temperature sensors and Heat Flow Rate sensors.

- The Heat Flow Rate Sensor block represents an ideal heat flow meter, that is, a device that converts a heat flow passing through the meter into a control signal proportional to this flow.

- The Temperature Sensor block represents an ideal temperature sensor, that is, a device that determines the temperature differential measured between two points without drawing any heat.

The model implemented for the thermal evaluation of the electric motor in question consists mainly of four parts. The windings heat up due to the current flow in the conductors and generate a heat flow to the slots in which they are housed, hence the first Conductive Heat Transfer block. A second heat flux results from the interaction between individual three-phase slots and the entire stator core. The core, heating up, generates a heat flow, due to the temperature difference, with the case covering the electric motor itself. As for the passage between windings and slots, in this case the materials of which they are composed are different, electrical steel for the stator core and aluminium for the stator case. A last heat flow is generated by the temperature

difference between the case and the environment, which as mentioned above is at a constant temperature. In this case it was considered a radiative heat exchange even if of low absolute value.

Temperature sensors evaluate the temperature of the three windings, as well as stator and external case temperatures. Instead, the heat flow rate sensors evaluate the heat flow between the different components of the motor, such as the one between windings and slots, between slots and stator core, between stator core and external case and between case and the environment.

In the modelling were not considered any internal heat flows to the electric motor, or among other elements, because in a normal use of the motor the temperature variations are quite low and considering all the interactions between the different components would make the model quite complex.

The complete thermal model of the electric motor under consideration is shown in Fig.5-16.
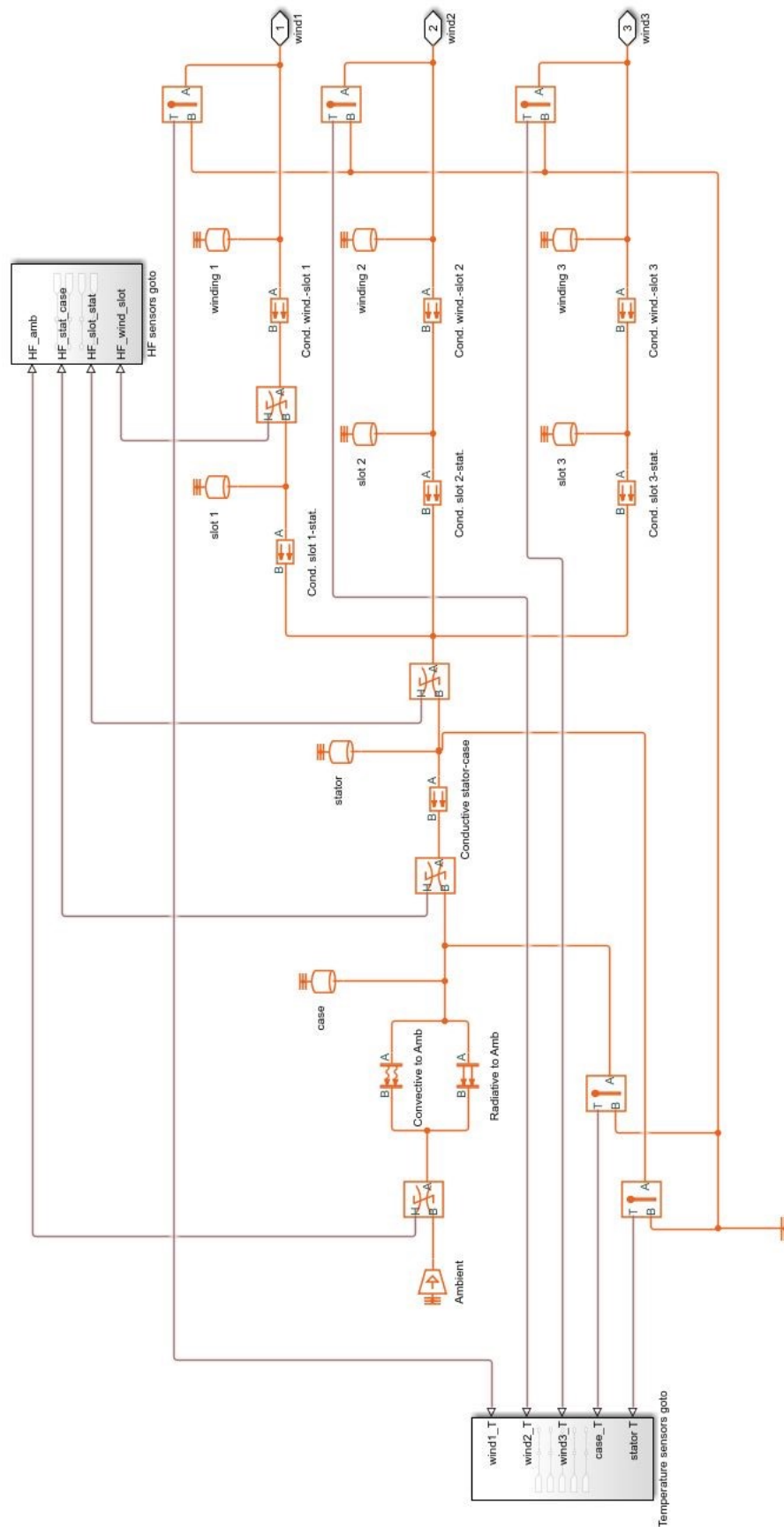
FIGURE 5-16 MOTOR THERMAL MODEL

6 Fault modes

The use of Electromechanical Actuators (EMA) for aerospace applications, as previously introduced, is having a rapid development in recent years. Civil aircraft, such as the Boeing 787 or the Airbus A350, use more electric power than the previous generation aircraft, also because a greater number of systems, previously powered by hydraulic power, are operated instead by electric power, such as the directional control system of the aircraft, but also for secondary systems, such as flaps and slats operation, the brake system, or the on-board environment control system.

In the first aircraft previously introduced, the EMA are used for secondary systems, leaving the hydraulic system the control of the primary surfaces, maintaining a conventional architecture of the hydraulic lines, to meet the safety requirements.

The latest Airbus aircrafts, such as the A380 and the A350, are equipped with a new generation of actuators also used for the primary control surfaces, the Electro hydrostatic actuators (EHA) and the Electric Backup Hydraulic Actuation (EBHA).

In the first case, these actuators replace the aircraft hydraulic system with self-contained hydraulic power, generated by a local electric pump, operated for example by a BLDC. Instead, the EBHA provides a normal operation with the aircraft hydraulic system, switching to a local operation in case of emergency. In order to meet the safety requirements of the aircraft, less hydraulic lines are sufficient compared to competitors, as shown in fig. 6-1 (2 hydraulic lines for A350 and 3 for the B787).
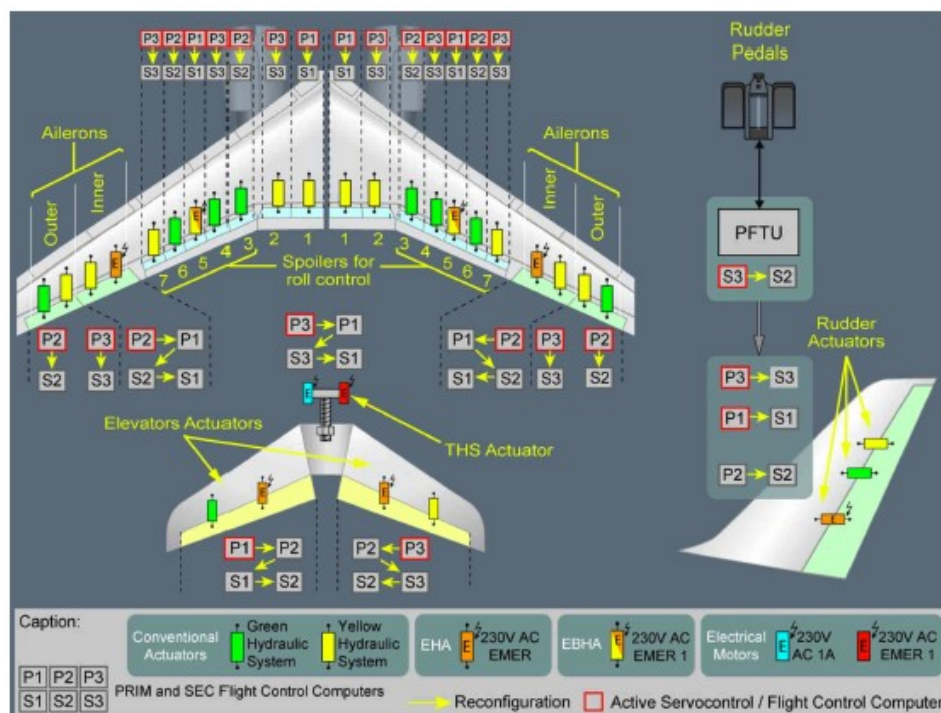
FIGURE 6-1 A350 ACTUATORS ARCHITECTURE

In the study of the electric motor operation, or for the entire EMA, it is necessary to evaluate all possible fault modes, since reliable fault statistics is not yet available and combined faults condition response is still not fully understood, compared to the most popular hydraulic actuators.

A typical EMA configuration involves the use of an electric motor connected to the user through a gear box, necessary for the high torques compared to the size of the motor and because usually it has the most efficient operation zone at very high RPM.

6.1 EMA fault modes

Failure modes of an EMA can be divided into four categories, mechanical and structural faults, motor faults, electrical or electronical faults and sensors faults. The purpose of prognostic methods is to identify every single fault before the functioning of the engine is compromised, evaluating the remaining useful life of the actuator (RUL). Risk management methods, such as the Failure Mode, Effects, and Criticality Analysis (FMECA), are used to identify potential failures in systems and equipment. Every single mode of failure is associated a coefficient that takes into account the probability of occurrence and one coefficient relative to the criticality that this can have on the entire system. The goal of FMECA is to determine which failure modes pose the highest risk to the entire system.
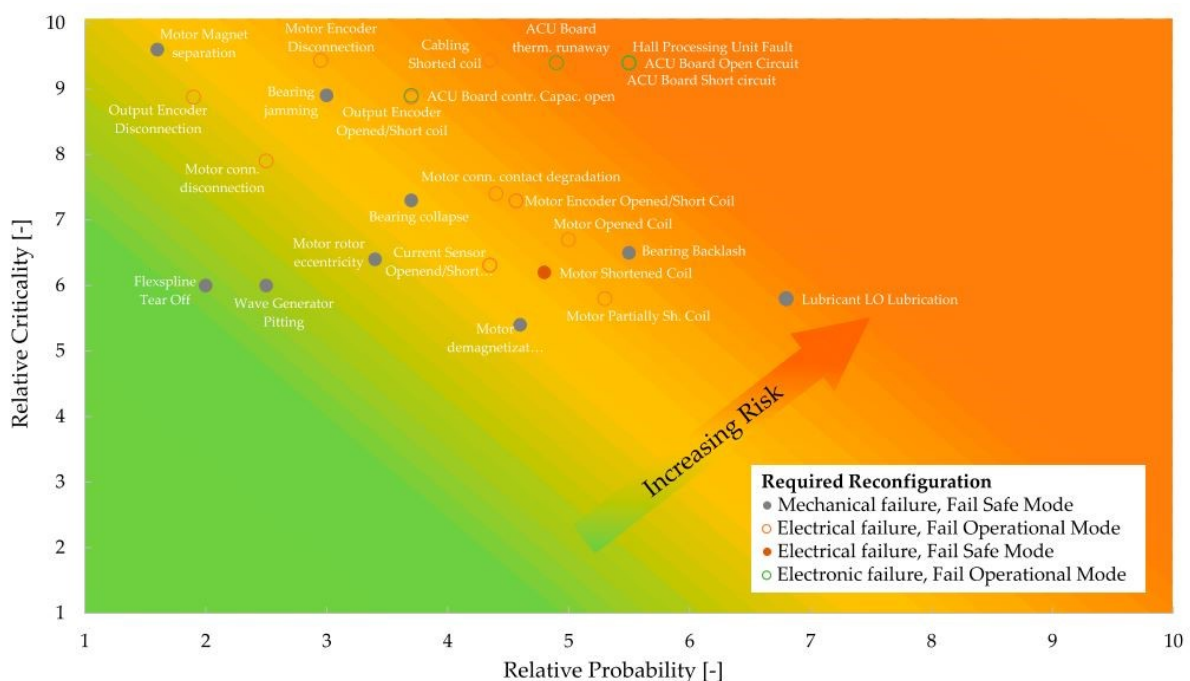
FIGURE 6-2 EMA RISK ANALYSIS

In the following points are explained the categories associated with the failure modes, previously introduced:

1. **Mechanical and structural faults**: these are consequences of the operating conditions of the electric motor, due to excessive loads, lubrification issues, manufacturing defects or environmental factors. in addition to the motor, this type of failure afflicts reducers and transmission. there are few prognostic or diagnostic models that identify this type of failure, except for bearing faults, of which there is a good knowledge of their behaviour.

2. **Motor faults**: Electric motors, such as PMSM or BLDC, are often operated at high RPM. this implies an increase in temperature within them, due to the power dissipated for Joule effect, which could lead to failures due to the breakage of the insulating layers of the winding conductors. A second effect of temperature rise is related to magnetization of the PM, because if the temperature is greater than the Curie temperature there will be a demagnetization of the rotor magnets. The high speed of the rotor could lead to failures related to the eccentricity of the rotor, subsequently implemented in the model under analysis

3. **Electrical Faults**: These are similar to failures already evaluated in other aerospace systems. The main causes are related to overheating, short circuits, over currents, over voltages, vibrations or electromagnetic compatibility problems leading to system failure.

4. **Sensor faults**: the operation of the EMA is based on feedback loops with data from sensors, included in the system. Their failure implies changes in operation, or the entire loss of the actuator. Sensor faults can be classified into three types, Bias, Drift or Scaling.

The possible fault modes of the previously introduced categories are grouped in the Tables 4-5-6, based on [20-25].

In the model presented in this work are implemented some fault, such as the short circuit fault, rotor eccentricity fault, noise fault and friction fault.

Component	Fault	Failure	Probability	Criticality	Model type
Screw	spalling	vibrations, metal flakes	5	3	Hybrid
	wear/backlash	backlash	7	3	Data
Nut	spalling	vibrations, metal flakes	5	3	Hybrid
	backlash	seizure/disintegration	7	3	Data
	degraded operation	seizure/disintegration	3	5	Data
	binding/sticking	seizure/disintegration	3	3	Data
	bent/dented/warped	seizure/disintegration	1	5	Data
Ball returns	jam	seizure/disintegration	5	8	Hybrid
Bearings	spalling	vibrations/metal flakes	5	3	Hybrid
	binding/sticking	seizure/disintegration	2	4	Data
	corroded	vibrations, metal flakes	2	5	Hybrid
	backlash	vibration, disintegration	7	3	Data
Piston	cracks	structural failure	1	10	Data
Dynamic seals	wear	structural failure	4	6	Physics
	structural failure	same	3	8	Data
Static seals	structural failure	same	2	8	Data
Balls	spalling	vibrations, metal flakes	5	3	Hybrid
	wear	backlash	7	5	Hybrid
Mountings	crack	complete failure	1	7	Data
Lubricant	contamination	seizure/disintegration	8	5	Data
	chemical breakdown	seizure/disintegration	4	5	Physics
	run-dry	seizure/disintegration	3	10	Hybrid

TABLE 4 MECHANICAL AND STRUCTURAL FAULT MODES

Component	Fault	Failure	Probability	Criticality	Model type
Controller capacitors	dielectric breakdown	short/open circuit	4	8	Hybrid
Controller transistors	dielectric breakdown	short/open circuit	4	8	Hybrid
Wiring	short circuit	same	5	10	Hybrid
	open circuit	same	5	10	Hybrid
	insulation deterioration	short/open circuit	5	8	Data
Solder joints	intermittent contact	disconnection	5	8	Hybrid
Power supply	short circuit	same	5	10	Hybrid
	open circuit	same	5	10	Hybrid
	intermittent performance	short/open circuit	5	8	Data
	thermal runaway	dielectric breakdown	6	10	Hybrid

TABLE 5 ELECTRICAL FAULT MODES

Component	Fault	Failure	Probability	Criticality	Model type
Connectors	degraded operation	disconnection	5	6	Data
	intermittent contact	disconnection	3	7	Data
Stator	stator coil fails open	same	4	4	Physics
	insulation deterioration	short circuit	5	5	Data
Resolver	coil fails open	same	4	10	Physics
	intermittent coil failures	permanent coil failures	5	7	Data
	insulation deterioration	short circuit	5	7	Data
Rotor/magnets	bond deterioration	magnet separation	2	10	Data
	rotor eccentricity	bearing failure	3	6	Physics

TABLE 6 MOTOR FAULT MODES

6.1.1 Short circuit fault

A short circuit inside an electric motor is an important failure as it could compromise its operation and can occur for several causes. A first case can be traced back to the presence of moisture or condensation between the coils of a motor, which in the case of high voltage differences could lead to the presence of leak currents, for this reason it is necessary to provide for the implementation of voltage regulators that take into account this effect in the presence of adverse environmental conditions.

A second cause, more common in the analysed electric motors, is due to the damage of the insulating layer of the conductors. the high temperature caused by the energy dissipation by joule effect could lead to the breakdown of the insulator, usually of nanometre thickness, generating a short circuit between adjacent turns of a coil.

This causes a reduction of inductance and resistance and a consequent increase of current flowing in the conductors, a greater energy dissipation and therefore a greater temperature of them.

Several types of short circuit can take place inside an electric motor:

- **Coil-coil short circuit**: fault due to contact between conductors of the same coil.

- **Phase-phase short circuit**: fault due to contact between conductors of different phases, important in slot-less electric motors.

- **Phase-ground short circuit**: failure due to contact between conductors of a phase and the stator core, or other components of the electric motor.

The first case can be implemented in the model as an indicator of the degradation status of the electric motor, as it continues to operate even if in the presence of this fault. The other cases introduced relate to worse conditions as it leads to the shutdown of the operation of the entire actuator. implement the first case could be a tool to evaluate the other effects introduced because it is generally the first effect to manifest.
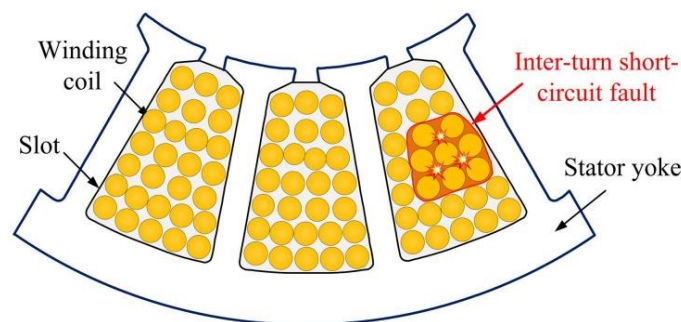
FIGURE 6-3 COIL-COIL SHORT CIRCUIT FAULT

6.1.1.1   Short circuit fault implementation

The implementation of the short-circuit effect within the model must take into account that both the resistance and the inductance decrease, in accordance with the above. A third effect concerns the variation of the counterelectromotive force as a function of the number of turns of the single coil, and therefore of the torque constant, as related to each other.

The generic BEMF coefficient may be expressed by the relationship:

$$k_{BEMF} = \frac{\partial \phi}{\partial \theta_m} = nA \frac{\partial}{\partial \theta_m} \left(\int_A \boldsymbol{B} \, \boldsymbol{n} \, dS \right)$$

Where n is the number of turns of each coil, A is the total winding area, and **B** is the magnetic flux density of the rotor.

Defining N_i as the normalized value of shorted coil windings in respect to n, the total number of coil windings, it is possible to define:

$$R_i = N_i R$$

$$L_i = N_i{}^2 L$$

$$k_{BEMF}^i = N_i k_{BEMF}$$

Where R_i, L_i and k_{BEMF}^i are Resistance, Inductance and normalized BEMF coefficient of the i-th phase, while R, L and k_{BEMF} are the nominal values, referring to a zero-fault condition.

6.1.2 Rotor eccentricity fault

The eccentricity defines the misalignment between the axis of rotation of the engine and the axis of symmetry of the entire engine in the most general case. Three types of eccentricity are defined in the literature, the Static eccentricity (SE), the Dynamic eccentricity (DE) and a Mixed eccentricity (ME).
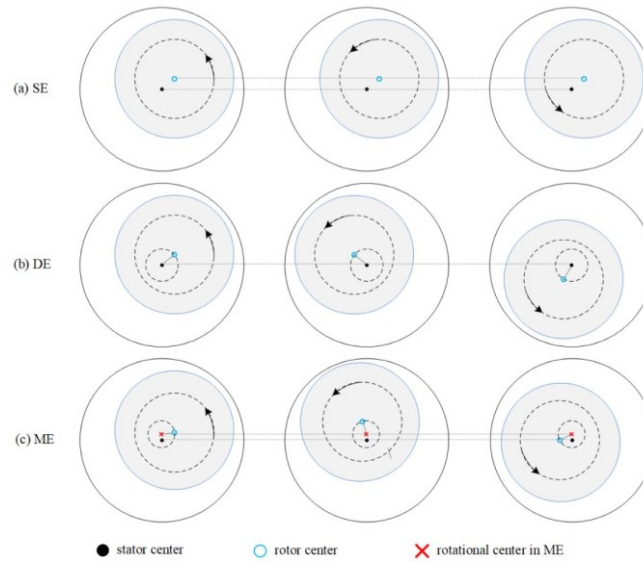
FIGURE 6-4 ECCENTRICITY FAULT TYPES

In the first case, that is the Static eccentricity, the rotational axes of the rotor and the axis of symmetry of the motor do not coincide, causing a variation of the air gap in the revolution of the motor.

The dynamic eccentricity instead indicates a misalignment between the axis of rotation of the rotor and its rotational inertial axis. In this case vibrations are generated due to the non-symmetrical mass distribution around rotational axis of the rotor, which imply possible breakage of the bearings that support the rotor or an irregular torque generation in the rotor revolution.

In the third case introduced, the Mixed eccentricity, are contained both SE and the DE conditions, and in this case the rotor revolves a third centre, other than the stator and the rotor centres. The three cases introduced are explained in Fig. 6-3.

In this model the only static eccentricity is implemented because, considering for example the second introduced case, it is possible to make the evaluations directly measuring the vibrations of the component as the air gap could be constant, but for the inertial effects the torque generated could vary in the rotor revolution.

The geometrical characteristics useful for evaluating the static eccentricity of the rotor are defined, according to the relation:

$$g = x_0 \cos \theta + R_s \sqrt{1 - \frac{x_0^2}{R_s} \sin^2\theta} - R_r \cong$$

$$\cong x_0 \cos \theta + R_s \left[1 - \frac{1}{2}\frac{x_0^2}{R_s} \sin^2\theta\right] - R_r \cong$$

$$\cong x_0 \cos \theta + g_0$$

Where $g_0 = R_s - R_r$ is the air gap value during nominal conditions, R_s is the stator inner radius, R_r is the rotor outer radius, x_0 is the distance between rotor rotational axis and the symmetric axis of the motor, θ is the angle relative to the rotation of the rotor, as the value of the air gap is a function of the position considered. The previously introduced relationship contains simplifications that take into account the order of magnitude of the various parameters contained in it.

The eccentricity parameter, described by the relationship below, is defined:

$$\zeta = \frac{x_0}{g_0}$$

The air gap value is then described by the equation:

$$g \cong g_0(1 + \zeta \cos \theta)$$

Once the air gap is evaluated as a function of the rotation angle of the rotor, the equation of the magnetic flux is introduced, calculated solving the circuit between two consecutives rotor poles.

$$\Phi = \frac{F_m}{\frac{g(\theta_1)}{\mu_0 S} + \frac{g(\theta_1 + \frac{\pi}{P})}{\mu_0 S}} = \frac{F_m \mu_0 S}{g(\theta_1) + g(\theta_1 + \frac{\pi}{P})}$$

Where F_m is the rotor permanent magnet magneto motive force (MMF), P is the number of poles pairs and S is the surface crossed by magnetic flux.
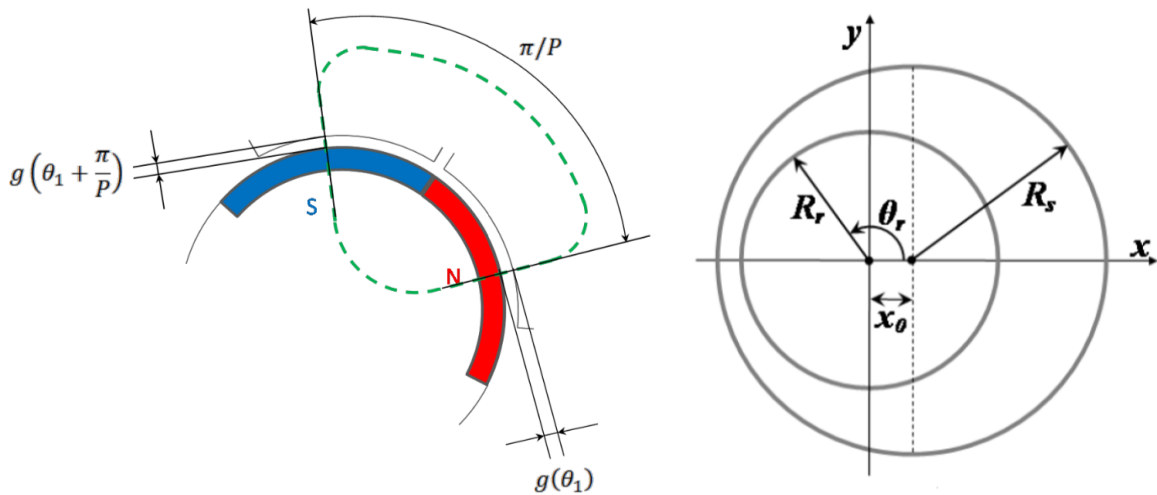
FIGURE 6-5 MAGNETIC FLUX SCHEME [LEFT], ECCENTRICITY GEOMETRY [RIGHT]

It is possible to express the calculated magnetic flux as a function of the magnetic flux under nominal conditions and the nominal air gap:

$$\Phi = \frac{2\Phi_0 g_0}{g(\theta_1) + g(\theta_1 + \frac{\pi}{P})}$$

From this relation it is deduced that, since the air gap has a periodicity of 2π, the BEMF coefficient, function of the magnetic flux time derivative, varies only if the number of pairs of poles is greater than one because in this case the sum at the denominator assumes a constant value, equal to $2g_0$:

$$g(\theta_1) + g\left(\theta_1 + \frac{\pi}{1}\right) = g_0(1 + \zeta \cos \theta_1) + g_0(1 + \zeta \cos(\theta_1 + \pi)) =$$

$$= g_0 + g_0 \zeta \cos \theta_1 + g_0 - g_0 \zeta \cos \theta_1 = 2g_0$$

6.1.2.1   Rotor fault implementation

The assessed static eccentricity is easily implemented in the model, within the calculation of the BEMF coefficient, together with the previously introduced coefficient taking into account the short circuit fault of the windings.

$$k_{BEMF,f}^i = k_{BEMF}^i (1 + \zeta \cos(\theta_m + \frac{2(i-1)}{3}\pi))$$

Where k_{BEMF}^i is the BEMF coefficient in the absence of faults and i the number of the i-th phase.

6.1.3 Friction fault

Friction is a dissipative force that is exerted between two surfaces in contact, opposing the relative motion between them. In the case where the surfaces are fixed to each other the force opposing the motion is called static friction force, if instead the surfaces have a relative motion, then it is called kinetic friction. Dry friction, subdivided in static and kinetic friction, causes malfunctions in the servomechanisms, such as position errors or stick slip phenomenon.

The purpose of a friction model is to accurately explain the behaviour of the mechanism under certain speed conditions, evaluating the force that is attached to the motion of the actuator, but the problem falls into the high nonlinearity of the phenomenon. There are different friction models, generally classified into continuous and discontinuous. Those who best describe the real condition are the discontinuous models, that is, where the friction force, which opposes the relative motion between

the surfaces, presents a discontinuity at zero speed, but their application is not simple because their formulations in conditions of zero and nonzero velocity are different.

6.1.3.1   Friction fault implementation

The simplest discontinuous model describing the trend of the friction force is the coulomb model, described by the relationship:

$$FF = \begin{cases} F_{act} & if\ v = 0\ \wedge |F_{act}| \leq FSJ \\ FSJ\ sgn(F_{att}) & if\ v = 0\ \wedge |F_{act}| > FSJ \\ FDJ \cdot sgn(v) & v \neq 0 \end{cases}$$
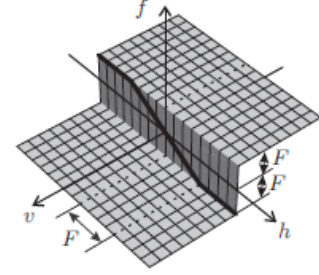
Where FF is the calculated friction force, F_{act} is the active force applied to the component, FSJ is the friction force in stick condition, FDJ the friction force in dynamic condition and v is the velocity of the component.

The problem of this model is related to numerical issues, in fact, taking into consideration the model under consideration, if in a step of integration two speeds with opposite sign are obtained, then the model does not notice the transition from zero, not verifying the possible stop of the motion.

Other models, such as that of Karnopp's or that of Quinn's friction models, try to solve this problem but they also present several aspects that could lead to errors of assessment, such as that of the Dead-band of Karnopp's friction model, where a wrong evaluation could lead to the trigger of numerical limit cycles.

The friction model implemented in the analysed servomechanism model is the Borello's friction model, defined by the relationship:

$$FF = \begin{cases} F_{act} & if\ v = 0\ \wedge |F_{act}| \leq FSJ \\ sgn(F_{att})FSJ & if\ v = 0\ \wedge |F_{act}| > FSJ \\ FDJ & v \neq 0 \end{cases}$$

The newly introduced model is quite similar to the Coulomb model but adapted to avoid evaluation problems in numerical integration.

In fact, the whole thing is based on evaluating the speed near zero, that is when it changes sign, imposing the following relationship:

$$v_{t+1} = 0 \quad if \quad v_{t+1} \cdot v_t \leq 0$$

In the case in which between two integration steps the speed changes sign, in the next timestep zero speed is set, passing from considering the dynamic friction force to evaluating the static one, imposing a stick condition.

In subsequent timesteps if the acting force, calculated as a function of the force generated by the actuator and all the contributions opposing it, is greater than the FSJ, that is the maximum stick force, then the speed is set to non-zero, passing to a dynamic condition.

Inside the model is implemented the Stribeck effect, which evaluates the friction between two lubricated surfaces, as a non-linear function of the contact load, lubricant viscosity and lubricant drag speed.
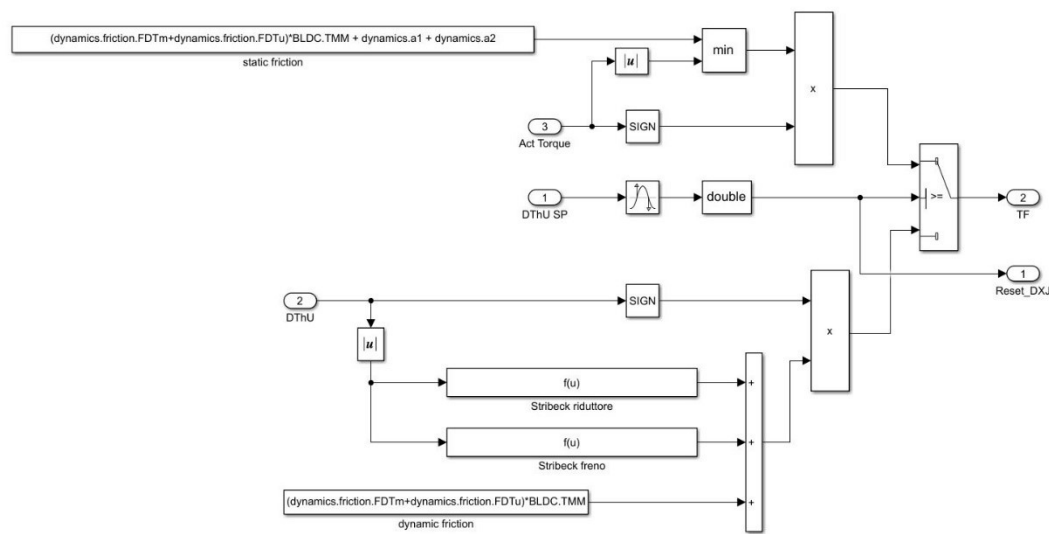
FIGURE 6-6 BORELLO'S MODEL BLOCK

6.1.4 Noise fault

In signal processing, noise is a general term for unwanted fluctuations that a signal may suffer during capture, storage, transmission, processing, or conversion.

The noise source can be classified according to three main contributions, the electromagnetic noise, the mechanical noise and the aerodynamic noise, in order to evaluate their causes and the possibly ways to reduce them.

The mechanical noise is generated by the components of the electric motor, such as bearings, fasteners or for the eccentricity between the stator and the rotor, as already mentioned in the previous paragraphs. mechanical noise is usually characterized by a low frequency range, and its source identification methods are well known.

Aerodynamic noise refers to electric motors equipped with a cooling system composed by an unspecify number of fans, which generate noise. In most cases electric motors

are not equipped with these fans but are cooled directly by air or by liquid cooling systems.

Electromagnetic noise is the largest and most complex contribution to be assessed compared to other sources of noise. Electromagnetic noise refers to the vibrations produced by the electromagnetic forces within the motor, of which the radial force on the stator teeth surface is the main component.
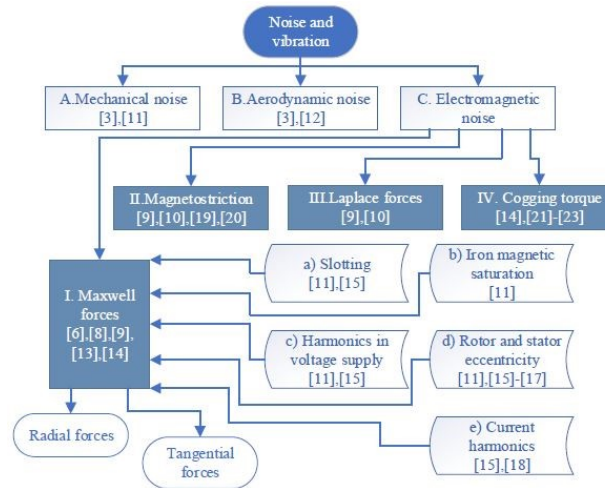
FIGURE 6-7 NOISE AND VIBRATION CAUSES SCHEME

Following the classification introduced in the fig. 6-6, electromagnetic noise can be break down into 4 contributions:

1. **Maxwell forces**: these are considered the major source of electromagnetic force, which act on roto and stator slots. Maxwell forces are produced in the radial and tangential directions. The first contribute is the source of most noises generated in the PMSMs, causing housing deformation. The second contribute is responsible for producing the acting torque, but at the same time leads to vibrations of the rotor and torque ripple.
   Maxwell forces are affected by a several number of contributes, such as the core magnetic saturation, which distorts the magnetic flux distribution or the effect of stator slots, which break the uniformity of the air gap, changing his reluctance. Another aspect to consider is the rotor eccentricity, because a small deviation of the air gap cause significant variation of his permeance

2. **Magneto-strictive forces**: the stator core is made of electrical steel, which becomes subject to magneto-strictive forces when immersed in a strong and rapidly changing external magnetic field and for this reason it can lead to vibration of the core.

3. **Laplace forces**: these forces act on the stator coils, which they can cause to vibrate. As introduced in the previous chapters, these forces can lead to any damage in the conductors and therefore to create possible short circuits.

4. **Cogging torque**: it can be described as a parasitic torque caused by the magnetic attraction forces exerted between the stator teeth and the permanent magnets (PM) in the rotor.

Noise could lead to signal transmission errors as electrical circuits could be affected by possible interference, such as those previously introduced. Specifically, a disturbed signal implies a wrong evaluation by the controllers, and therefore a lower performance of the system that could lead to its complete loss.

A white noise source is implemented in this model. White noise is a random signal having equal intensity at different frequencies, which gives it a constant power spectral density (PSD). It is a discrete signal whose samples are considered as a sequence of unrelated random variables in series with zero mean and finite variance
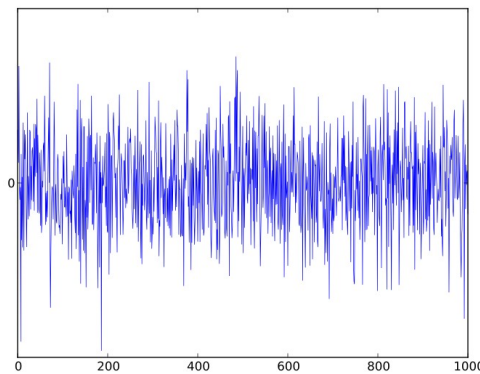
FIGURE 6-8 WHITE NOISE SPECTRUM

6.1.4.1 Noise fault implementation

In the model, a band-limited white noise is introduced, since, as previously proved, white noise is related to infinite power. To obtain accurate results, the highest noise frequency is set at less than half of the sampling rate. White noise is added to the reference current signal, then after the most sensitive electronic subsystems.

This approach makes it possible to simulate the final effect of the noise, introduced by the electronic systems, in the reference signal that in the following steps controls the operation of the servomechanism.
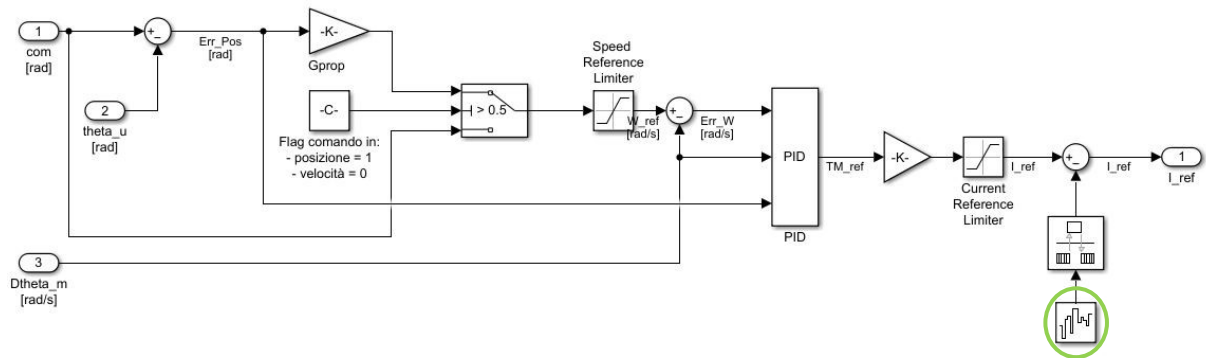
FIGURE 6-6-9 WHITE NOISE IMPLEMENTATION (INSIDE CONTROL ELECTRONICS BLOCK)

7 Results of EMA model

To verify the proper functioning of the actuator model it is useful to analyse its response to a given operating condition. Specifically, as a first case, a sinusoidal command is imposed, with an external load applied at a given time.

Simulation	Command	External Load	Fault
1	Amp=1.3 rad *f*=0.25 Hz	1350 Nm @ t=1 sec	No faulty condition

The choice of these parameters is arbitrary but takes into account the limit conditions of the actuator, in fact, from datasheet, the maximum torque that can be released by the electric motor is 11,842 Nm and taking into account the transmission ratio of the gearbox, the actuator stall torque shall be calculated, and it is 1468.4 Nm.

It is important to remember that the electric motor may not be able to follow the command imposed, even if the external load is less than the stall torque of the motor, this because the torque demand is also a function of the actuator control, and specifically the angular speed, as the viscous effects of the actuator are a function of this parameter, thus dissipating a part of the torque generated by the motor. Therefore, choosing a well determined external load value, combined with the instantaneous operating conditions of the motor, it is possible that this is not able to follow the command imposed.

In figure 7-1 it is possible to evaluate the system response according to the command imposed, the real instantaneous position of the rotor of the electric motor and its speed. After a second of simulation the external load is applied, easily understood by the speed trend that undergoes a change, but the system tends almost instantaneously to maintain the controlled position, readjusting itself through the modulation of the phase currents, generating a greater torque contribution.

Once reached the apex of the width of the control, begins an operating phase in which the direction of application of the external load is equal to the direction of rotation of the shaft. In this case the control system modulates the power supply of the phases to brake the shaft of the electric motor.
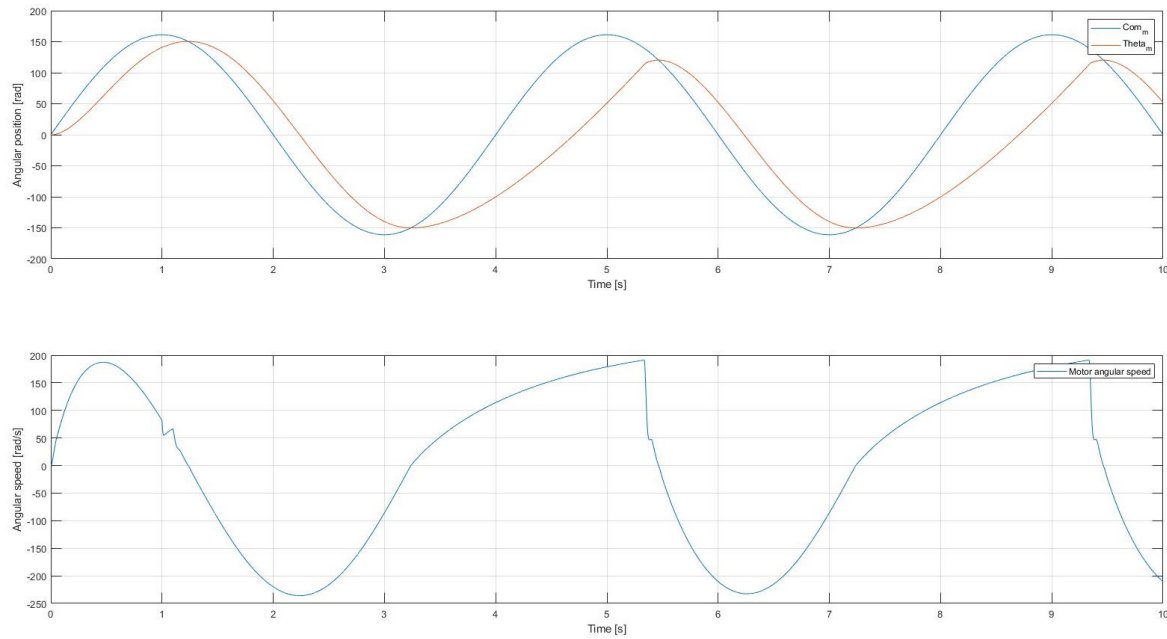
FIGURE 7-1 COMMAND-REAL ANGULAR POSITION (TOP), ANGULAR SPEED (BOTTOM)

After half a period of sinusoidal control, in a new phase of operation of the motor the external load is opposed to the control, as opposite direction. In this case the motor cannot follow the command due to the saturation of the generated torque due to the stall torque of the motor, the external load, and the viscous effects due to the rotor speed.

In the figure 7-2 the winding currents are evaluated in function of the reference current, as an output of the control system of the electric motor (I_{REF}).

After an initial normal operation of the motor, in which the imposed sinusoidal control is followed, after applying the load there is a rapid increase of the required current, necessary to oppose the external load. In a first operating phase the load has the same direction of the control, then the control system switches the phases to ensure that the rotor is braked, as previously introduced, still remaining within the operating limits of the motor.

In the operational phase in which force and command have opposite direction, the current reaches the saturation limits because the torque required by the motor has the same order of magnitude as the sum of the torque delivered and the viscous effects due to the shaft speed of the electric motor.

In this case, as seen in figure 7-1, the motor fails to perfectly follow the command imposed due to the lack of net torque generated, deviating from this until the operational phase is reached when the external load and the control have the same direction.
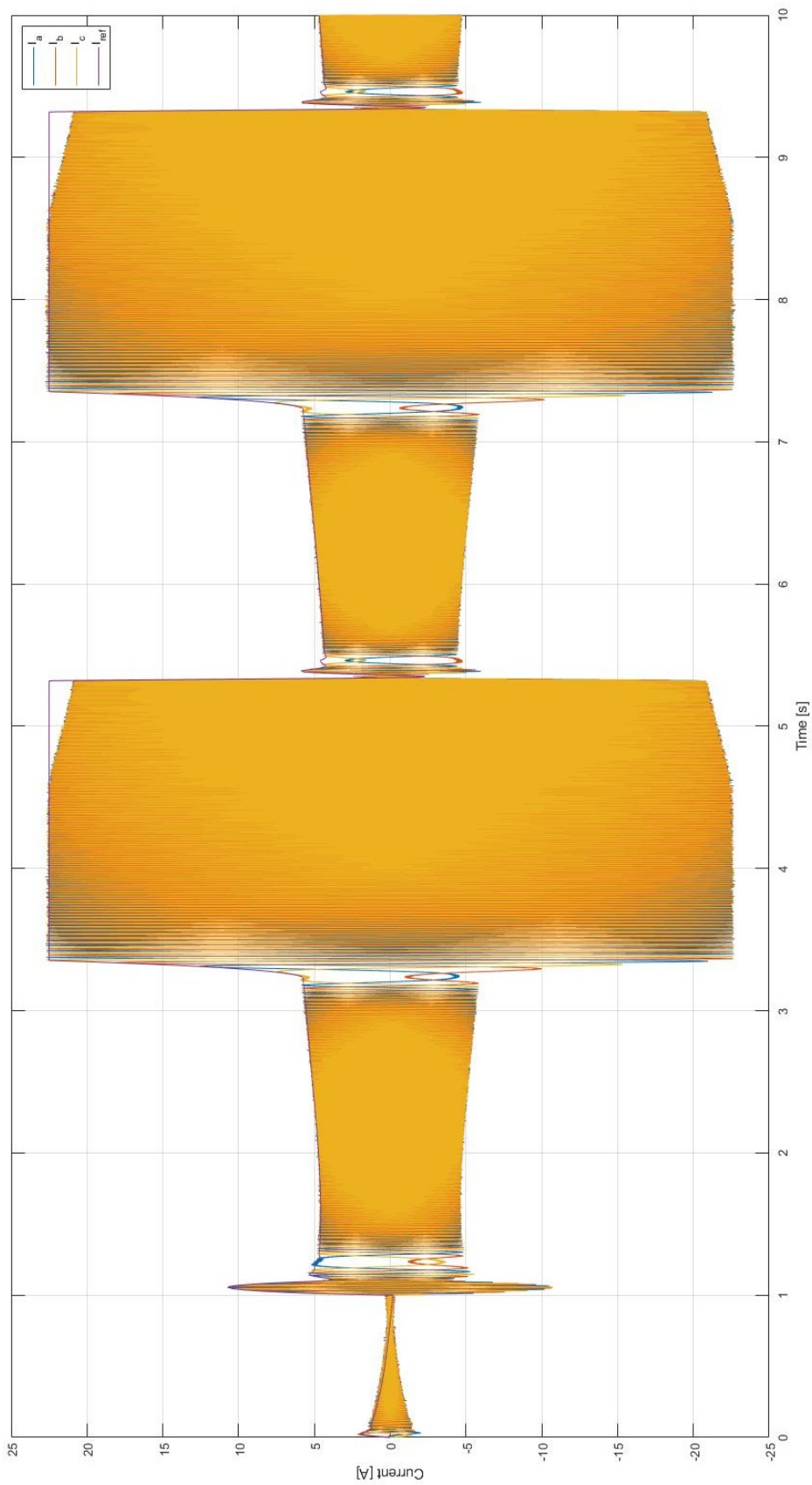
FIGURE 7-2 WINDINGS CURRENT

It is useful to analyse the final part of the saturation peak as the actual currents in the windings decrease, deviating from the reference value (I_{REF}), output of the control system. This is an effect due to BEMF, a function of the magnetic flux variation between rotor and windings, then function of the shaft speed of the electric motor. At high angular speeds, the BEMF achieves a value that contrasts with the voltage source in a tangible way, thereby reducing the current in the windings. The motor cannot hinder this effect as the reference current is in saturation condition.

When the actual position of the rotor is again close to the control imposed, and then the error drops below a certain threshold, the control system is no longer in saturation condition, resuming normal motor operation, as the control and the load are again operating in the same direction.

In fig. 7-3 the supply voltages of the three stator windings are evaluated, with a magnification of a portion of graph, in order to better evaluate the course of these. In the operating phase of the electric motor, when the saturation limits are reached, the feeding time of the phases is greater than in a normal condition, as it is necessary that greater currents flow in the conductors.
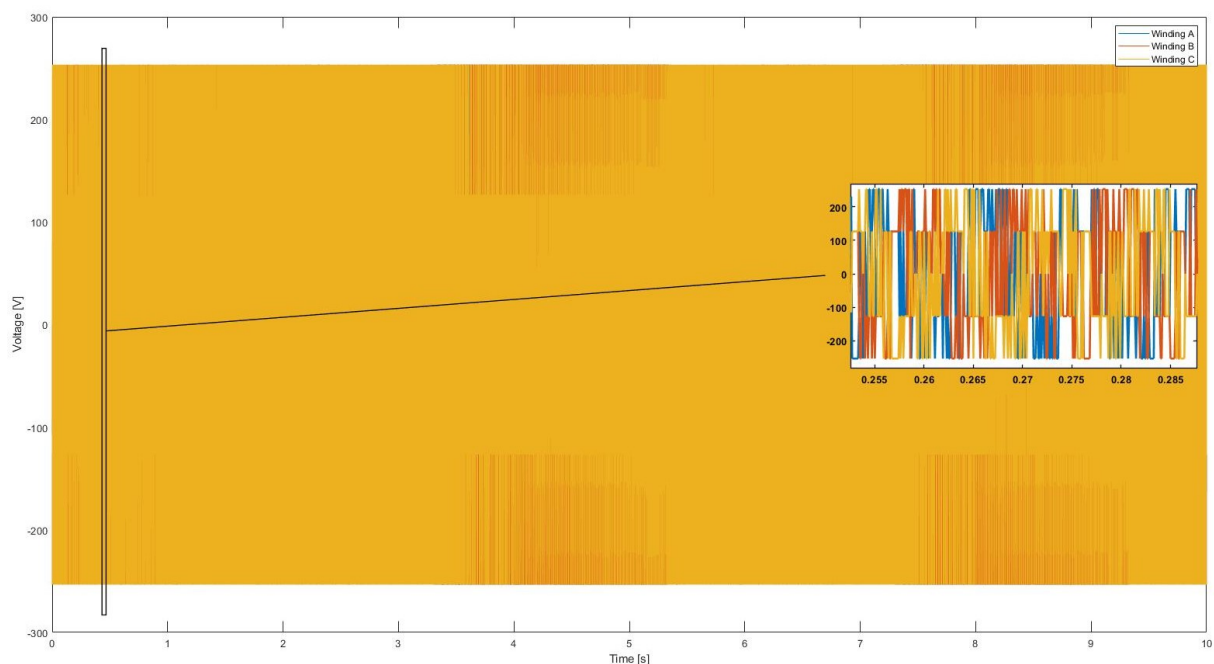
FIGURE 7-3 WINDINGS VOLTAGE

In Fig. 7-4 are introduced the trends of the temperatures of the stator windings, the stator and the case, on the top, and the thermal flows referred to a single winding, on the bottom.

Due to the high currents in the opposing phase between the control and the external load, the energy dissipation due to the joule effect is high, with a consequent increase in the temperature of the windings themselves. In this operational phase also increases the heat flow between the winding and the slot where it is contained.

As a result, with the temperature rise of this, as a chain reaction, increase the heat flows between the different components of the electric motor, thereby dissipating the heat generated by the operation of this.
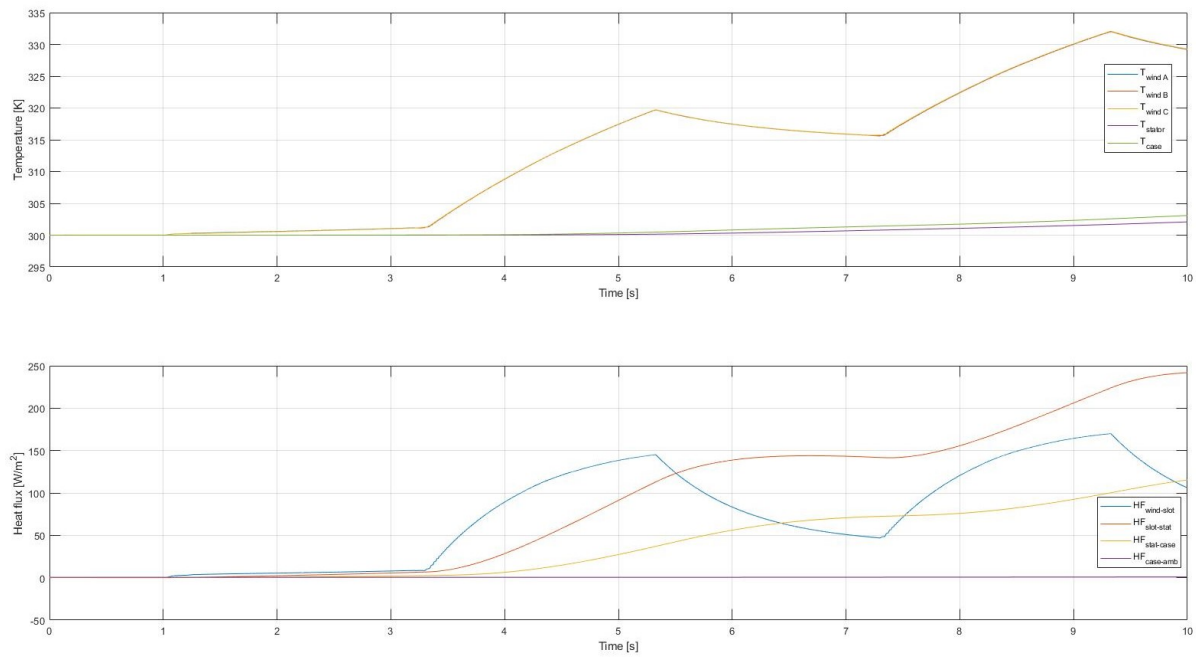
FIGURE 7-4 ELECTRIC MOTOR TEMPERATURES (TOP), HEAT FLUXES (BOTTOM)

7.1 Example: Electric motor stall

It is useful to analyse the response of the actuator in case the external load, probably due to a control surface, is equal to the stall torque of the electric motor. In this specific case a step load is applied in T=1s and Amp=1468.4 Nm width, this is because is necessary to consider the gear box transmission ratio. At the Fast Shaft, i.e., the rotor of the electric motor, this resistant torque is 11.842 Nm, because the transmission ratio is 1/124, and this is the stall torque value of the electric motor under consideration.
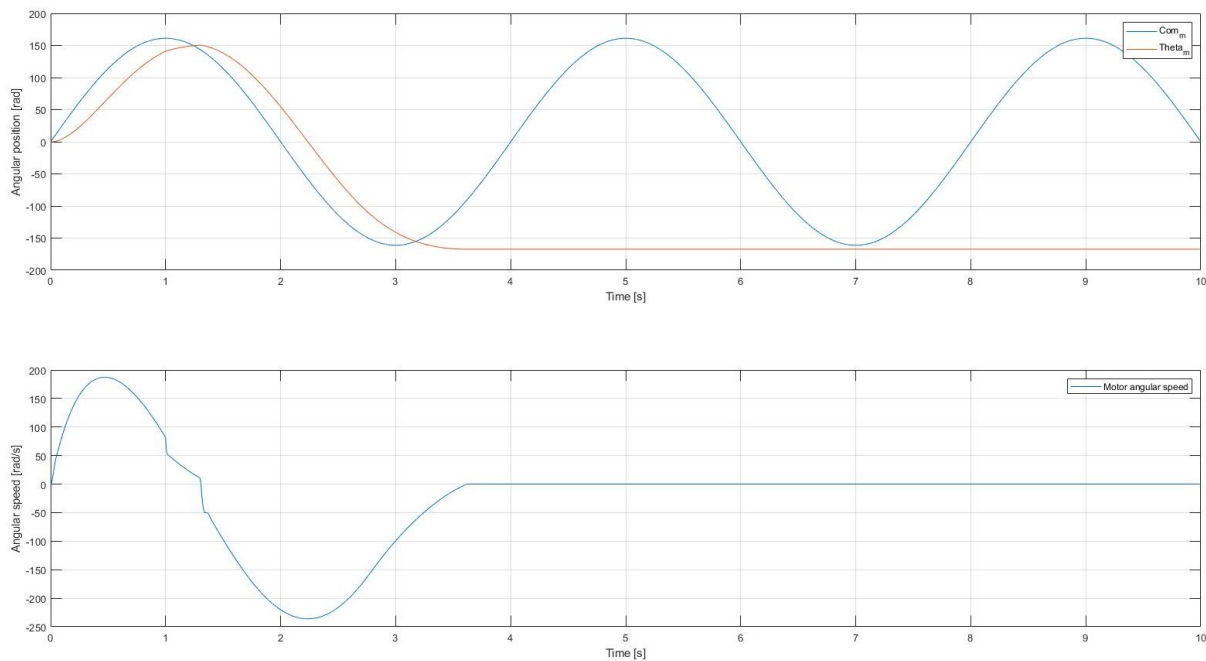
FIGURE 7-5 COMPARISON BETWEEN COMMAND AND REAL POSITION (TOP) - FAST SHAFT ANGULAR SPEED (BOTTOM)

Figure 7-5 evaluates the actuator model response when the load type previously introduced is applied. In the first phase of operation the actuator behaves normally as F_{ext} is not yet applied. As seen in the previous example, when the load is applied the actuator acts as a brake since the movement of the shaft and the external load have the same direction of application.

When the two components are in opposition, the motor cannot counteract the external load and the fast shaft will lock in a position with zero speed, as the torque generated by the motor and the external load have the same amplitude.
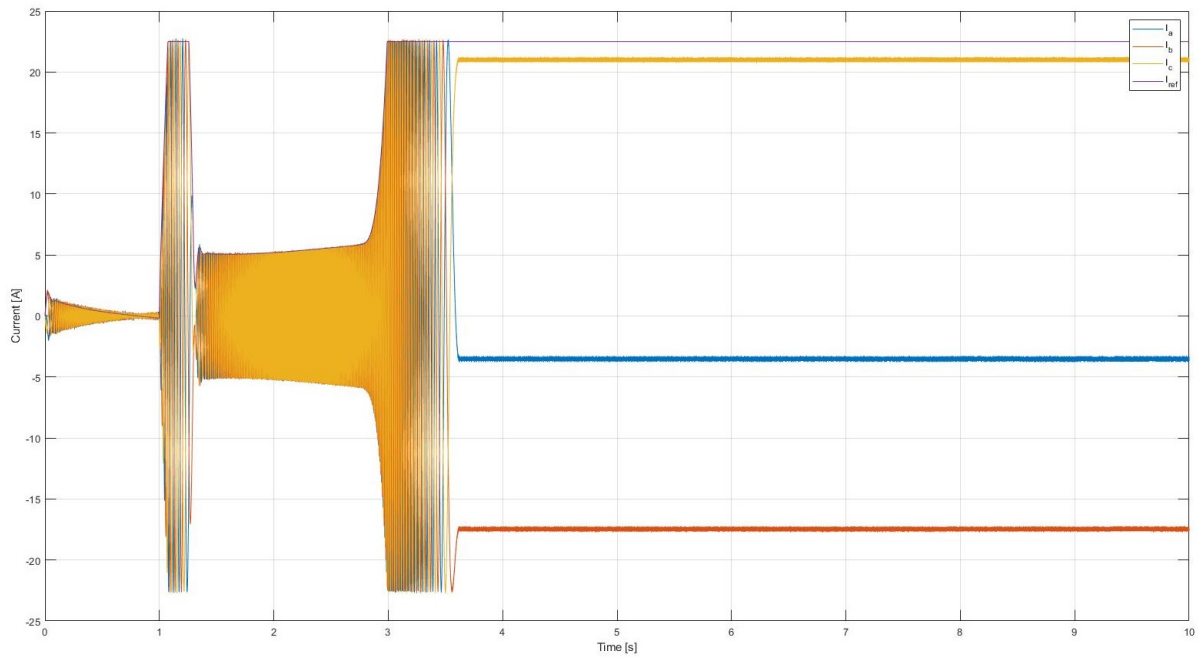
FIGURE 7-6 WINDINGS CURRENT

Figure 7-6 shows the trend of the currents in the three stator windings. In the first operating phase the motor, since no external force is applied, behaves optimally, with relatively low current values. Then, when the load is applied, at first the actuator acts as a brake, but when the external load is in opposition to the direction of the fast shaft movement, these stabilize on a constant value such that a magnetic vector is generated to balance the external load, because the rotor speed is null.
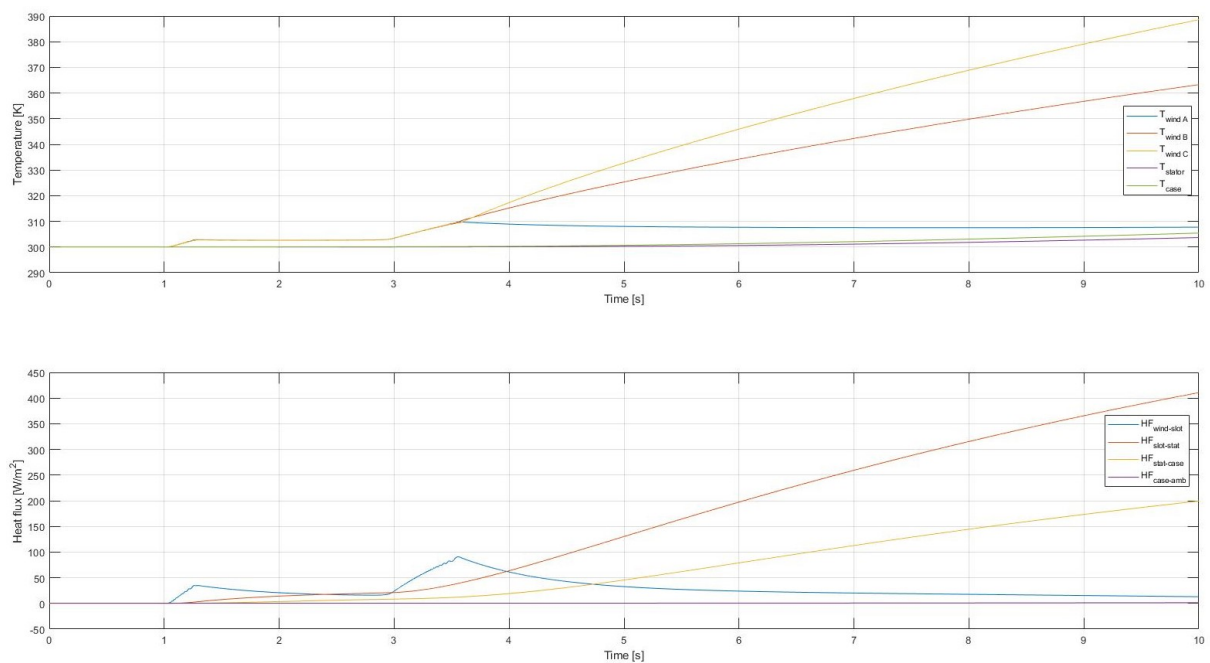
FIGURE 7-7 ELECTRIC MOTOR COMPONENTS TEMPERATURE (TOP) - HEAT FLUXES (BOTTOM)

The latest graphs, in Fig. 7-7, show the temperature trends of the three windings and the additional components of the motor, and the heat flows between the different components of the electric motor. When the rotor locks in a position due to the external load, there is a particular condition. Due to the constant current value the temperatures of the windings increase very quickly but not as expected. In fact, the rotor, being blocked, needs a magnetic vector with specific direction, and this implies that the currents in the windings are different. In this specific case the first winding has a relatively low constant current value, and for this reason the heat generated due to the Joule effect is optimally dissipated, decreasing the temperature of this. In the other windings instead, the current value is at a fairly high constant value and since the components are not able to dissipate quickly the heat generated outwards, their temperature rises. In this graph is also shown the course of the thermal flows for the first winding, that is that for which its temperature drops during the simulation. Specifically, the heat generated by the windings is dissipated through the heat exchange between the various components of the electric motor, decreasing the temperature of the conductors, and therefore also decreasing the heat exchange between these and the components of the stator.

8 Comparison with the previous model

The implementation of a thermal model of the electric motor derives from a previous model that includes electrical components, such as resistors, inductors and voltage generators used for BEMF, through Simpowersystem, a toolbox of Matlab software.

Citing MathWorks Simpowersystem user's guide:" SimPowerSystems was designed to provide a modern design tool that allows scientists and engineers to rapidly and easily build models that simulate power systems".

The main advantage of Simscape, used in the newest model, is that, compared to Simpowersystem, which works only in the electrical domain, in this toolbox, introduced with Matlab R2007a version, it is possible to model also physical domains, such as Mechanical, hydraulic, pneumatic, and thermal domains, in addition to the electrical part.
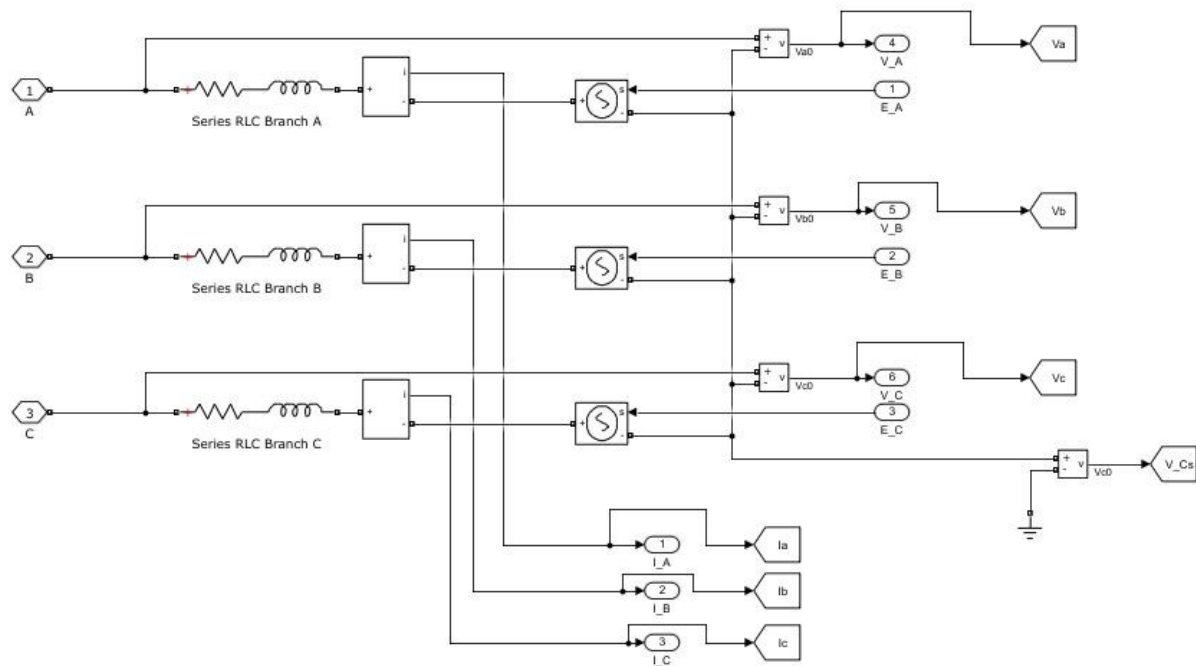
FIGURE 8-1 PREVIOUS SSC MODEL

The main problem of implementing a Simscape model in the existing Simpowersystem one, is the need to include precautions that allow a correct communication between the various blocks with different programming languages.

To do this, unlike the previous case, where there is a continuity between output of the three-phase bridge and input of the PMSM block, in the new model a new three-phase bridge was implemented, built using Simscape electrical blocks, driven by PWM through a signal converter, which has the task of converting the signal according to the block that requires it (Inherit via back propagation).

In the previous model instead, the data coming from the PWM are channelled directly into a block called "Universal Bridge", which simulates the block previously introduced in Simpowersystem language, which outputs the signal for the motor block.
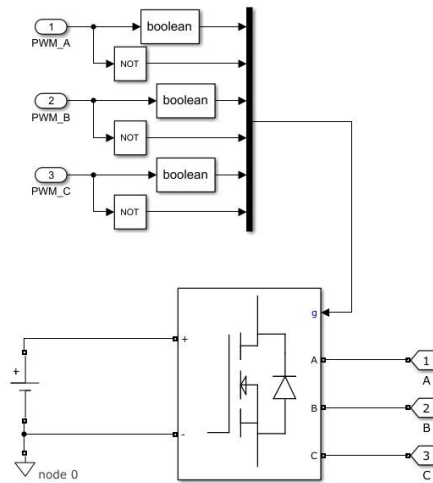
FIGURE 8-2 PREVIOUS H-BRIDGE BLOCK

To verify the correct functioning of the model, simulations were carried out, equal for both models, verifying their response by analysing certain parameters. Specifically, the simulations are always based on the same command imposed on the entire EMA, a sinusoidal input ($\omega = 0.25\ Hz$, Amp $= 1.3\ rad$), a simulation time of 10 seconds and under the following operating conditions:

Simulation	F_{ext} (@ T=1s)	SC-Fault
1	0	0
2	1350	0
3	1350	50% N_A

TABLE 5 SIMULATIONS FOR MODELS COMPARISON

Where F_{ext} is the external load that could be subject to the EMA, imposed at T=1s and the fault conditions are related to the percentage of stator windings in short circuit.

The data taken into account for the comparison between the two models are divided into electrical data, such as windings current (I_A, I_B, I_C), BEMF coefficients (k_A, k_B, k_C), windings voltages (V_A, V_B, V_C), and mechanical data, such as input command, rotor angular position and its angular speed.

8.1 Simulation 1

In nominal conditions the actuator is supposed to operate in a no-faults condition. This is the reference simulation, used to evaluate an eventual damage in the system and in this case to compare the models under consideration and evaluate the introduction of the thermal model within the actuator model.
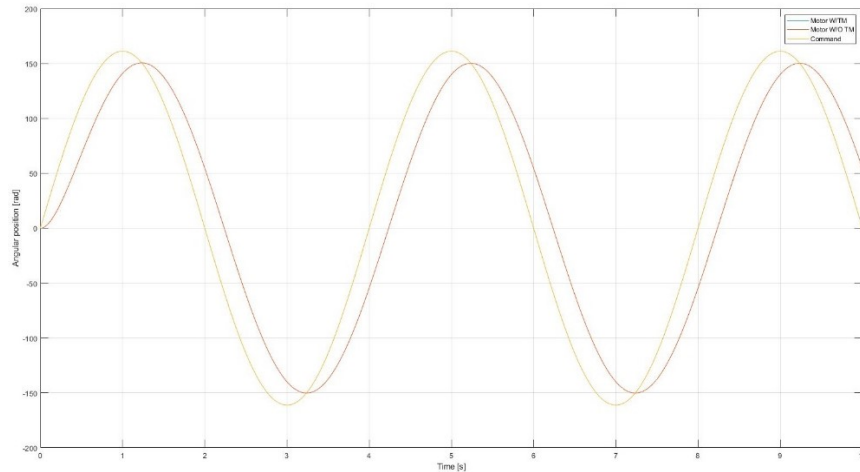
FIGURE 8-3 COMMAND VS REAL SHAFT ANGULAR POSITION
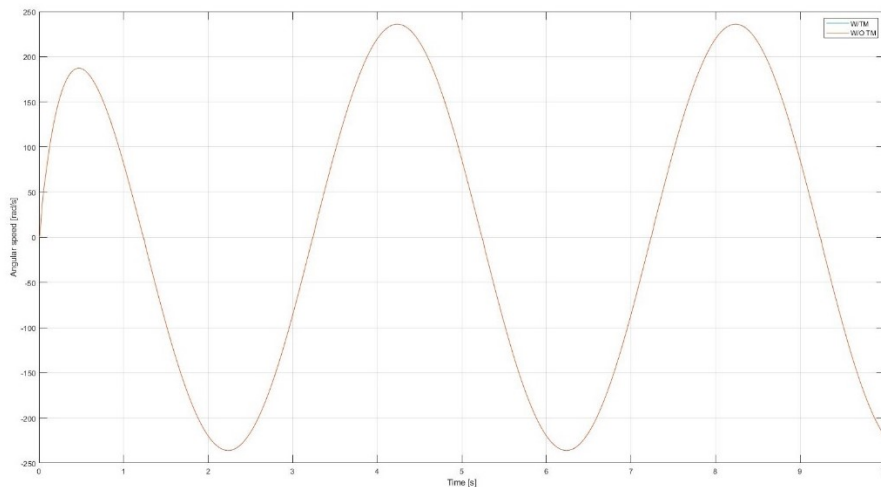
FIGURE 8-4 SHAFT ANGULAR SPEED

The figures 8-3 and 8-4 show respectively the position of the fast shaft of the actuator, then of the electric motor, compared to the imposed command and its speed for both models under consideration, the generic one and in the new one in which the thermal model has been implemented. In these cases, there are no differences, as can be estimated from the previous graphs, as the model is based on nullifying the error in the actuator position.
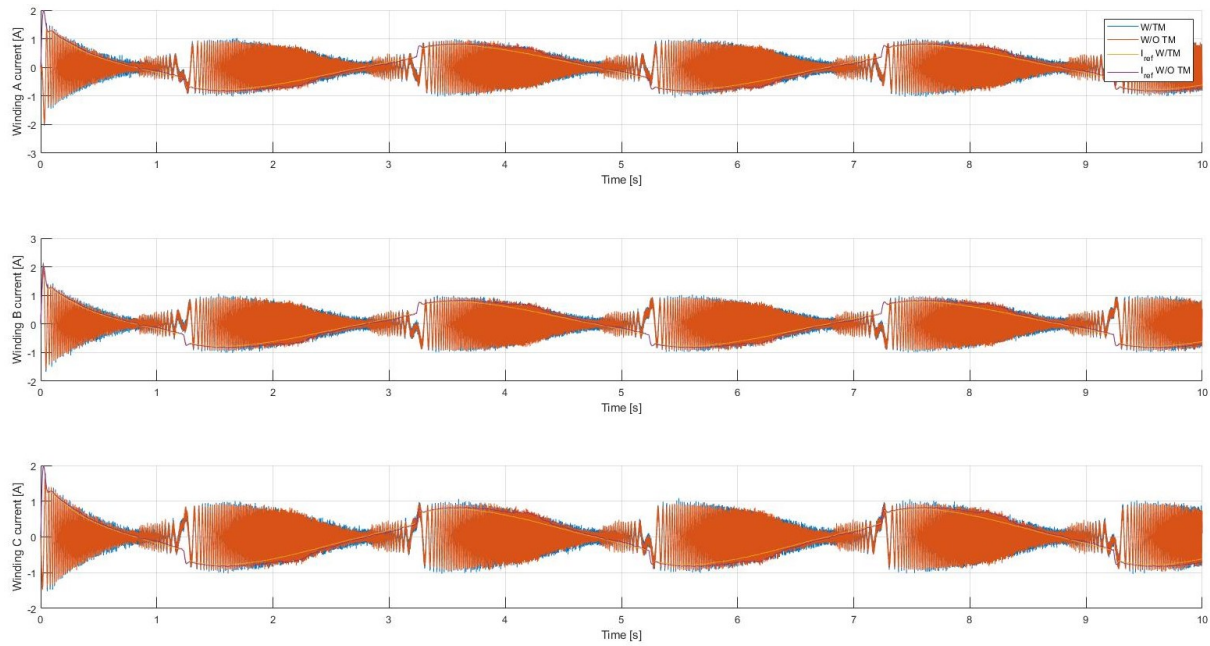
FIGURE 8-5 WINDINGS CURRENT VS REFERENCE CURRENT FOR BOTH MODELS

The fig. 8-5 shows the trends of the currents in the three stator windings, a function of the reference current, also shown in the graphs. In this case the values between the two models are very similar because the temperature change of the windings, shown later, is minimal
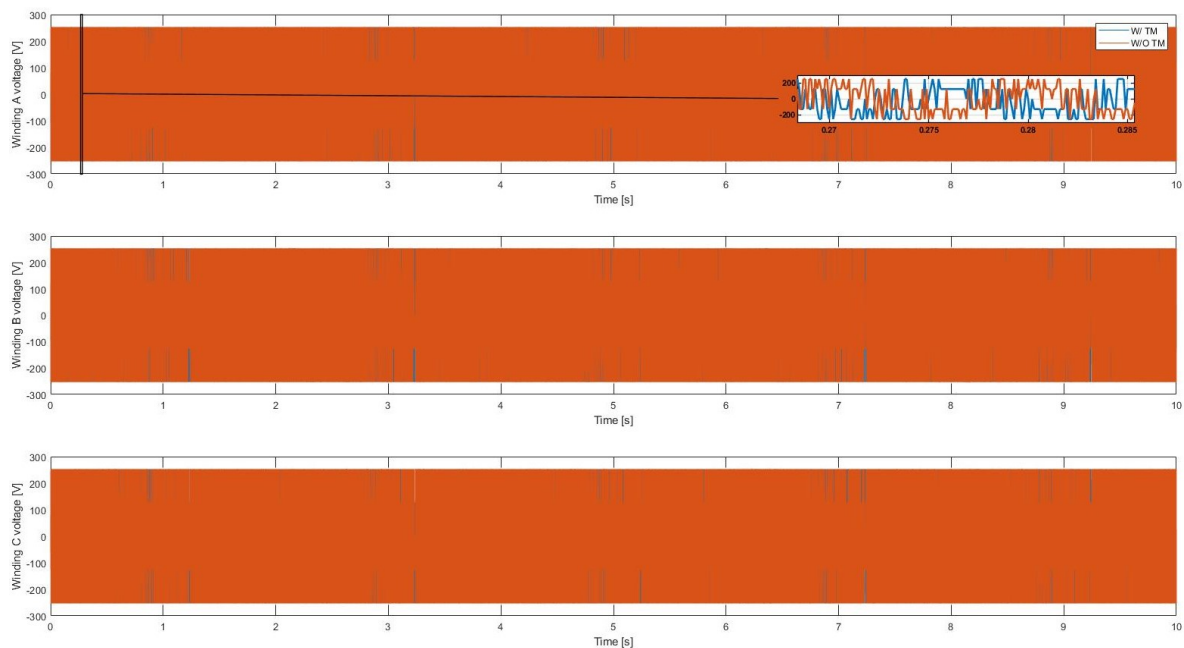
FIGURE 8-6 WINDINGS VOLTAGES FOR BOTH MODELS

The diagram in Fig. 8-6 shows the trends of the winding supply voltages. In this case the operating limits are the same, as a function of the constant voltage source, controlled by the PWM controller, even if they have some differences in the application time, indifferent in the operation of the actuator, as also shown by the enlargement of the chart under consideration
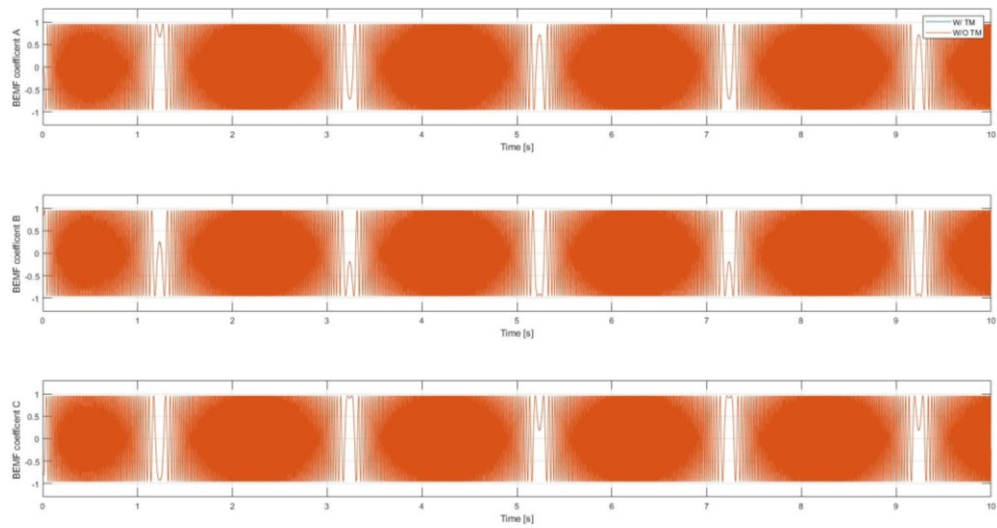
FIGURE 8-7 PHASES BEMF COEFFICIENT
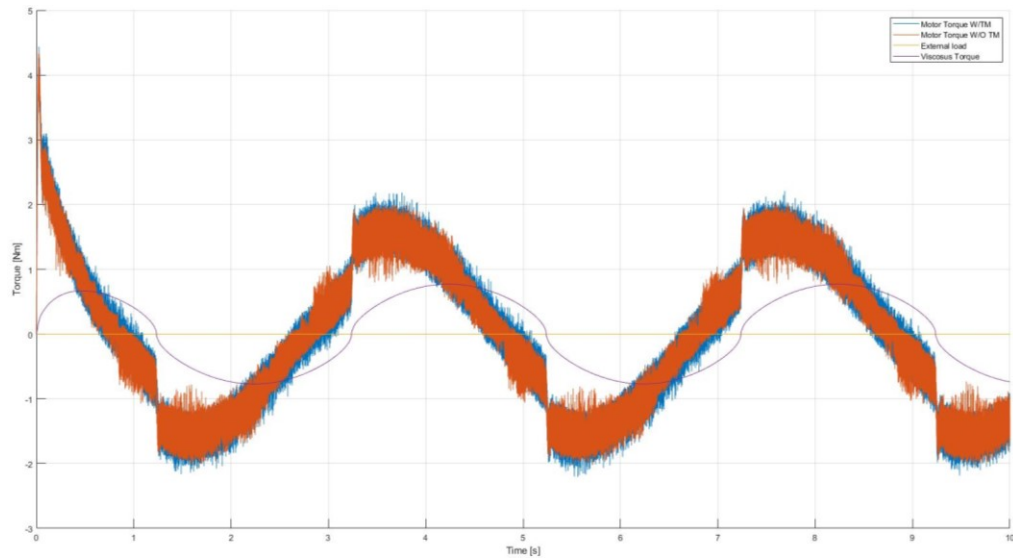
FIGURE 8-8 ELECTRIC MOTOR TORQUE VS EXTERNAL LOAD VS VISCOUS EFFECTS IN BOTH MODELS
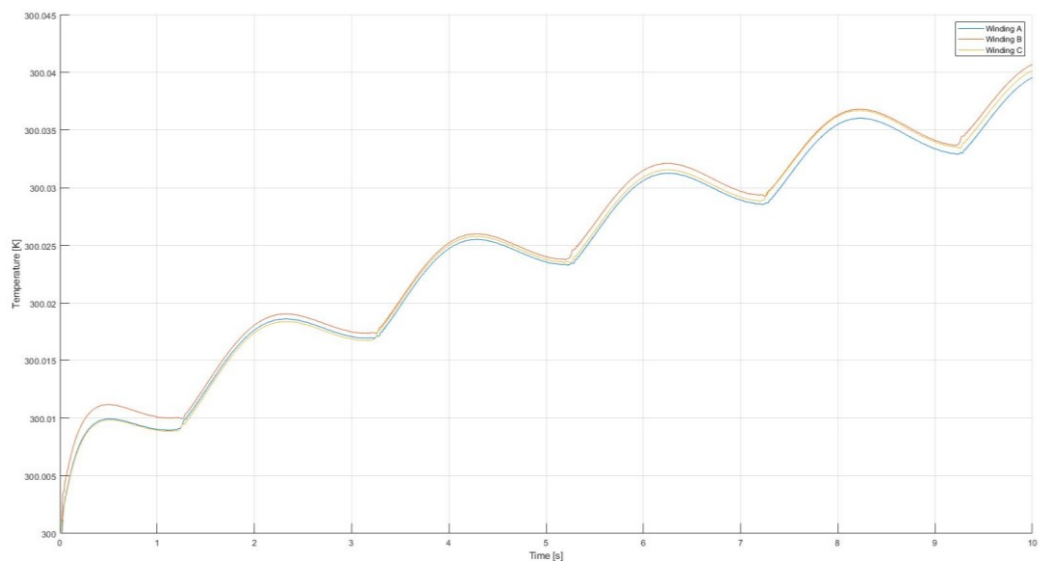
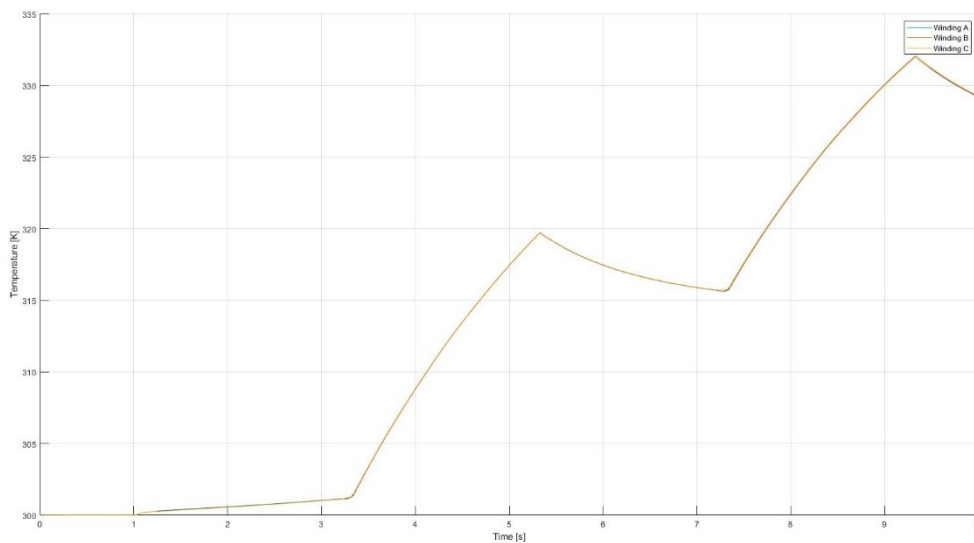**FIGURE 8-9 WINDINGS TEMPERATURE**

As in the previous cases, also the trends of the BEMF, shown in the figure 8-7, do not present particular differences, symptom of a correct functioning of the thermal model implemented, because they almost accurately trace the trends of the previous model. In this case, the trends are a function of the position of the rotor, in addition to the various factors related to any fault conditions, then offset each other in a constant value.

The graph in the Figure 8-8 shows the actuator response in terms of torque, as the sum of the effects due to the torque generated by the electric motor, a function of the required command, the external load, zero for this simulation, and the contribution due to viscous effects inside the motor, function of the rotor speed. It is important to note that motor torque has a high frequency ripple due to control with PWM.

The last graph, in Fig.8-9, shows the temperature trend of the three stator windings in the simulation. In this case, given the normal use of the actuator not in critical conditions, the temperature values do not differ much from the initial conditions as the currents of the three windings do not reach critical values, and then the heat generated by joule effect is easily dissipated by the various components of the electric motor.

8.2 Simulation 2

In this simulation the response of the two models is evaluated, with and without thermal model, in the case where the command is equal to the previous case, but with a load applied, with width close to the stall load and a no-fault condition.
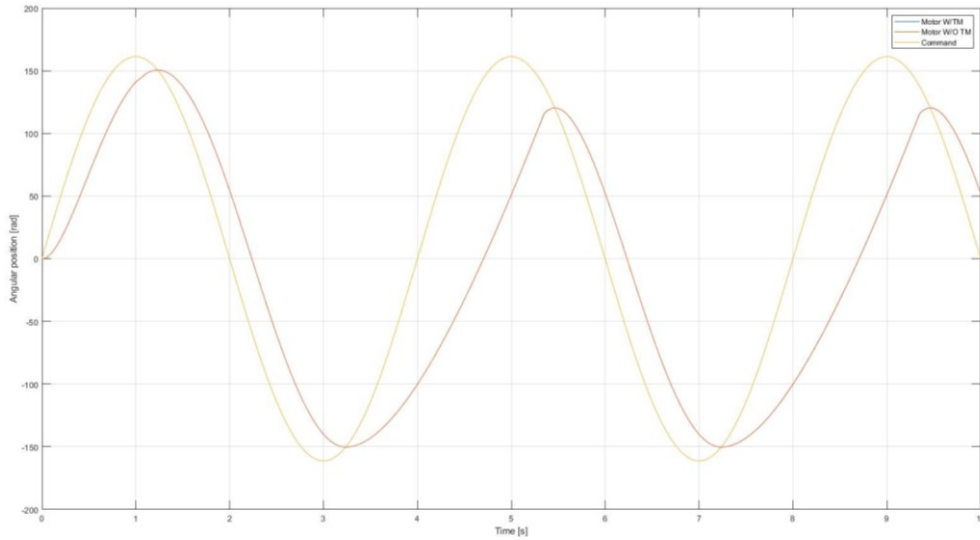
FIGURE 8-10 COMMAND VS REAL SHAFT ANGULAR POSITION
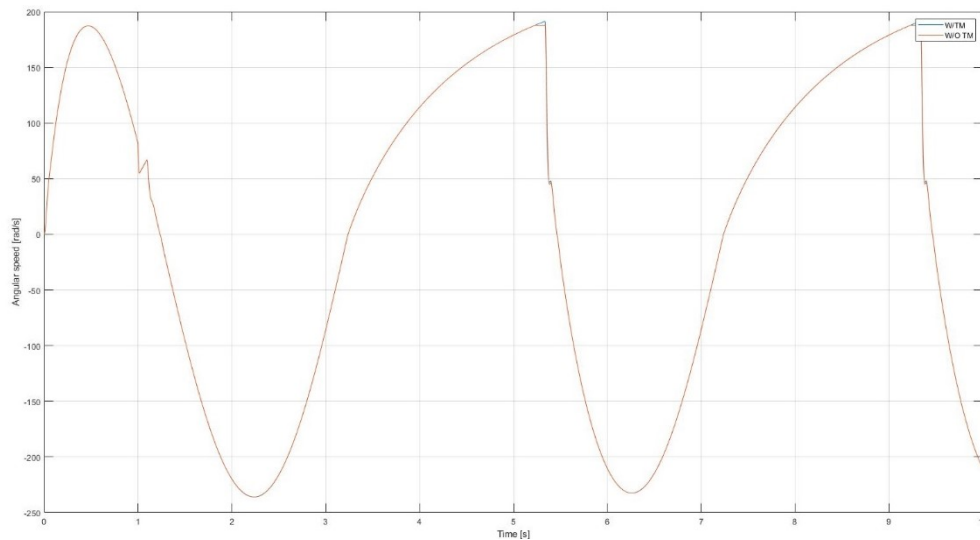
FIGURE 8-11 SHAFT ANGULAR SPEED

Also, in this case the model tends to reduce the error of position, because of this no particular differences between the two models are noticed, as shown in Fig. 8-10. Similarly, the angular speed trend is very similar between the two models under consideration, with low order differences, especially as the temperature of the windings increases, as shown in Fig. 8-11.
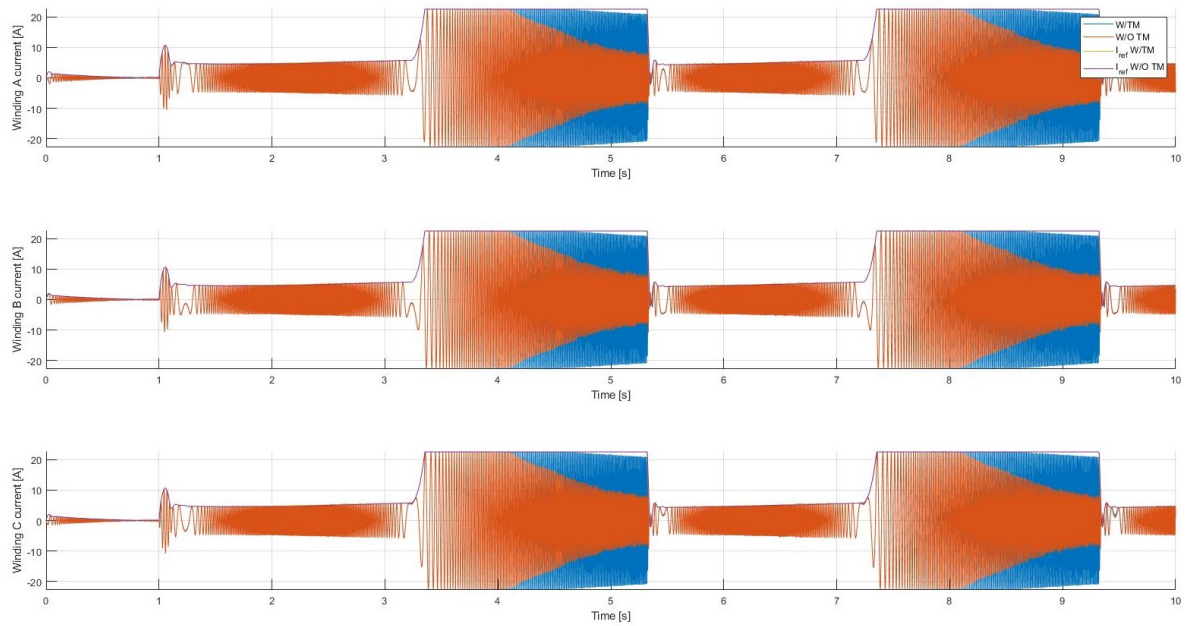
FIGURE 8-12 WINDINGS CURRENTS

The first major difference between the two models is visible in the Fig.8-12, where the currents of the three windings are represented for the two cases under examination. In this case the different models generate different values of currents in the windings, even if they have the same trend. Specifically, their reduction in the opposing phase is mainly due to the presence of BEMF. Due to the current saturation imposed on the model, the increase in the angular velocity of the rotor implies a decrease in the supply voltage of the windings, implying a decrease in current flowing into them. The difference between the two models is mainly due to the increase in the temperature of the windings, which implies a change in the resistance of the conductors.
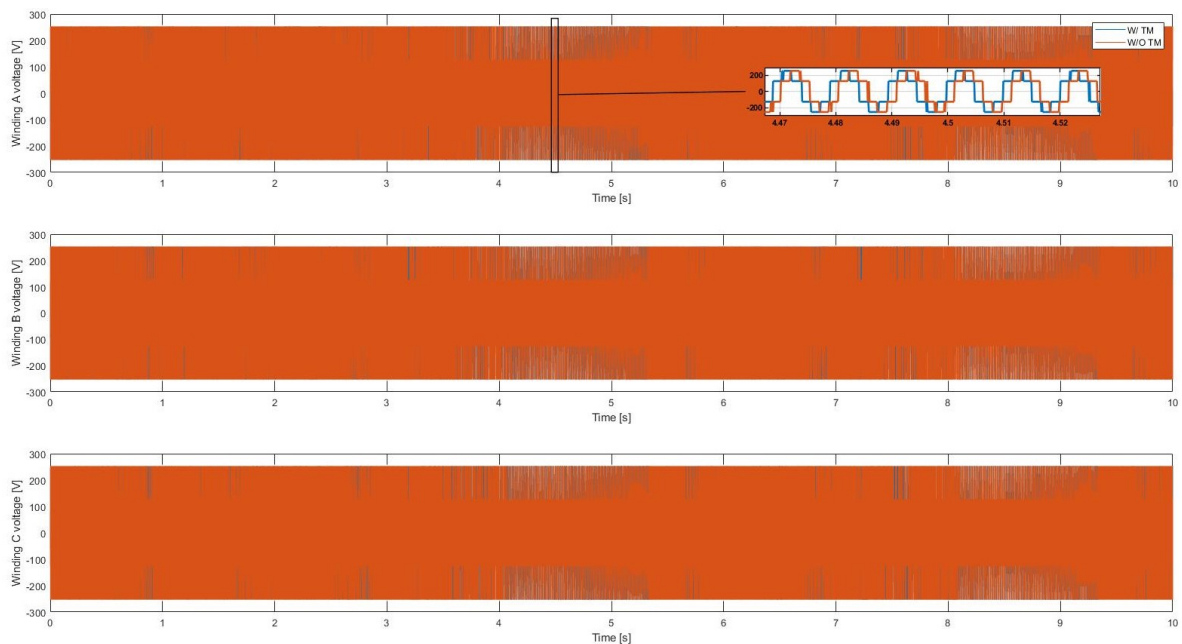
FIGURE 8-13 WINDINGS VOLTAGES
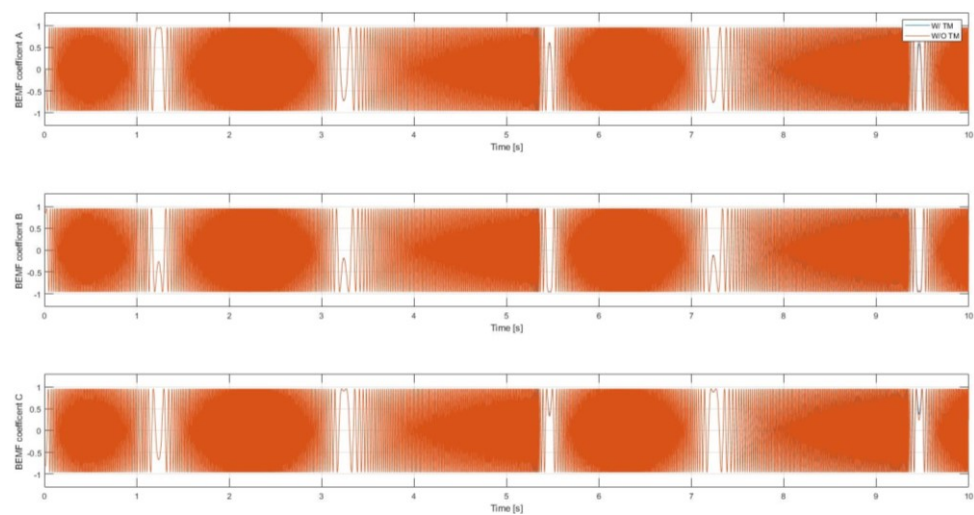
FIGURE 8-14 PHASES BEMF COEFFICIENT
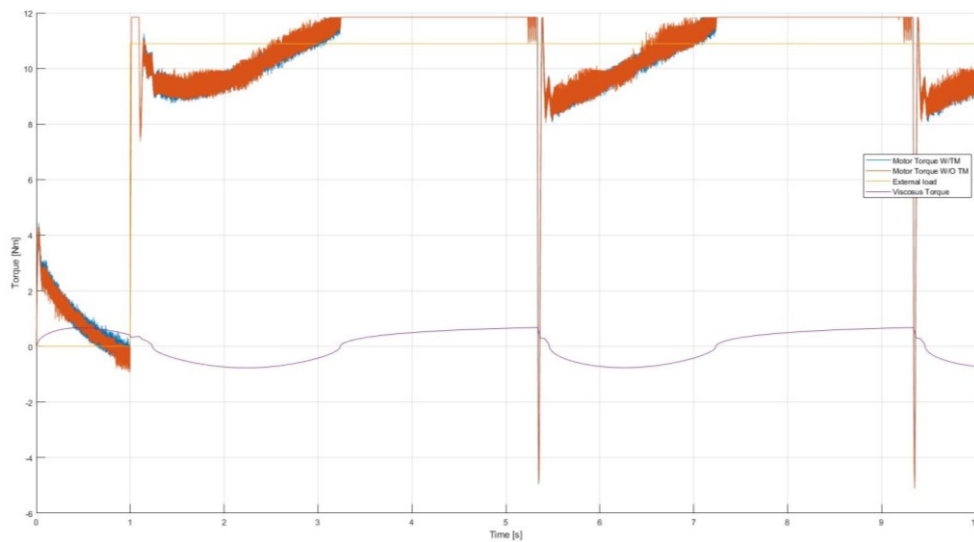
FIGURE 8-15 ELECTRIC MOTOR TORQUE VS EXTERNAL LOAD VS VISCOUS EFFECTS IN BOTH MODELS

FIGURE 8-16 WINDINGS TEMPERATURE

As in the previous case, the trend of the voltages in the three windings is very similar, as a function of the PWM controller, as shown in Fig 8-13.

In Figure 8-14 it is shown the course of the BEMF coefficient during the simulation. In a first operational phase the two models generate about the same output for the three stator windings. As the temperature increases, at the end of the simulation, it is possible to evaluate a variation between the two models in terms of amplitude, even if minimal, mainly due to a difference in rotor speed in the two models, possible effect of electric motor operating temperature.

Figure 8-15 shows the trend of the torque contributions, the torque generated by the motor, the external load, and the torque due to viscous effects inside the actuator model. After initial normal operation, with torque fluctuation present in both models mainly caused by PWM switching, when the external load is applied, in a first phase the motor acts as a brake, as the drive direction is equal to the load direction. Then the torque generated by the electric motor reaches saturation values because the engine is not perfectly able to follow the control, due to the high external load value.

The last graph shows the temperature trends of the windings, in the system in which the thermal model is implemented. The alternating temperature trends are mainly due to the alternation between the two phases of brake and opposing, where a heating phase alternates with a cooling of the windings, as shown in the Fig. 8-16.

8.3 Simulation 3

A fault condition, specifically a short-circuit failure, is implemented in the last simulation. In this specific case the operating conditions of the previous simulation are considered, but where the winding A has a short circuit of 50% of the coil.
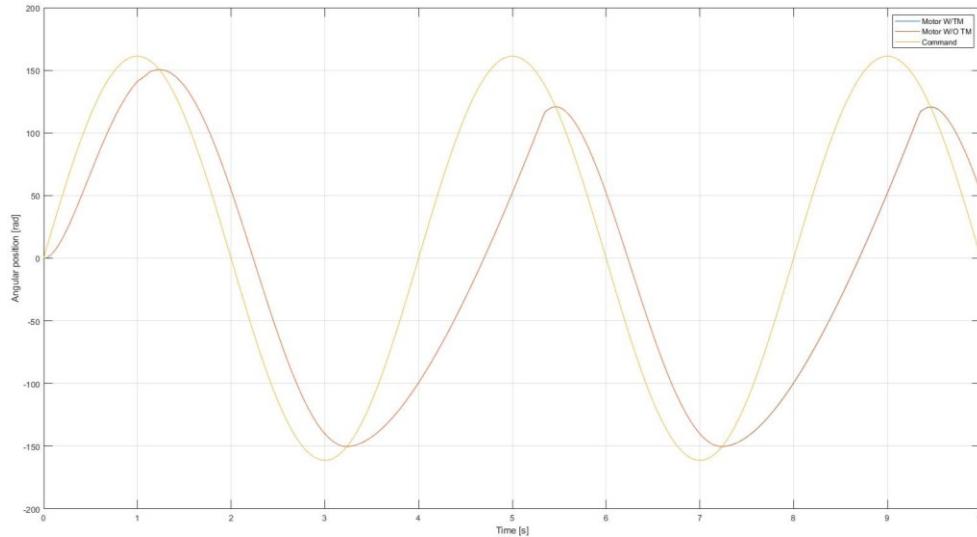
FIGURE 8-17 COMMAND VS REAL SHAFT ANGULAR POSITION
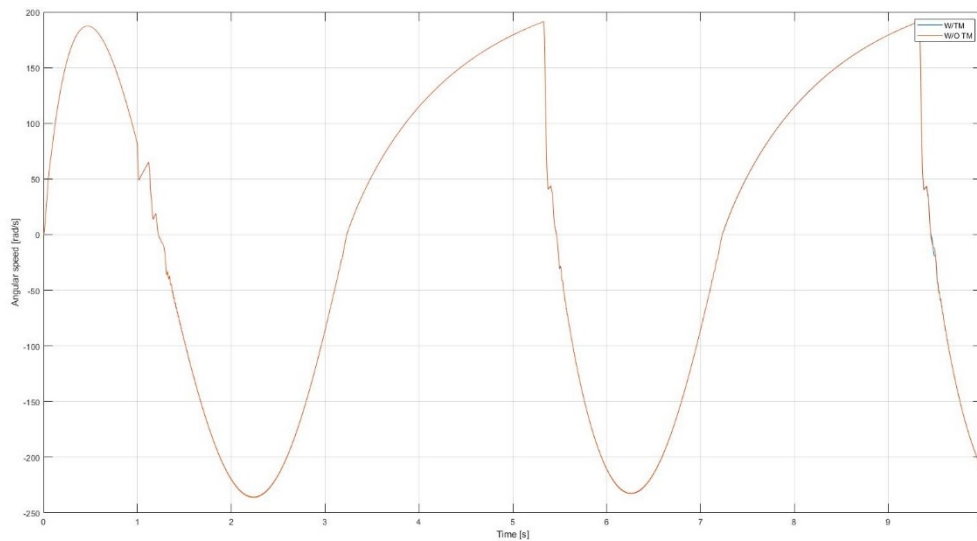
FIGURE 8-18 SHAFT ANGULAR SPEED

Also in this case, as shown in the Figure 8-17, the angular position of the rotor has no particular difference with the previous model, where, as explained above, there is an operating phase in which the motor behaves like a brake and an opposing one, where the electric motor does not succeed in optimally following the imposed control.
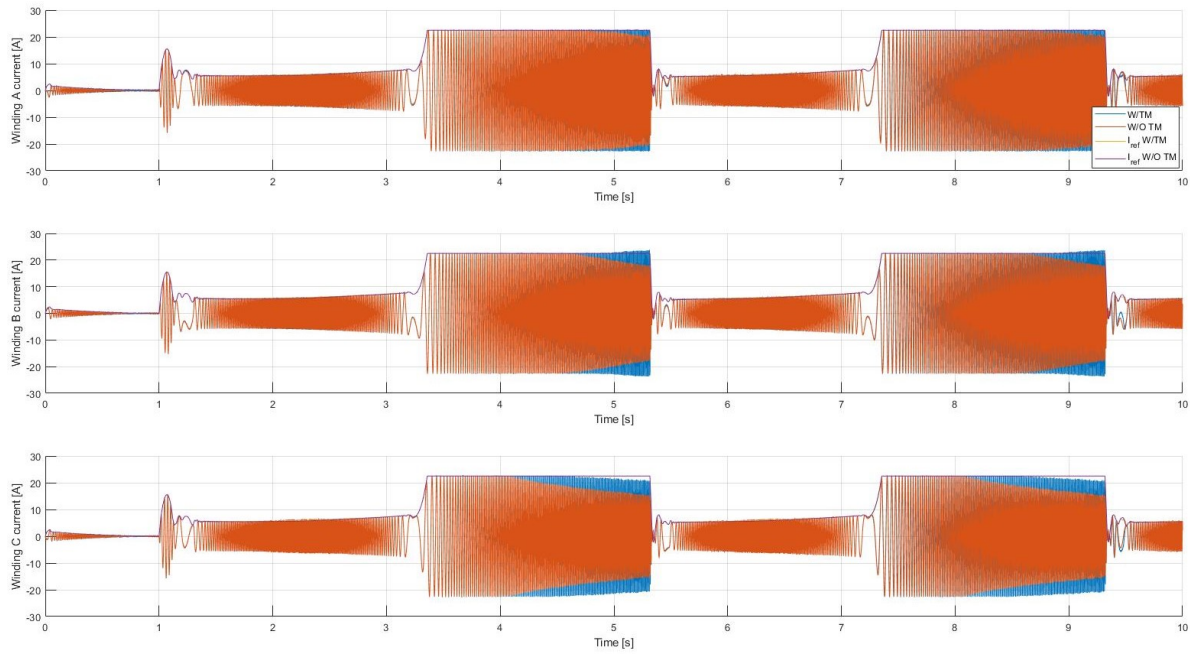
FIGURE 8-19 WINDINGS CURRENTS
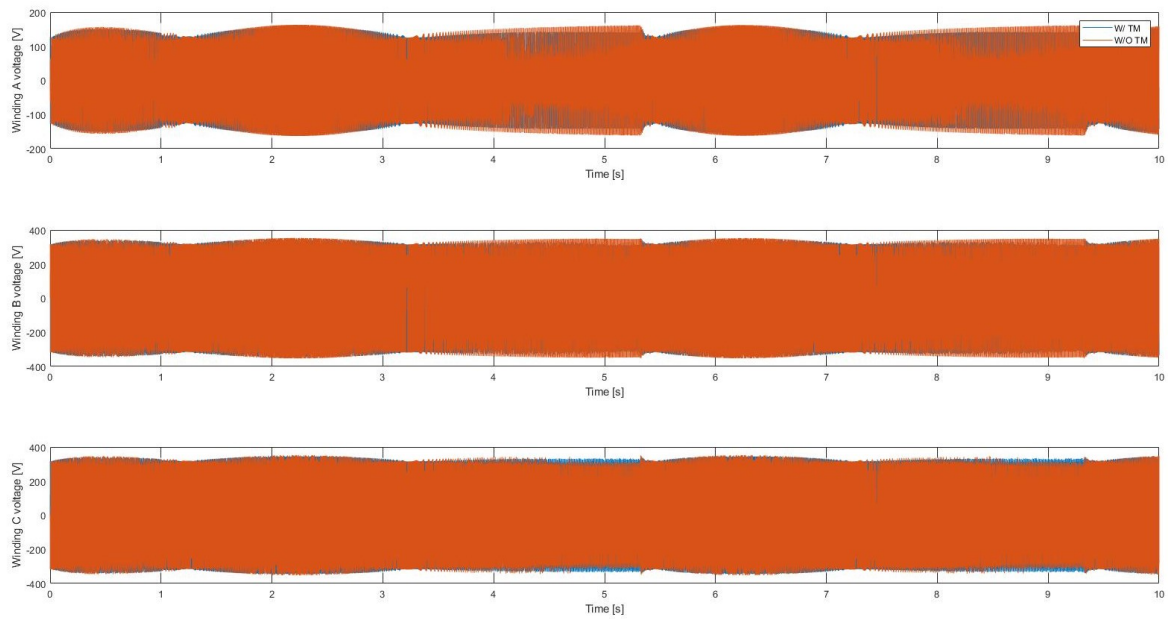
FIGURE 8-20 WINDINGS VOLTAGES

In the Figure 8- 18 is shown the trend of the angular velocities for the two models under examination. In this case there are no particular differences between the two systems, but it is useful to evaluate the angular velocity fluctuation, present in both models, caused by the presence of the fault in one of the three windings, which implies a difficulty in following the imposed command.

As shown in the Figure 8-19, the currents have different values for the two models under examination, mainly caused by the operating temperature of the electric motor. Due to the presence of the short circuit fault, the healthy windings must compensate for the fault, optimally modulating the switching between the phases.
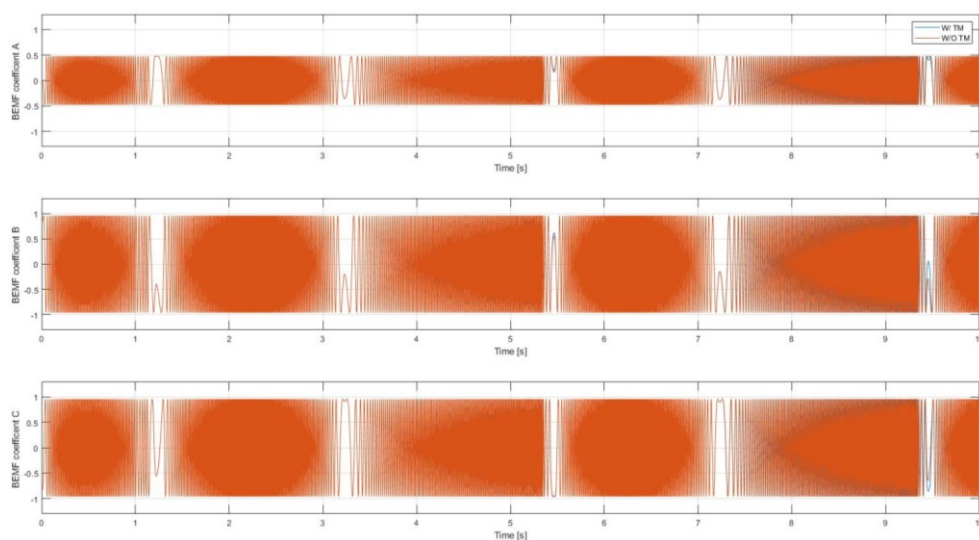
FIGURE 8-21 PHASES BEMF COEFFICIENT
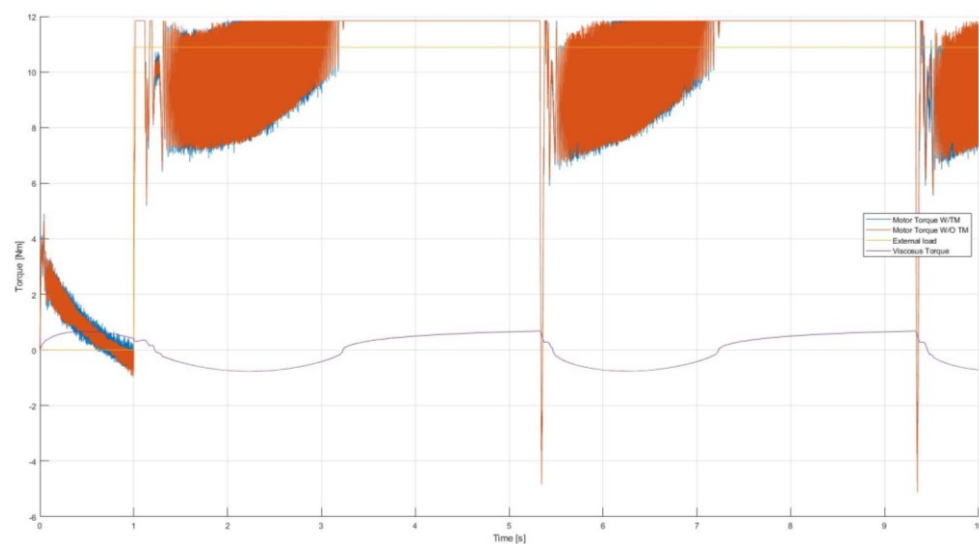
FIGURE 8-22 ELECTRIC MOTOR TORQUE VS EXTERNAL LOAD VS VISCOUS EFFECTS IN BOTH MODELS
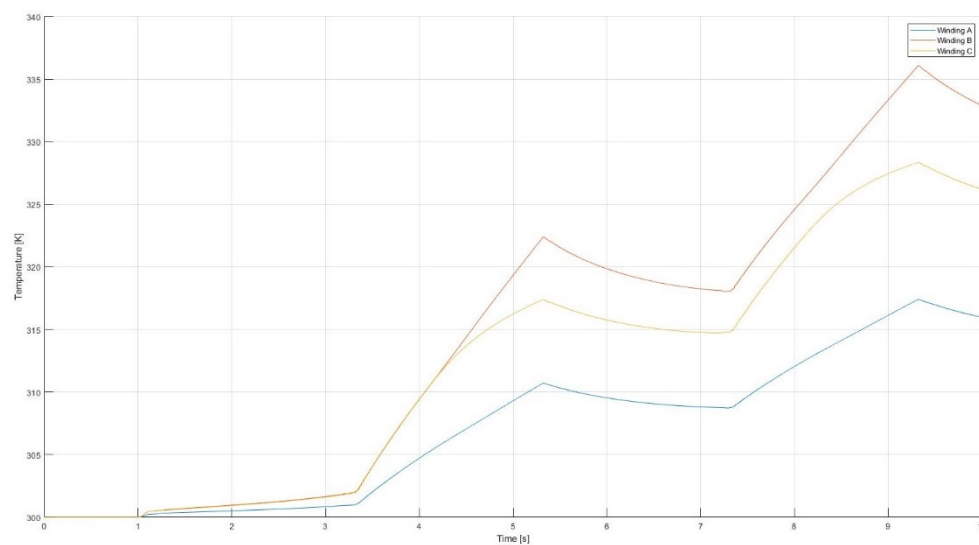
FIGURE 8-23 WINDINGS TEMPERATURE

Since the resistance is halved due to the short circuit of the winding, the supply voltage of the phase under consideration has an amplitude proportional to the fault, therefore almost halved. Also, in this case there are fluctuations due to the present fault. The two models behave in the same trend, even if for the increase of temperature of the windings there are minimal differences, as shown in Fig.8-20.

As seen in the previous simulation, the BEMF coefficient has variations at the end of the simulation, that is when the operating temperature of the electric motor increases. In this specific case, as shown in Fig. 8-21, the BEMF coefficient of the first winding has a decrease proportional to the fault value, therefore also halved.

The Figure 8-22 shows the trend of the torques inside the actuator. In this specific case there are no particular differences between the two models in examination as the new model almost perfectly traces the torque fluctuations generated by the electric motor, present due to the PWM control and the failure of the single motor phase.

The winding temperatures graph show different trends due to the different energy dissipation between the three phases of the electric motor. In the failed winding, due to the reduction in resistance, the heat dissipation by Joule effect and therefore its temperature decreases. The other windings due to the different switching caused by the fault, have a different temperature trend, even if similar to each other, as shown in Fig.8-23.

9 Conclusions and future works

The aim of this work is to implement and evaluate the effects of a thermal model for a sinusoidal permanent magnet brushless motor in a detailed electromechanical actuator model used for aerospace applications.

The thermal effects were considered by updating the stator winding block, using Matlab's Simscape toolbox, compared to the previous model developed in SymPowerSystem.

In this particular case, only the stator windings have been modelled, and their interaction with the other components of the electric motor, i.e. the stator and the case, evaluating the dispersion of heat with the external environment and the effect of the change in the resistance value of the conductors due to the rise in temperature of the windings themselves. It is important to remember that the heat exchanges with the rotor and the environment inside the electric motor have not been considered for two reasons, an unnecessary complex model in that the temperatures do not reach particular values such as to compromise a large error in the simulations, and because the paper wants to consider a general case, which entails a high modularity of the model, since, as mentioned, it only considers the components that contribute most to the rise in temperature.

As seen in the chapter dedicated to the comparison between the old model and the new, the results are completely comparable, symptom of a correct functioning and implementation of the part related to the thermal effects. Taking into consideration one of the performed tests it is possible to notice as in almost the totality of the simulation, the trends of the characteristics parameters of the electric motor, like the currents of the windings, are quite similar, excepting some intervals of time, where the temperature, reaching fairly high values, helped to change the system response, quite normal for the case under examination, validating the work done.

In order to have the certainty of the functioning of the implemented model it would be necessary to implement two strategies, the first one being the evaluation of the thermal exchanges between the various components of the electric motor, using for example a finite element model (FEM), or measure the actual temperature values through a test bench, so as to calibrate the model optimally, and thus have confidence of simulations.

Future work on the implemented model may concern different fields, for example:

- Analyse thermal flows due to heating of stator windings, under different operating conditions

- Create a dataset, such to make opportune considerations in the order to estimate the Remaining Useful Life (RUL) of the actuator.

In this last case, evaluating the data output of the model, as folded in the previous paragraphs, it is possible to make evaluations by developing an algorithm of Artificial Neural Network (ANN).

The probabilistic ANN models are used in this particular case to estimate the remaining life of the actuators, starting from parameters that characterize their state of health, such as the BEMF coefficient. A model-based approach is required to calibrate the algorithm, giving it the most information from the model's output data as input. In this particular case, by simulating a correct number of possible actuator operating conditions, with their failure status, it is possible to evaluate a different waveform relative to the characteristic parameter.

With this calibration tool the algorithm will be suitable to evaluate the status of the actuator in a generic simulation, a key feature to assess the degree of safety of the system, making their implementation possible even for users of primary importance within an aircraft.

10 Bibliography

1. *EVOLUTION OF AIRCRAFT FLIGHT CONTROL SYSTEM AND FLY-BY-LIGHT FLIGHT CONTROL SYSTEM.* **Gp Capt Atul Garg, , Rezawana Islam Linda, Tonoy Chowdhury.** 2013.

2. *Notes from "Modellazione, simulazione e sperimentazione di sistemi aerospaziali".* **Matteo D.L Dalla vedova, Paolo Maggiore.** 2022.

3. *Electrohydraulic actuators affected by multiple failures: proposal of an alternative model-based prognostic paradigm.* **M. D. L. Dalla Vedova, P. Maggiore, and F. Marino.** 2016.

4. *THE A380 FLIGHT CONTROL ELECTROHYDROSTATIC ACTUATORS, ACHIEVEMENTS AND LESSONS LEARNT.* **Bossche, Dominique van den.** 2006.

5. *Prognostics of Onboard Electromechanical Actuators: a New Approach Based on Spectral Analysis Techniques.* **D. Belmonte, M. D. L. Dalla Vedova, P. Maggiore.** 2018.

6. **www.drivelines.co.uk/2020/02/04/ball-lead-screw/.** Ball screw for linear actuators.

7. **Eitel, Lisa.** How roller-screw and ball-screw actuators compare in high-force applications. *www.linearmotiontips.com/how-roller-screw-and-ball-screw-actuators-compare-in-high-force-applications/.*

8. *Energy optimization analysis of the more electric aircraft.* **Yitao Liu, Junxiang Deng, Chao Liu, Sen Li.** 2017.

9. **The Boeing Company.** 787 Electrical System Architecture.

10. **(FAA), Federal Aviation Administration.** Pilot's handbook of aeronautical knowledge. Chapter 6: Flight controls. 2003.

11. *A Review of electromechanical actuation system for more electric aircraft.* **Jianming Li, Zhiyuan Yu, Yuping Huang, Zhiguo Li.** 2016.

12. **Vincenzo Madonna, Paolo Giangrande, Weiduo Zhao,He Zhang,Chris Gerada, Michael Galea.** Main flight control surfaces in a typical mid-sized aircraft. *Electrical Machines for the More Electric Aircraft: Partial Discharges Investigation.* 2021.

13. **Hanselman, Duane.** *Brushless Permanent Magnet Motor Design.* 2003.

14. *Brushless DC (BLDC) Motor Fundamentals.* **Yedamale, Padmaraja.** s.l. : Microchip Technology Inc, 2003.

15. *Trapezoidal Motors vs. Sinusoidal Motors.* **Sidelsky, Adam.** s.l. : Texas Instrument.

16. *Brushless DC machine.* **Emetor AB.**

17. *Design Criteria for High-Efficiency SPM Synchronous Motors.* **Nicola Bianchi, Silverio Bolognani, Paolo Frare.** 2003.

18. *Permanent Magnets Characteristics.* **Magfine Corporation.**

19. *Permanent magnet pole pairs comparison.* **www.edn.com/brushless-dc-motors-part-i-construction-and-operating-principles/.**

20. **Quattrocchi, Gaetano.** *Development of innovative prognostic methods for EMAs Applied to aerospace systems.* 2019.

21. *ANALYSIS OF PULSE WIDTH MODULATION TECHNIQUES FOR AC/DC LINE-SIDE CONVERTERS.* **Michał KNAPCZYK, Krzysztof PIEŃKOWSKI.** 2006.

22. **Mathworks.com.** *Simscape user's Guide.*

23. *European Aviation Safety Agency (EASA) Issues a Safety Warning for the Airbus A350.* **Daigle, Connor.** 2017.

24. *A Diagnostic Approach for Electro-Mechanical Actuators in Aerospace Systems .* **Abhinav Saxena, Kai F. Goebel.** 2009.

25. *Design and Evaluation of Fault-Tolerant Electro-Mechanical Actuators for Flight Controls of Unmanned Aerial Vehicles.* **Mohamed A A Ismail, Simon Wiedermann, Colin Bosch, Christoph Stuckmann.** 2021.

26. **encyclopedia.pub/entry/12700.** *Eccentricity Fault types.*

27. *Dry Friction Discontinuous Computational Algorithms.* **L. Borello, M. D. L. Dalla Vedova.** 2014.

28. *Electromagnetic Noise and Vibration in PMSM and Their Sources: An Overview.* **Niccolò Remus, Mohammad Sedigh Toulabi, Shruthi Mukundan, Himavarsha Dhulipati, Wenlong Li, Member, Colin Novak, Narayan C. Kar,.** 2020.

11 List of Figures